Annals of Nuclear Energy 214 (2025) 111122

Contents lists available at ScienceDirect

Annals of Nuclear Energy

journal homepage: www.elsevier.com/locate/anucene

A half-century of nuclear research, education and training: Story of the JSI TRIGA reactor

Luka Snoj [a,b], Klemen Ambrožič [a,b], Loïc Barbot [c], Ljudmila Benedik [a], Arne Bratkič [a], Ivana Capan [d], Christelle Reynard-Carette [e], Vladimir Cindro [a], Dušan Čalič [a], Christophe Destouches [c], Benoit Geslot [c], Alireza Haghighat [f], Romain Henry [a], Milena Horvat [a], Elchin M. Huseynov [g], Grégoire de Izarra [c], Radojko Jaćimović [a], Anže Jazbec [a], Igor Jenčič [a], Robert Jeraj [a], Malcom Joyce [h], Domen Kotnik [a,b], Gregor Kramberger [a], Igor Lengar [a], Jan Malec [a,b], Igor Mandić [a], Valerio Mascolino [f], Vid Merljak [i], Marko Mikuž [a,b], Gilles Noguère [c], Julijan Peric [a,b], Anže Pungerčič [a,b], Vladimir Radulović [a,b], Sebastjan Rupnik [a], Borut Smodiš [a], Zdenka Šlejkovec [a], Marko Štrok [a], Žiga Štancar [j], Ingrid Švajger [a,b], Nicolas Thiollay [c], Iztok Tiselj [a,b], Andrej Trkov [a,b], Bojan Žefran [a], Gašper Žerovnik [a], Ylenia Kogovšek Žiber [a], Tanja Goričanec [a,b,*]

[a] Jožef Stefan Institute, Jamova cesta 39, SI-1000 Ljubljana, Slovenia
[b] University of Ljubljana, Kongresni trg 12, SI-1000 Ljubljana, Slovenia
[c] CEA, DES, IRESNE, DER, Laboratoire de Dosimétrie, Capteurs et Instrumentation, Cadarache, 13108, Saint Paul-lez-Durance, France
[d] Institut Ruđer Bošković, Bijenička cesta 54, 10000 Zagreb, Croatia
[e] Aix-Marseille University, Jardin du Pharo 58, bd Charles Livon-13284, Marseille Cedex 07, France
[f] Virginia Tech Research Center (VTRC) Nuclear Engineering Program, Mechanical Engineering Dept., 900 N. Glebe Road Arlington, VA 22203, USA
[g] Institute of Radiation Problems of Ministry of Science and Education, AZ 1143, B. Vahabzade 9, Baku, Azerbaijan
[h] Lancaster University, Lancaster LA1 4WA, United Kingdom
[i] Krško Nuclear Power Plant, Vrbina 12, 8270 Krško, Slovenia
[j] UK Atomic Energy Authority, Culham Science Centre Abingdon, Oxfordshire, OX14 3DB, United Kingdom

ARTICLE INFO

Keywords:
Research reactor
TRIGA
Jožef Stefan Institute
General Atomics

ABSTRACT

The TRIGA Mark II research reactor at the Jožef Stefan Institute is a key facility in the field of nuclear research, characterized by its versatility and applicability in a wide range of scientific disciplines. This document highlights its operational history, contributions to nuclear safety, education and various scientific applications, including advances in reactor and radiation physics, neutron activation analysis, environmental science and even contributions to the fight against the COVID-19 pandemic. It highlights the reactor's significant role in fostering international collaborations, improving computer modeling techniques for nuclear research, and providing invaluable educational experiences. The great versatility and applicability of the JSI TRIGA reactor is emphasized by its adaptability to various research needs and its ability to enable groundbreaking studies in both fundamental and applied sciences.

Contents

* Corresponding author at: Jožef Stefan Institute, Jamova cesta 39, SI-1000 Ljubljana, Slovenia.
E-mail address: tanja.goricanec@ijs.si (T. Goričanec).

https://doi.org/10.1016/j.anucene.2024.111122
Received 25 October 2024; Accepted 3 December 2024
Available online 21 January 2025

1. Introduction

A nuclear renaissance is currently under way. Nuclear energy is being recognized evermore as an important means of combating climate change through the decarbonization of the energy sector as well as a safe, stable and reliable power source contributing significantly to our energy security and power grid stability (Lee et al., 2023; Nuclear Energy Agency (NEA), 2022). Since the start of the development of nuclear energy, research reactors have been the focal point of research, scientific progress, development and education in the nuclear field. In the future, utilization and upgrades of research reactors will represent a crucial step in furthering development, education and training, and research needed for the development of nuclear technology.

In recent years, a significant number of research reactors in Europe have ceased to operate due to political decisions, financial constraints or issues related to aging of the facilities. Consequently, it has become essential to evaluate the present state of the research reactor fleet. In the scope of the EU Horizon 2020 project TOURR — Towards Optimized Use of Research Reactors in Europe (Pungerčič et al., 2023a; Anon, 2023), a comprehensive analysis of the current status of research reactors in Europe has been performed to address this challenge, by coordinating the optimization of available research reactors in Europe. Recently, several documents have been published that explore the use of research reactors, their future, and potential opportunities for scientific and technological applications. One such document, titled "Strategic Planning for Research Reactors" (Anon, 2017), published by the IAEA, primarily focuses on enhancing the use of existing research reactors and offers guidance for the development and the implementation of a strategic plan for new research reactor projects. Another document, "Neutron scattering facilities in Europe, Present status and future perspectives" (Carlile et al., 2016), published by the Physical Sciences and Engineering Strategy Working Group — ESFRI, provides a detailed overview of the current status of neutron scattering applications using research reactors and outlines various scenarios and perspectives for the future. Notably, the document identifies a crucial gap: the need for a reactor-based neutron source in addition to the existing spallation neutron source in Europe.

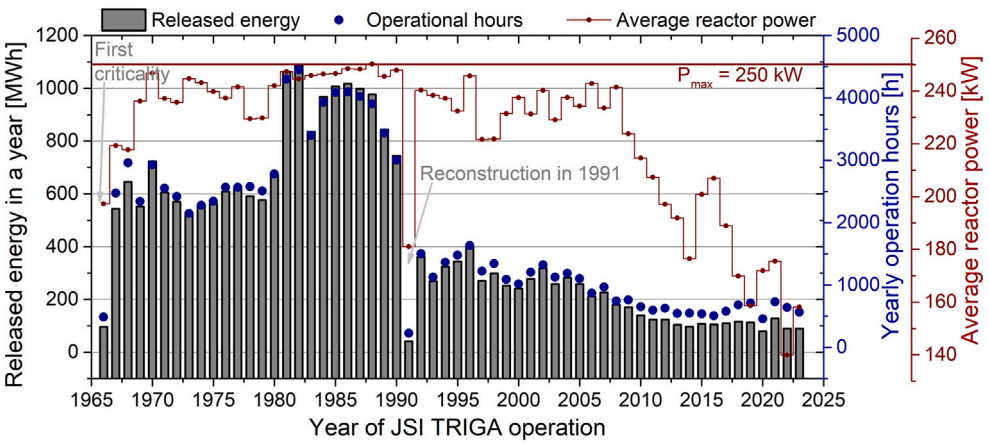

Fig. 1. JSI TRIGA Mark II reactor operation by year from its start in 1966 to the present. Annual released energy, operational hours and average reactor power are displayed for each year of operation. The average reactor power was calculated by taking into account only when the reactor was in operation in a single year (Pungerčič et al., 2020).

The IAEA Research Reactor database (IAEA) provides publicly available general information about research reactors, including details such as power, year of construction, and type. Notably, no new research reactors have been constructed in Europe from 1992 to 2023, when the subcritical VR-2 reactor was commissioned at the Czech Technical University in Prague, and the majority of existing research reactors were built during the 1960–1970 period. Consequently, the average age of European research reactors is 56 years, with a median age of 62 years. This indicates that the European research reactor fleet is relatively older than the global average, emphasizing the need for proactive measures to address future requirements.

An example of meaningful impacts of research reactors in the development of nuclear technology, safety culture, nuclear education, personnel training and research in various scientific fields is presented in this paper for the case of the TRIGA Mark II research reactor at the "Jožef Stefan" Institute (JSI) in Ljubljana, Slovenia. TRIGA is an abbreviation, which stands for Training, Research, radionuclide production, General Atomics, and is the most widely used type of research reactor in the world, with 66 facilities built since 1958, the year the first TRIGA reactor achieved criticality.

The JSI TRIGA reactor achieved first criticality on 31 May 1966 at 14:15 and has since been extensively utilized for training, research, and radionuclide production. The annual reactor operation history is graphically presented in Fig. 1, where the released energy, operational hours and average reactor power are displayed for each year of operation. Before 1991 the reactor was used in large part for radionuclide production, in 1991 it underwent a comprehensive refurbishment, after which radionuclide production ceased and the reactor utilization transitioned to research, education and training.

In the early years of operation, a time-of-flight spectrometer with a rotating monocrystal of lead, a cold neutron source with solid methane as a moderator, and a neutron diffractometer were installed and utilized for investigations in the field of solid state physics (Dimic and Petkovsek, 1971). The instruments were used mainly to measure fluid and ferroelectric crystals, respectively. The experimental devices were later dismantled and are presently not available. The description of different components, mentioned in the history description of the JSI TRIGA reactor, is given in next Section 2.

In 1974, a neutron radiographic facility was constructed (Rant et al., 1972). A conical cadmium neutron beam collimator was designed to fit into the thermal column or the tangential beam of the reactor to create a collimated thermal neutron beam outside the heavy concrete shield. Neutron radiography was performed by irradiating objects of interest in the beam and exposing photographic film or later neutron-sensitive imaging plates located behind the objects to be imaged. The facility was reconstructed in 1995. In the early years, the facility was mainly applied to examine metal adhesives combined with glass fibers and to study different binary alloy systems (Lazaru et al., 1999). Later, it was also used for the inspection of TRIGA fuel, applications in metallurgy, inspections of aviation components, archaeological objects, and quantitative measurements of moisture in building materials (Nemec et al., 1999). At present the use of the original facility is discontinued, however work is in progress to reinstate radiographic/tomographic capabilities at the JSI TRIGA reactor using modern components and systems currently available.

In the seventies and eighties, the reactor was extensively utilized for the production of radionuclides for medical purposes — ^{18}F, ^{131}I, ^{85m}Kr, ^{99m}Tc (Najzer et al., 1974; Dimic, 1976) and industrial applications — ^{82}Br, ^{60}Co, ^{24}Na, ^{65}Zn. Dedicated equipment for routine production of ^{99m}Tc based on solvent extraction from irradiated ^{98}Mo was developed and later upgraded as a semi-automatic facility. Dimic (1986) Also, doping of silicon monocrystals was performed. Over the years, the production decreased and was finally discontinued after the refurbishment of the reactor.

Originally, the reactor was equipped with several irradiation channels in the reactor core, a pneumatic system to irradiate samples in the core periphery (the outer "F" ring of the reactor core) and a rotary irradiation device – the carousel – in the graphite reflector. Around 1970 a pneumatic transfer system was installed connecting the pneumatic sample irradiation system to the hot cell facility, adjacent to the reactor, which was completed after the reactor itself (Dimic and Gabrovsek, 1972). Later in the decade, a replacement carousel, manufactured by the JSI workshop was installed and a pneumatic device was added to facilitate the withdrawal of irradiated samples (Kristan et al., 1978). In 2001 a fast pneumatic sample transfer system was installed to enable activation measurements of very short-lived radionuclides, with a sample transit time of approximately 2 s (Jacimovic et al., 2002).

During 1991–1994, the reactor underwent a significant reconstruction and upgrade (Dimic et al., 1995; Mele et al., 1994b). The reconstruction comprised the replacement of both reactor grid plates, control rod mechanisms and the control unit, new wiring of the electric power supply system, a new air exchange system, and a new spent fuel storage facility. The upgrade also included the installation of a pulse control rod (Mele et al., 1994a). After the reconstruction, the core was loaded with fresh 20 % enriched fuel elements, and in 1999, all spent fuel elements were shipped to the USA. In 2015, the original manually operated standard pneumatic transfer system for short irradiations was replaced with a new, computer-controlled system with an automatic loader for irradiation capsules in the framework of a technical cooperation project, financed by the IAEA. In 2020, the system was further upgraded to allow interconnection with the second original pneumatic system, the carousel pneumatic transfer system.

During the reconstruction in 1991, a new vertical channel, the so-called "triangular" channel, occupying three standard fuel element positions was introduced, enabling irradiations of larger samples in the reactor core. As the channel cross-section in the active core volume was irregular, in 2015 an improved version of the channel was manufactured, starting with custom-extruded aluminum tubes matching the shape of the triangular cutouts in the top reactor grid plate. A second triangular irradiation channel was added in the opposite part of the reactor core. In 2016 (Radulovic et al., 2017) and 2019 two horizontal tangential channels were modified, allowing for the irradiation of even larger samples in a close to homogeneous neutron flux. Work in currently in progress on the design of a cadmium shield in one of the horizontal channels to limit the activation due to thermal neutrons, as well as a high temperature irradiation device enabling irradiations in conditions representative of nuclear power plant reactors or high-temperature reactors.

The reactor has amply been utilized for neutron activation analysis (NAA) for a variety of sample matrices, including geological, environmental, biological, and industrial: in the sixties, seventies, and eighties mainly for radiochemical NAA, i.e., where an element or group of elements to be determined is chemically separated after neutron irradiation to lower detection limits. Emphasis was on the determination of essential and toxic elements, including speciation analysis of some biologically important ones (e.g., As, Cr, Hg, I, Mn, Se, V). With the development of gamma-ray spectrometric equipment in the late seventies and early eighties, instrumental NAA was applied, where the sample is measured without chemical processing, thus offering the possibility of simultaneous determination of many elements in the sample. Instrumental NAA gradually replaced radiochemical NAA. In the late 1980s, a semi-empirical instrumental k0-based NAA was introduced, completely replacing the relative instrumental NAA (Jaćimović et al., 2012).

It is evident that the JSI TRIGA reactor has been playing an important role in the development of nuclear technology and safety culture in Slovenia. It is one of a few centres of modern technology in the country. Its international cooperation and reputation are important for the promotion of the JSI and Slovenian science in the world. The reactor has been mainly used for training and education of university students, future operators at the Krško Nuclear power plant (NPP) as well as on-the-job training of staff working in public and private institutions, radionuclide production, neutron activation analysis, neutron radiography, testing and development of a digital reactivity meter, verification of computer codes and nuclear data, comprising primarily criticality calculations and neutron flux distribution studies. In the past few years, it has been extensively used for irradiation of various components for the ATLAS detector in the European Organization for Nuclear research (CERN). Due to the comprehensive characterization of the irradiation channels the reactor has become a reference centre for neutron irradiation of detectors developed for the ATLAS experiment.

This paper is structured as follows: Section 2 describes the JSI TRIGA reactor in detail, Section 3 focuses on the application fields, Section 4 summarizes the education and training activities conducted at the JSI TRIGA reactor, and Section 5 presents the development of computer codes and programs. Section 6 gives some concluding remarks.

2. JSI TRIGA MARK II reactor description

The JSI TRIGA Mark II reactor is in operation in Ljubljana, Slovenia, since 1966. It has been used as a training facility for reactor operators, as a production facility for medical radionuclides and for conducting various reactor physics experiments. It is a pool-type light-water thermal research reactor, with a maximum power of 250 kW and a maximum neutron flux of about 2×10^{13} 1/(cm^{2}s). The reactor core has a cylindrical configuration and consists of cylindrical fuel elements clad with stainless steel. The fuel material is a homogeneous mixture of uranium and ZrH with 12 wt.% uranium and 20 % enrichment. The schematic side and top views of the reactor are shown in Figs. 2 and 3.

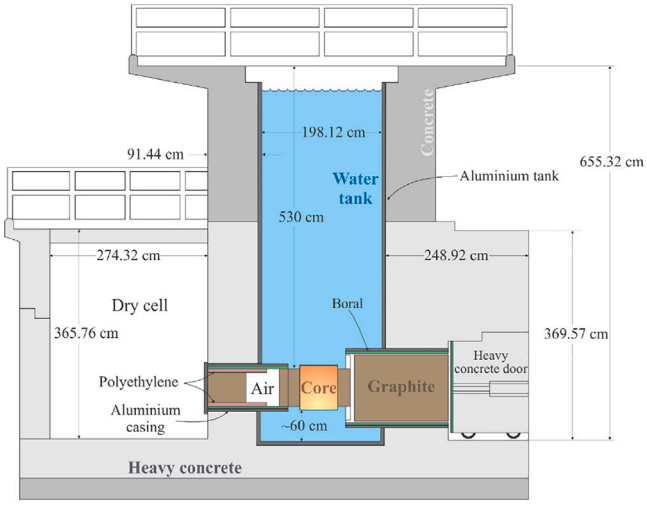

Fig. 2. Side view of the TRIGA Mark II reactor.

Table 1
Position of rings from core center.

Ring	Positions	Ring position [cm]
A	1	0
B	6	8.108 ± 0.005
C	12	15.961 ± 0.005
D	18	23.891 ± 0.005
E	24	31.831 ± 0.005
F	30	39.776 ± 0.005

The core of the TRIGA reactor is located at the bottom of the reactor pool, about 5.30 m from the platform bridge. The reactor pool is filled with demineralized water and has the shape of an aluminum cylinder with a height of 6.25 m and a diameter of 2 m. The core itself has a cylindrical configuration and consists of fuel elements retained by two aluminum support grids. Holes are present in both support grids to allow the insertion of fuel elements, control rods, irradiation channels and a neutron source. In addition, smaller holes with a diameter of 10.5 mm or 8 mm are also present in the grids. These are intended for the insertion of specially adapted instrumentation guides that enable the use of neutron detectors in the core of the TRIGA reactor. Two larger triangular cutouts are used for the installation either of three fuel elements or a triangular irradiation channel. A schematic view of the upper support grid is shown in Fig. 4.

The fuel elements inside the core are arranged in six concentric rings, labeled A, B, C, D, E and F, with 1, 6, 12, 18, 24 and 30 locations, respectively. Each location corresponds to a hole in the aluminum upper grid plate of the reactor. The distances between the center of the core and the rings are given in Table 1.

The fuel of the TRIGA Mark II reactor is contained in cylindrical fuel elements clad in stainless steel (SS-304), as can be seen in Figs. 5 and 6. The height of a single element is 73.2 cm — the top and bottom ends of the element are designed to be safely positioned in the core and can be manipulated remotely by the reactor operator. The central part has a cylindrical shape with an outer diameter of 3.7 cm. The fuel meat is made of a homogeneous mixture of uranium and zirconium hydride U-ZrH and is in pellet form. Three pellets are stacked vertically inside the fuel element, with no significant gaps between them, the total height of the fuel meat is 38.1 cm. The fuel has a 12 % mass fraction of 20 % ^{235}U enriched uranium.

At the upper and lower ends of the fuel material there are two cylindrical graphite plugs about 8.7 cm in length. These serve as local

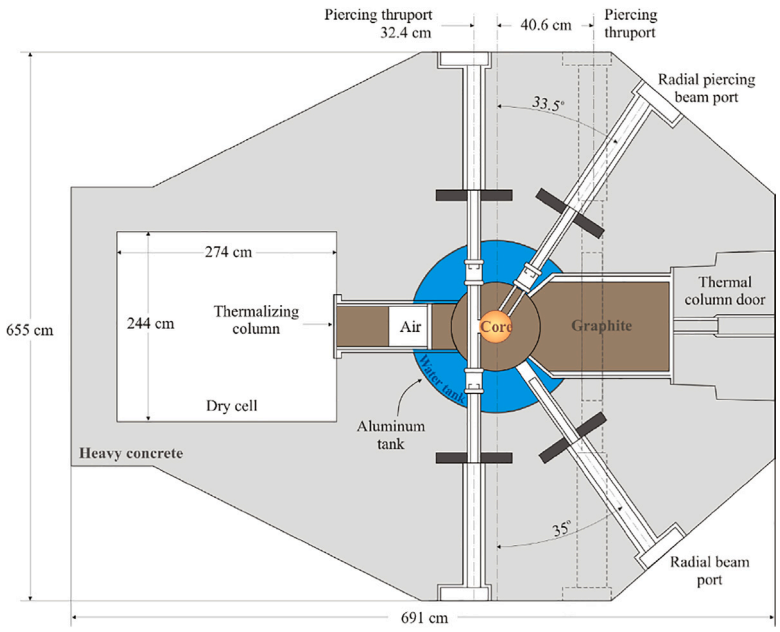

Fig. 3. Top view of the TRIGA Mark II reactor.

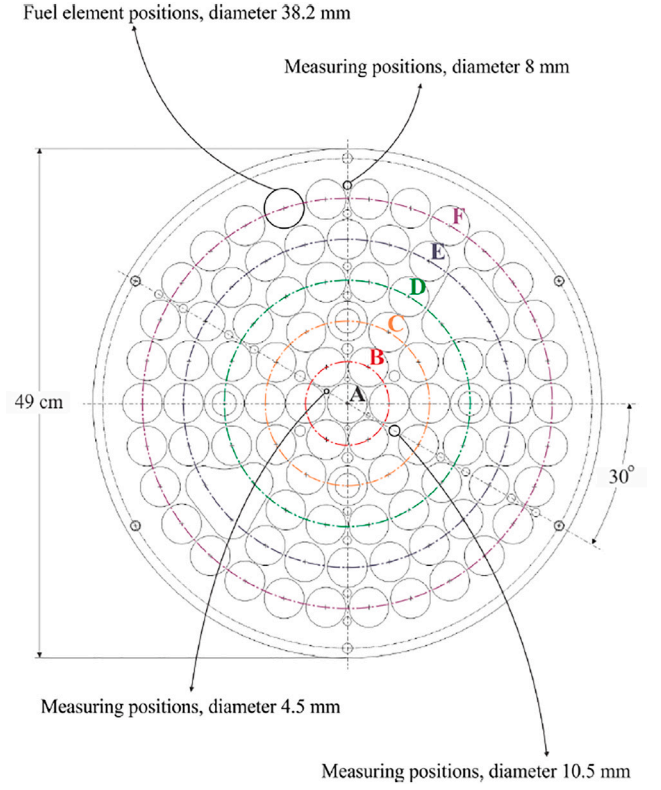

Fig. 4. Schematic view of the JSI TRIGA core configuration with marked fuel rings with letters and colors.

axial neutron reflectors. A zirconium rod with a diameter of 0.635 cm is inserted in the middle of the fuel material. The lower graphite plug is additionally separated from the Zr rod and the fuel material by a thin molybdenum support disk.

Surrounding the core is a ring-shaped neutron reflector consisting of dry graphite blocks. It is surrounded by a protective watertight aluminum housing with a thickness of 1.27 cm, isolating the reflector from the water in the reactor core. There is a 6.44 cm wide annular groove in the upper part of the graphite reflector, which hosts the carousel irradiation device. The carousel is made of aluminum and consists of 40 circularly distributed irradiation positions with an inner diameter of 3.8 cm. A schematic drawing of the graphite reflector is shown in Fig. 7.

There are two horizontal channels that penetrate the graphite reflector — the radial channel ends at the inner radius of the reflector and is located 7 cm below graphite reflector horizontal mid-plane. The tangential channel is at the same height and passes the core at a distance of 32.44 cm from core center. The channels are dry and clad with aluminum. A schematic view of the irradiation channels can be found in Fig. 3.

Three control rods of fueled-follower type are used in the TRIGA reactor: Regulating (R), Compensating (C) and Safety (S). They take the form of cylindrical rods encased in stainless steel, the lower part of which is filled with fuel material and the upper part with B_4C neutron absorber. Similar to the fueled-follower control rods, the transient (T) control rod also consists of an upper absorber part (B_4C) and an air-follower below. The latter is an empty cylinder that reduces the power peaks when the transient rod is in its fully withdrawn position. When transient rod is pneumatically ejected it creates a pulse. The position of the control rods is measured in steps, with full withdrawal being achieved at 200 steps (0 steps for the transient rod) and full insertion at 900 steps. The end positions of the control rods are approximate and vary between control rods, i.e. some control rods may be inserted as far as step 915 or withdrawn as far as step 181, but due to the low reactivity of the control rods in their limit positions, the movement of the rods in this range has a negligible effect. The schematic drawing of the control rods is presented in Fig. 8.

The neutron source has a cylindrical shape with aluminum cladding and has the approximate dimensions of a fuel element. It contains an Ra-Be source with an activity of 10^6 1/s. Its outer diameter is 3.754 cm and it is 71.755 cm long. Except for the part of the cylinder containing the Ra-Be source, the volume is filled with air. A schematic representation of the neutron source can be found in Fig. 9. The source can be installed in the fuel element positions in the reactor core and its location is periodically changed, depending on the experimental configuration of the core.

Fig. 10 displays a schematic view of the reactor core. There are five instrumentation channels on the outside of the graphite reflector,

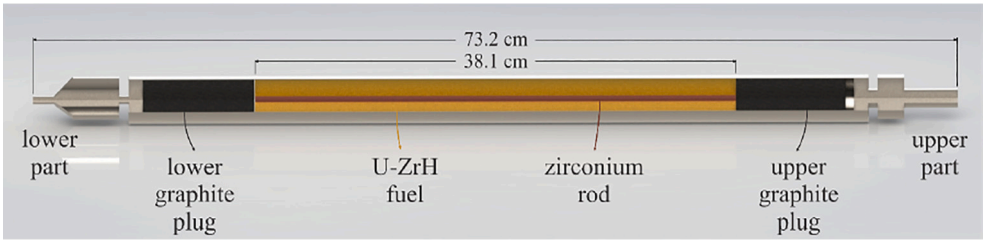

Fig. 5. Cut view of the fuel element with the U-ZrH fuel, zirconium rod and graphite plugs.

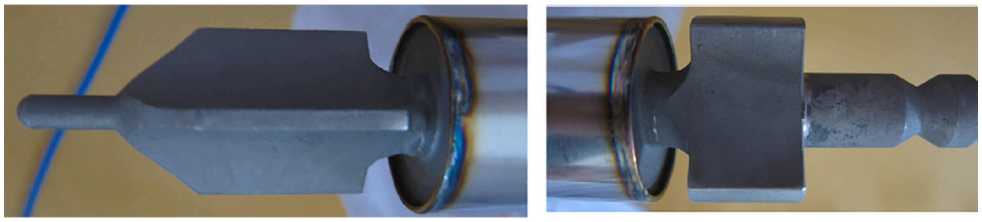

Fig. 6. Photograph of the lower (left) and upper (right) stainless steel pin of the fuel element.

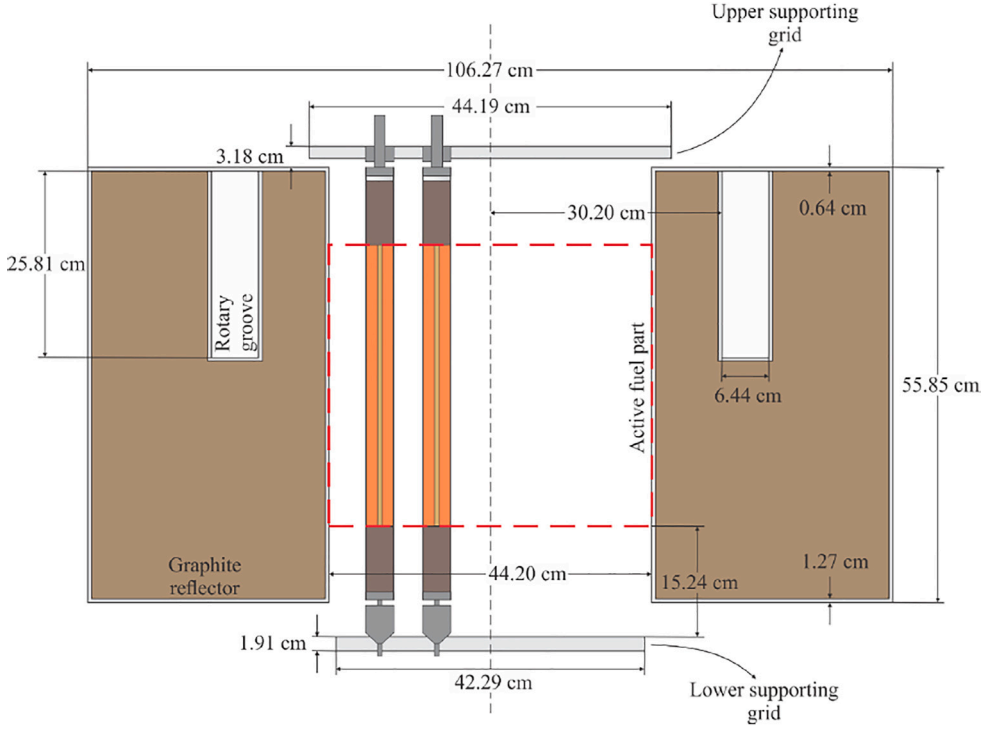

Fig. 7. Schematic side view of the reactor core and the annular graphite reflector.

which are used to measure the thermal power of the reactor. The instrumentation channels consist of sealed aluminum housings containing neutron detectors. They are referred to as the Start-up, Pulse, Safety, Logarithmic and Linear channel, with each channel having a specific power measurement range. For example, the start-up channel is used to measure low reactor power levels during reactor start-up with a range between 0.1 mW and 100 W. The logarithmic and safety channels are used for power measurements in the range from 1 W to about 1 MW, while the pulse channel is used in reactor pulse operation mode, during which power levels of up to 1 GW can be achieved. The widest power range, i.e. from 100 mW to 300 kW, is covered by the linear channel, which is mainly used for power measurements during normal reactor operation. The position of the ex-core detectors is shown in Fig. 10, where they are marked with circles on the edge of the graphite reflector.

Dimension and material composition of all JSI TRIGA components is given in Table 2.

3. Application fields

The diverse applications of the TRIGA research reactor underline its central role in advancing scientific and technological boundaries in various disciplines. This section highlights the reactor's contributions to nuclear research, technology development and practical applications utilizing its unique capabilities and emphasizes its adaptability and importance in various fields. A more detailed description of specific application areas is presented, including reactor physics, radiation

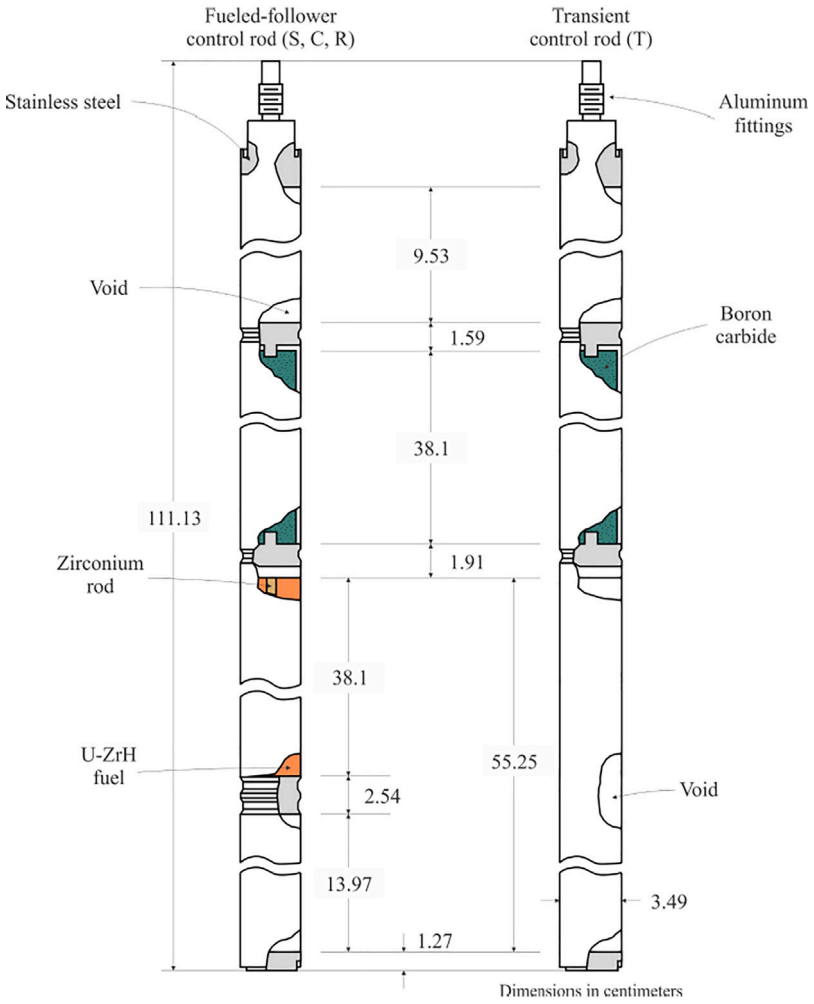

Fig. 8. Dimensions of the TRIGA control rods — regulating (R), compensating (C), safety (S) and transient (T).

physics, environmental science, and more, illustrating the integral role of the reactor in advancing scientific knowledge and technological capabilities.

3.1. Reactor physics

The contribution of the JSI TRIGA reactor to the development of reactor physics is presented, emphasizing its crucial role in theoretical and practical applications in the field of nuclear science. The importance of the reactor in conducting benchmark experiments, validating computational models and studying reactor response under different conditions is highlighted.

3.1.1. Benchmark experiments

With the development of new high-fidelity computational methods, the improvement of nuclear data and multi-physics modeling, the need for benchmark experiments to experimentally validate the models, methods and input data is increasing. Many of the nuclear facilities designed to perform reactor physics benchmark experiments have been shut down. Therefore, research reactors offer a great opportunity for benchmark experiments as long as they are well designed and performed with great care and accuracy. In this section, we provide an overview of past and ongoing activities related to benchmark experiments at the JSI TRIGA Mark II research reactor. The following experiments have been performed: criticality with fresh fuel, ^{197}Au(n, γ) and ^{27}Al(n, α) reaction rate measurements in irradiation channels, absolute and relative ^{197}Au(n, γ), ^{235}U(n,f) and ^{238}U(n,f) reaction rates in the core, burnup, kinetic parameters, control rod worth, isothermal reactivity coefficient, self-shielding, slow and fast (pulse) transients, nuclear heating, prompt and delayed gamma ray production, temperature profiles for multi-physics. Some of the experiments have already been evaluated and are available to the worldwide community Jeraj and Ravnik (1999), Štancar et al. (2017a), while others still need to be evaluated.

3.1.1.1. Criticality and burnup benchmark.

The benchmark experiments were performed as a part of startup test of the JSI TRIGA after reconstruction and upgrading in 1991, during which all core components (top and bottom grid plates, fuel, control rods, irradiation channels), with the exception of the graphite reflector around the core, were replaced with new ones. The experiments in steady-state operation were performed with completely fresh fuel (including instrumented elements and fueled followers of control rods) in a compact and uniform core (i.e. all elements including the fueled followers of control rods were of the same type with no nonfuel components in the critical core configuration) at well-controlled operating conditions. Subsequently, a computational model of the reactor for use with the MCNP code (Goorley et al., 2013) was developed in 1999 to evaluate the experimental uncertainties and provide computational support for the reactor experiments. The evaluated criticality benchmark experiment was later documented in the International Handbook of Evaluated Criticality Safety Experiments (ICSBEP) (Briggs et al., 2006). Until recently, this benchmark was the only publicly available TRIGA criticality benchmark featuring a homogeneous mixture of fuel,

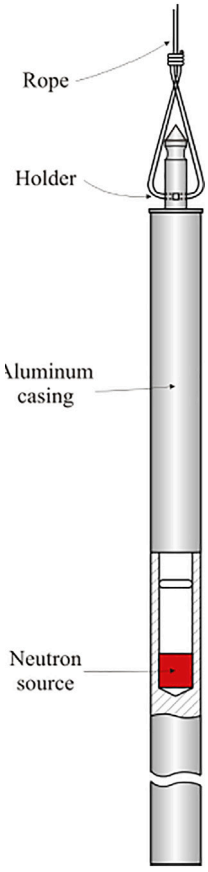

Fig. 9. Dimensions and composition of the TRIGA neutron source.

Table 2
Table of JSI TRIGA component dimensions, materials, and densities (Štancar et al., 2017b).

Component	Dimension [cm]	Material	Density [g/cm^3]
Fuel		U-ZrH	6.045[a]
Outer diameter	3.645 ± 0.008		
Inner diameter	0.64 ± 0.01		
Height	38.1 ± 0.1		
Graphite plug		Graphite	1.60
Diameter	3.632 ± 0.003		
Height upper plug	8.67 ± 0.05		
Height lower plug	8.81 ± 0.05		
Zirconium rod		Zirconium	6.49
Diameter	0.64 ± 0.01		
Height	38.1 ± 0.1		
Supporting disk		Molybdenum	10.2
Height	0.07938 ± 0.00001		
Cladding		SS-34	7.889
Outer diameter	3.75 ± 0.02		
Thickness	0.051 ± 0.003		
Height upper part	8.2 ± 0.1		
Height lower part	8.7 ± 0.1		
Reflector		Graphite	1.60
Outer diameter	106.27 ± 0.05		
Inner diameter	45.47 ± 0.05		
Height	53.95 ± 0.05		
Cladding		Aluminum	2.70
Thickness (inner, top)	0.64 ± 0.01		
Thickness (outer, bottom)	1.27 ± 0.01		
Thickness (groove lining)	0.318 ± 0.001		
Rotary specimen rack		Air	0.0013
Outer diameter	73.3 ± 0.2		
Inner diameter	60.4 ± 0.2		
Height	25.8 ± 0.2		
Specimen hole diameter	3.8 ± 0.05	Aluminum	2.70

moderator, and Zr. Due to the U-ZrH fuel, it has a high sensitivity to Zr absorption and scattering cross-sections (Snoj et al., 2012b). In addition, the criticality benchmark was repeated after several years of operation utilizing spent fuel (Peršič et al., 2000). This benchmark provides valuable data to validate depletion calculation codes and to evaluate the reactivity effects of burnup. In addition, the burnup of individual fuel elements was estimated by reactivity experiments (Ravnik et al., 1992a, 1993).

Recently, initiatives have been launched to comprehensively document the operating history of the reactor, together with measurements of excess reactivity and control rod worth. These records can be helpful in the verification of core management codes. One of the largest uncertainties in determining fuel burnup comes from the measured reactor power level (Štancar and Snoj, 2017). In the JSI TRIGA Mark II reactor, neutron flux redistribution or radial tilt due to asymmetric control rod insertion is a significant source of uncertainty. Since the reactor power is usually measured with a single detector, the deviations in the measured power levels can reach 20–30 % in extreme cases. This issue can be addressed by applying correction factors (Kaiba et al., 2015) or by using multiple detectors for power measurement (Žerovnik et al., 2014b).

3.1.1.2. Reaction rate benchmark.

The neutron activation technique was used to experimentally validate the calculated reaction rates in the irradiation channels of the reactor. In this experiment, aluminum–gold (Al(99.9 wt. %)–Au(0.1 wt. %)) foils (disks with diameter of 5 mm and a thickness of 0.2 mm) were irradiated in 33 locations (irradiation channels); 6 in the core and 27 in the carousel facility in the reflector (Snoj et al., 2011a). After irradiation, the activation of the individual samples was measured with a High-Purity Germanium detector (HPGe). Specifically, two activation reactions were investigated in the experiment (see Fig. 11): ^{27}Al(n, α) and ^{197}Au(n, γ).

In addition, axial ^{197}Au(n, γ)^{198}Au reaction rate measurements were performed in four in-core positions at full power. This was achieved by irradiating aluminum probes, containing 5 mm long Al–0.1% Au wires with a diameter of 1.0 mm (Radulović et al., 2014).

Fission rate measurements were performed with a fission chamber containing approximately 10 μg of 98.49% enriched ^{235}U. Axial measurements (23 axial positions) of the fission rate along the entire core height at 9 radial measurement positions were performed and are presented in Section 3.2.2. These measurements were also used for verification and validation of the computational model. An interesting feature of the above experiments is that they provided absolute values of the reaction rates that are normalized to the total reactor power and can therefore also be used to validate the normalization (Žerovnik et al., 2014a).

3.1.2. Reactor physics parameters

Over the past 25 years, extensive efforts have been made to evaluate the physical parameters of the JSI TRIGA reactor, starting with core criticality, power peaking factors, control rod worth analysis, kinetic parameters, and fuel depletion effects. The reactor physical parameters were determined both experimentally and computationally using Monte Carlo codes such as MCNP (Goorley et al., 2013), Serpent-2 (Leppänen et al., 2015) and TRIPOLI (Petit et al., 2008), deterministic codes such as TRIGLAV (Peršič et al., 2017), GNOMER (Trkov and Merljak, 1994; Trkov et al., 1990; Merljak et al., 2017a) and the hybrid code RAPID (Walters et al., 2018).

3.1.2.1. Control rod worth.

The JSI TRIGA reactor has four control rods. Their integral and differential reactivity worth curves are commonly measured by the Rod

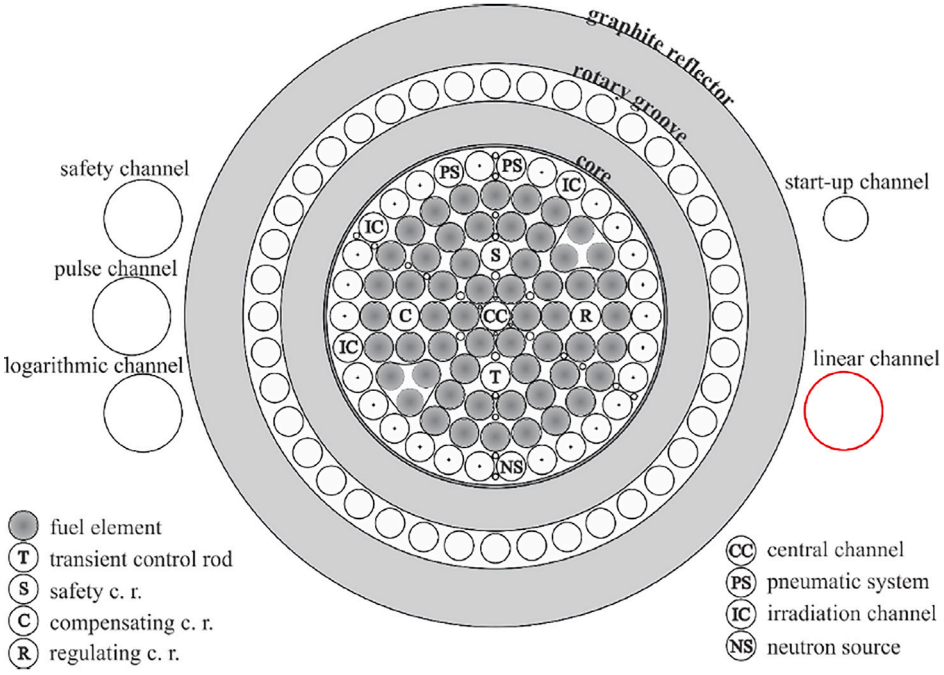

Fig. 10. Schematic of the reactor core with denoted fuel elements, control rod positions and irradiation channels with the surrounding graphite reflector and five ex-core instrumentation channels.

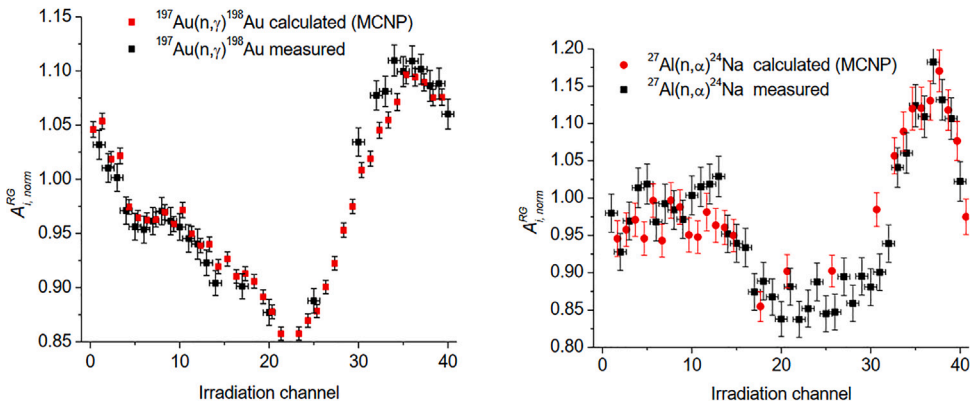

Fig. 11. Calculated and measured Au(n, γ) and Al(n, α) reaction rates in the carousel facility, normalized to the average over all considered measuring positions in the carousel facility. The Y error bars represent 1σ uncertainty in measured or calculated results. The X error bars represent the uncertainty in the irradiation channel position during the experiment (Snoj et al., 2016).

Swap and the Rod Insertion methods. A comparison of the experimentally measured values with those obtained from numerical simulation by the Monte Carlo method is performed with differences analyzed and uncertainties estimated (Merljak et al., 2014). As seen from Fig. 12 the simulation of control rod worth measurement by the rod-swap method yields results that are qualitatively and quantitatively comparable to the experimental values.

3.1.2.2. Power peaking factors.

Modern neutron transport codes (e.g. MCNP (Goorley et al., 2013), Serpent-2 (Leppänen et al., 2015), RAPID (Walters et al., 2018)) allow calculation of the power distribution in 3D geometry assuming detailed geometry without unit-cell homogenization. The power distribution (and its maximum value — the peaking) can be calculated in a 'point-wise' fashion with a spatial resolution of approximately 1 mm. The detailed power distribution was calculated using MCNP (Goorley et al., 2013) for the JSI TRIGA reactor, assuming various realistic and hypothetical core-loading patterns with focus on the mixed cores (Snoj and Ravnik, 2008). Combinations of 8.5 w/o, 12 w/o, 20 w/o and 30 w/o low-enriched (20% ^{235}U) fresh TRIGA fuel elements were systematically treated in the mixed cores. The power peaking factor value and position strongly depends on the core configuration. Power peakings are usually found in fuel elements with higher uranium content especially if they are inserted near the core center. The results are conservative and can be applied in planning realistic mixed core-loading patterns. Power peakings, calculated with both Monte-Carlo MCNP (Goorley et al., 2013) and deterministic TRIGLAV (Peršič et al., 2017) code are presented in Fig. 13.

It is clearly seen in Fig. 13 that the highest power density is at the periphery of a fuel element, as the flux of thermal neutrons arising from water decreases rapidly inside the fuel region. If 12 w/o fuel elements or 20 w/o fuel elements are inserted in the core, the radial power density peak location in most cases coincides with the location

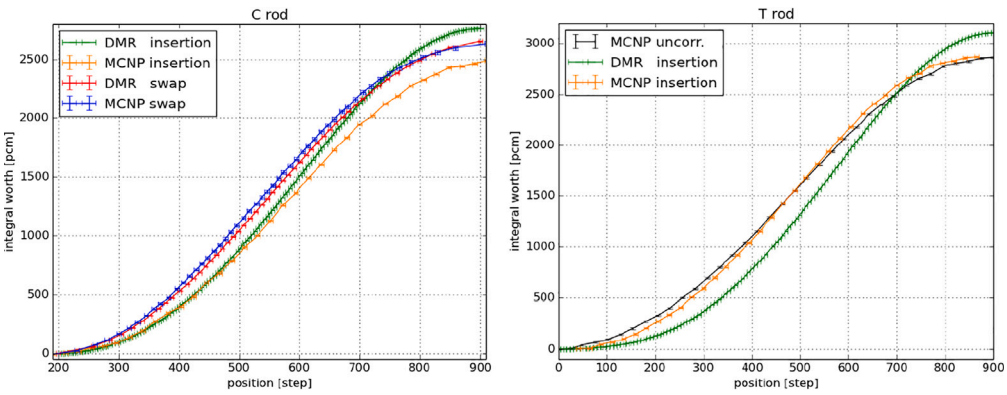

Fig. 12. Integral reactivity worth curves for the Compensating (C) rod (left) and Transient (T) rod (right). "DMR" stands for measurements done using Digital Meter of Reactivity (Trkov et al., 1992; Lengar et al., 2012) and "MCNP" stands for calculations done using the MCNP code (Goorley et al., 2013). Also, a curve uncorrected for initial insertion depth and total travel length is plotted to illustrate the magnitude of the correction.

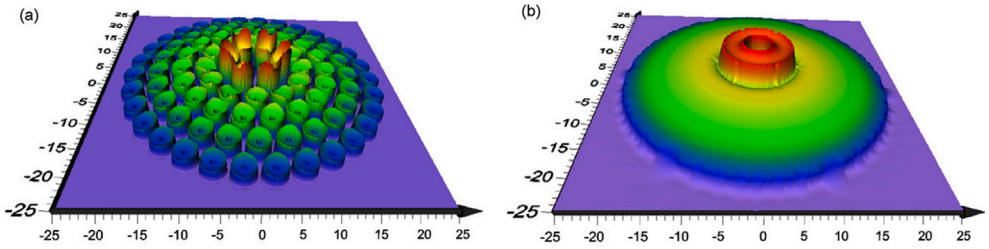

Fig. 13. Relative power distributions (relative units) of 8.5 w/o fuel element core with 6 20 w/o fuel elements in B ring calculated with MCNP (a) and TRIGLAV (b) code. Numbers on x- and y-axis represent the distance from the center of the core in centimeters. Due to homogenization in the TRIGLAV code, power distribution in the unit-cell cannot be determined.

of the hot rod peak, while in case 30 w/o fuel elements are used, the radial power density peak location is always found in the 30 w/o fuel elements. Due to homogenization in the TRIGLAV code, power distribution in the unit-cell cannot be determined.

3.1.2.3. TRIGA kinetic parameters.

Modern Monte Carlo transport codes in combination with fast computer clusters enable very accurate calculations of the most important reactor kinetic parameters. Such are the effective delayed neutron fraction, β_{eff}, and mean neutron generation time, Λ. We calculated β_{eff} and Λ for various realistic and hypothetical annular TRIGA Mark II cores with different types and amounts of fuel (Snoj et al., 2010). It is observed that the effective delayed neutron fraction strongly depends on the number of fuel elements in the core or on the core size. β_{eff} varies for 12 wt% uranium standard fuel with 20% enrichment from 0.0080 for a small core (43 fuel elements, subcritical core) to 0.0070 for a full core (90 fuel elements, supercritical core). It is found that calculated value of β_{eff} strongly depends also on the nuclear data set used in calculations. The prompt neutron lifetime mainly depends on the amount (due to either content or enrichment) of ^{235}U in the fuel as it is approximately inversely proportional to the average absorption cross-section. It varies from 28 μs for 30 wt% uranium fuel to 48 μ s for 8.5 wt% uranium fuel.

The reported values of mean neutron generation time for 12 w/o fuel range from 32 μs to 53 μs, depending on the reflector type. The realistic value for the JSI TRIGA core is probably somewhere in between. Looking at the values of 35 μs for a water reflected core and 53 μs for a graphite reflected core, we could speculate that in case of the benchmark core (Snoj et al., 2016), which is surrounded first by 5–10 cm (E and F rings, see Fig. 4) of water and then by the graphite reflector, the true value of the mean generation time would lie somewhere in between the two values, that is around 40 μs. Our value of 42 μs agrees well with the pulse experiments performed at JSI TRIGA after reconstruction in 1991 (Mele et al., 1994b,a; Ravnik, 1997; Ravnik et al., 1990, indicating that our calculations are correct. Our ratio between β_{eff} and Λ (1.79 ± 0.04)×10^{-4} μs^{-1} is also in good agreement (within the uncertainty) with the experimental values (1.71 and 1.75 μs^{-1}). Thus we can conclude that our method can properly calculate β_{eff} and Λ and can be used in kinetics and reactivity analysis of TRIGA reactors. The calculations of kinetic parameters were further experimentally verified (Filliatre et al., 2015) by neutron noise measurements using an Agilent spectrometer. The experimental values for both β_{eff} and Λ parameters agree with the calculated values.

3.1.2.4. Hydrogen moderation ratio.

In the TRIGA Mark II research reactor, neutron moderation occurs by elastic scattering on ^{1}H in two different materials: the TRIGA fuel (U-ZrH mixture) and the surrounding water. We were interested in the fraction of total moderation that occurs in the fuel elements as it becomes important due to fuel temperature changes (e.g. during pulse experiments) (Švajger et al., 2023). The fraction of total moderation in TRIGA fuel was determined by simulations with the Serpent-2 Monte Carlo particle transport code (Leppänen et al., 2015) using different tallies. We tallied the total number of elastic scattering events (MT2 in ENDF terminology) on H in the fuel (U-ZrH) and water (H_2O). It was determined that 44% of all scattering events occur in the fuel region. In order to further understand the moderation process in the TRIGA reactor, particle histories immediately before fission were analyzed. Previously, all occurring moderation events (elastic scattering on hydrogen) were tallied, not taking into account that not all scatterings result in equal energy loss or probability of fission occurring afterwards. Consequently, a different approach was taken, where scattering events which occur right before the fission process were analyzed by determining the material (fuel, water) on which the scattering events occur. The scattering ratio for individual scattering events before the occurrence of fission was determined using the PTRAC option in the MCNP Monte Carlo neutron transport code, where all neutron events are recorded, and the results are presented in Fig. 14.

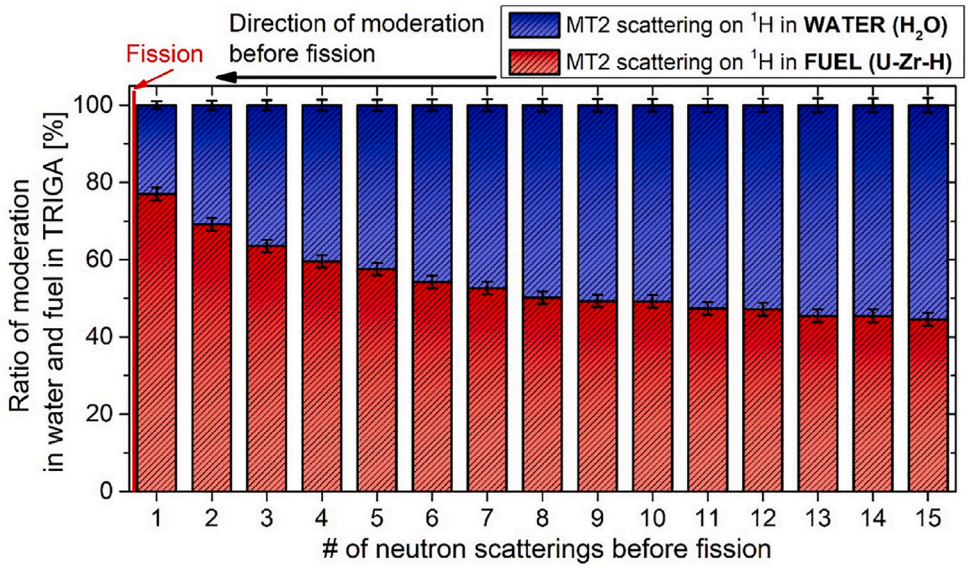

Fig. 14. Ratio of elastic scatterings (MT2 ENDF's reaction type) in water (H_2O) and TRIGA's fuel (U-ZrH) as a function of number of scatterings before the occurrence of fission (#1 representing the last scattering before fission, and #5 fifth scattering before fission). The 1 σ statistical uncertainty for all values is below 3% and is presented with error bars (Švajger et al., 2023).

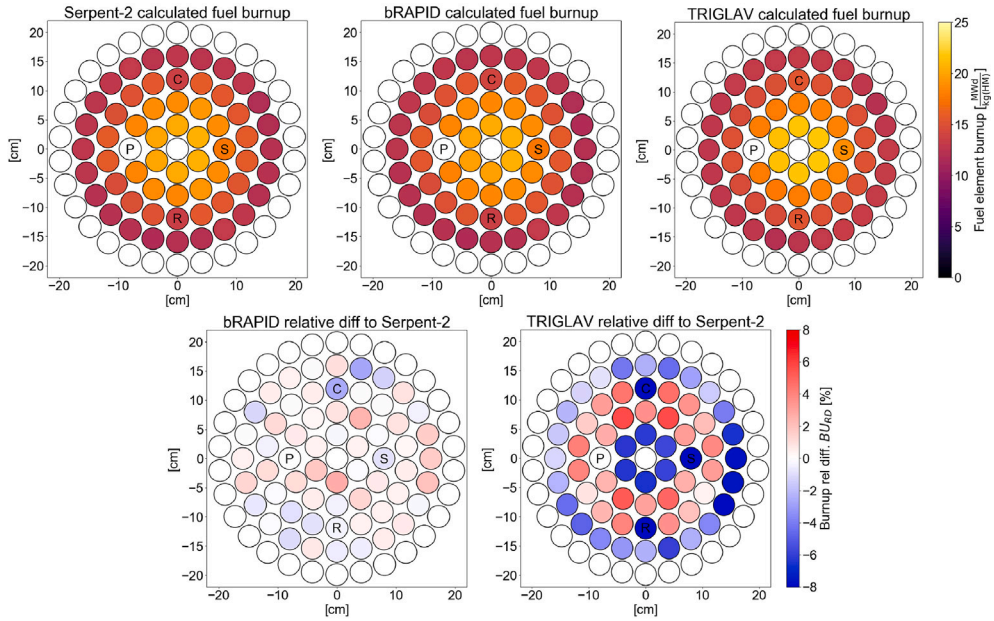

Fig. 15. Top three figures: 2D fuel element burnup profile for JSI TRIGA core configuration 239, obtained with three different codes Serpent-2, bRAPID and TRIGLAV (from left to right). Bottom two figures: relative differences between the calculated fuel element burnup using bRAPID and TRIGLAV compared to Serpent-2. It should be noted that Serpent-2 and RAPID are capable of 3D fuel burnup, the axial average was used for the comparison of the 2D profiles. Pungerčič et al. (2023b).

3.1.2.5. Fuel depletion effects.

The fuel burnup of the JSI TRIGA Mark II reactor at present was determined by taking into account the complete operational history (almost 60 years of operation) (Pungerčič et al., 2020). Burnup is determined from the energy released during reactor operation. Therefore, each reactor start-up and shut-down sequence accounted for in the reactor logbooks was analyzed. In total, 51 logbooks or approximately 21 000 pages were analyzed. Our goal was to digitalize all the needed parameters for future depletion calculations. The energy released can be calculated from the reactor power level, date and time of both reactor start-up and shut-down or power change. Using the reactor operation data, the annual released energy in the reactor core was obtained, as was presented in Section 1 of this paper, depicted in Fig. 1.

Another important part of the determination of fuel burnup is the fuel shuffling history. Throughout the history, the fuel element positions in the core have been changed several times. To acquire the positions, all core configurations (in total 240) were analyzed and digitalized so their loading patterns could be used in the depletion calculations or for other activities. The last part of the operational history analysis was to record all the excess reactivity measurements. The excess reactivity has been determined regularly every Monday since the start of reactor operation in 1966. As these changes can be used to validate depletion calculations, we have decided to analyze all 2000 measurements performed in the complete operational history.

In the past at the JSI TRIGA, multiple depletion calculations and measurements have been performed (Ravnik et al., 1999; Zagar and Ravnik, 1996; Jeraj et al., 2002; Peršič et al., 2000). Measurements

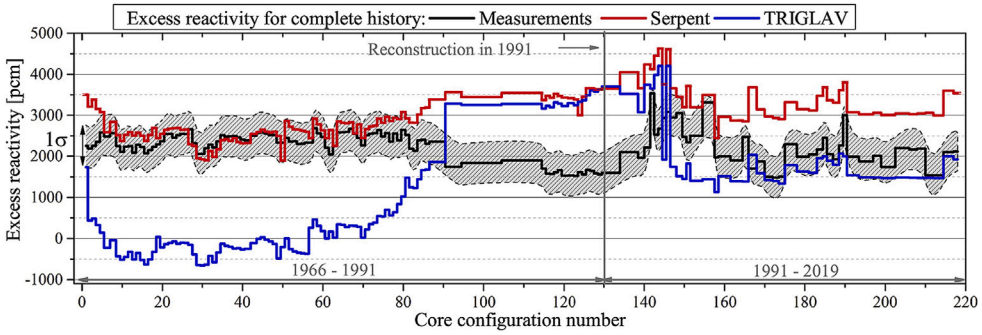

Fig. 16. Excess reactivity at the beginning of each core configuration for the JSI TRIGA reactor (top graph). Measurements and results of complete operational history simulation using the Serpent and TRIGLAV codes are presented. The excess reactivities for benchmark core configuration No. 132 (not included in the graph) determined with both codes agree within 1σ. Pungerčič et al. (2020).

were performed using the fuel element reactivity worth method (Ravnik et al., 1992b). depletion calculations for the JSI TRIGA reactor were performed using only part of the operational history with simplified operational data; this was done because the operational history analysis was not available. Burnup was calculated with deterministic codes, such as the in-house developed TRIGLAV code (Jeraj et al., 2002; Peršič et al., 2017). With the obtained operation history data, the complete history was simulated and fuel element burnup was obtained in both 2D with the deterministic TRIGLAV (Peršič et al., 2017), 3D Monte-Carlo Serpent-2 (Leppänen et al., 2015), and 3D hybrid RAPID (Pungerčič et al., 2023b). The distribution of fuel burnup among fuel elements for core configuration No. 239 in operation in 2020 is presented in Fig. 15.

The main analysis was the experimental validation of the depletion calculations, which was performed using the obtained excess reactivity measurements throughout the whole history. The comparison between measurements of excess reactivity performed at the beginning of each core configuration and calculations of the excess reactivity performed using TRIGLAV and Serpent-2 is presented in Fig. 16. For the measurements, a 1σ uncertainty of 500 pcm is assumed, as the same uncertainty was determined for the benchmark core configuration (Snoj et al., 2016). This uncertainty is underestimated for individual absolute measurements but overestimated for relative changes on the same core configuration. Thus, we have focused our results on the shape of the burnup curve rather than absolute results. Very good agreement between Serpent and the measurements is observed for the first 80 core configurations and relatively good for the rest. Almost all values are within the 1 σ uncertainty. The differences after core No. 80 can be explained by the introduction of older fuel elements in 1992 with poorly known burnup.

The second experimental validation was performed by repeating the fuel element reactivity worth experiment, as was already done in the past (Ravnik et al., 1992b). The fuel reactivity worth, compared to the reference fuel element in one of the positions in C-ring (see Fig. 4) of the TRIGA core, change in core reactivity $\Delta\rho_{\mathrm{worth}}$ for seven JSI TRIGA fuel elements was measured. The fuel elements were chosen such that their burnups differed in the range of 1–20 MWd/kg. The measured $\Delta\rho_{\mathrm{worth}}$ reactivity change was simulated using the RAPID, Serpent-2, and TRIGLAV neutron transport codes. Good agreement between measured and calculated fuel element reactivity worth can be observed for the RAPID and Serpent-2. For all seven fuel elements, the calculated values using Serpent-2 and RAPID agree with the measured values within their 1σ uncertainties. This indicates that both the burnup of individual fuel elements and simulation of small reactivity changes in the JSI TRIGA core are calculated accurately. Discrepancies between measured and calculated fuel element reactivity worth are observed for the TRIGLAV code system, especially for the fuel elements with higher $\Delta\rho_{\mathrm{worth}}$ value. The results also indicate that the methodology of simulating the complete operating history of the JSI TRIGA reactor, presented in Pungerčič et al. (2020), is accurate (see Fig. 17).

3.1.3. Pulse experiments

Theoretical models of the reactor response during pulse operation were validated with experimental data from the JSI TRIGA Mark II research reactor. The data from all pulse experiments since 1991 have been collected, analyzed and are publicly available in Švajger et al. (2023) and Švajger and Snoj (2021). This paper summarizes the validation study, which focuses on the comparison between experimental values, theoretical predictions (Fuchs–Hansen and Nordheim–Fuchs models) and calculations using a JSI-developed program named Improved Pulse Model (Vavtar and Snoj, 2019; Vavtar et al., 2020). The results show that the Improved Pulse Model predicts the reactor power behavior more accurately compared to the theoretical models. The theoretical models predict a higher maximum power but a lower total released energy, a shorter pulse width at half maximum as well as a shorter time at which the maximum power is reached (Švajger and Snoj, 2020).

We evaluated the uncertainties in the pulse physical parameters (maximum power, total released energy and full width at half maximum) due to uncertainties in the reactor physical parameters (inserted reactivity, delayed neutron fraction, prompt neutron lifetime and effective temperature reactivity coefficient of the fuel). It was shown that assuming an overestimated correlation between the reactor physical parameters does not significantly affect the estimated uncertainties in the pulse physical parameters (Švajger et al., 2020). The relative uncertainties of the pulse physical parameters decrease with increasing inserted reactivity. If all reactor physical parameters feature an uncorrelated uncertainty of 10 % the estimated total uncertainty in peak pulse power at an inserted reactivity of 3 $ (effective delayed neutron fraction — β_{eff}) is 59 %, where significant contributions come from uncertainties in the prompt neutron lifetime and effective temperature reactivity coefficient of fuel. In addition, we analyzed the contribution of two physical mechanisms (Doppler broadening of resonances and neutron spectrum shift) that contribute to the temperature reactivity coefficient of the fuel. The Doppler effect contributes about 30 % to 15 % while the rest is due to the thermal spectrum hardening in a temperature range between 300 K and 800 K.

3.1.4. Digital meter of reactivity

During refueling outages in nuclear power plants, part of the nuclear fuel is replaced, which has a significant impact on the reactor properties. The parameters of the new reactor core are determined by nuclear design calculations and must be verified experimentally before normal reactor operation resumes. A reactivity measurement device is required to accurately determine these properties during an NPP start-up.

A digital meter of reactivity (DMR), which was developed in the 1980s at the Reactor Physics Department at the JSI has been in use for real-time measurements of reactivity in research and power reactor cores (Trkov et al., 1992). The development of the DMR was based on measurements at the JSI TRIGA reactor, the DMR enabled reactivity measurements under a wide range of operating conditions.

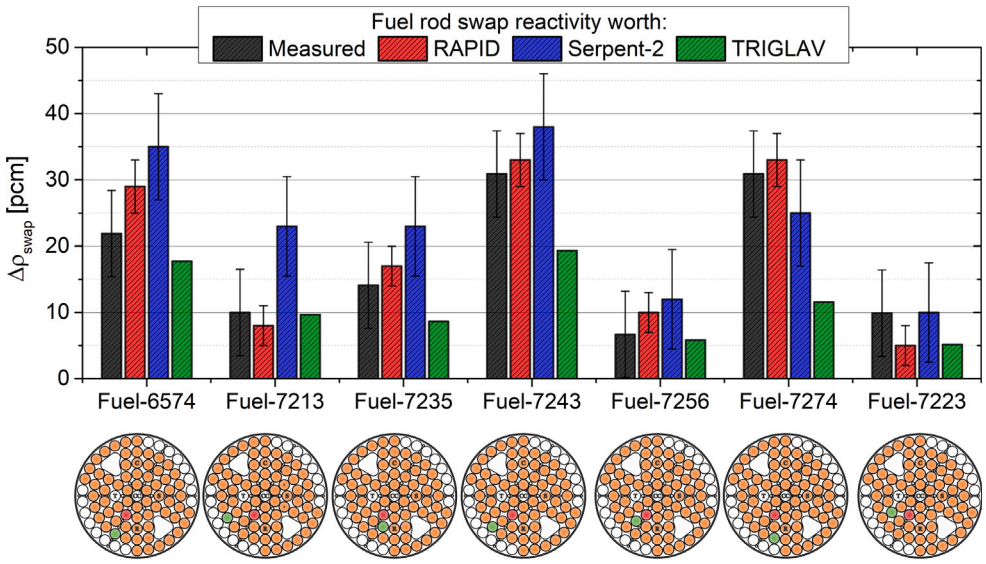

Fig. 17. Comparison of measured $\Delta\rho_{\mathrm{worth},i}$ during the fuel reactivity worth experiment and simulations of the experiment using three different neutron transport and depletion codes (RAPID, Serpent-2 and TRIGLAV). On the x-axis the position of fuel elements in the core during last 20 years of reactor operation is highlighted in *green*. The reference position C2 is highlighted in *red*. $\Delta\rho_{\mathrm{worth},i}$ is proportional to the difference in fuel burnup between the reference fuel element and the measured one.

The input signals for the DMR are the current signal, which is assumed proportional to the neutron flux (and reactor power), obtained from boron-lined ionization chamber(s) or other detector types, and the signal representing the temperature of the core (Lengar et al., 2012). The output is the value for the reactivity ρ, presented in real-time. Before starting the measurements, the reactor kinetic parameters for the specific reactor to be measured are also required as input.

The basis for the calculation of reactivity is the recurrence relation for numerical integration in solving the inverse reactor point-kinetics equations in the DMR, but several practical problems related to signal processing have to be solved in order to achieve a device that can be used and provide meaningful results. The strength of the DMR compared to some other reactivity meters is its ability to provide correct results for ρ in a very broad range of reactor operating conditions that include the following:

- operation at low power, where the neutron flux is dominated by the source term,
- in a deeply subcritical reactor,
- during measurements of transients,
- during redistribution effects of the neutron flux due to control bank movements.

Special solutions had to be implemented in order to cover the described cases.

The measurement of reactivity in a deeply subcritical reactor enables the DMR to determine the integral and differential reactivity worth of control rods during their insertion into the core. This new method has been termed the "Rod Insertion Method" and makes full use of the special features available in the DMR. It is used for bank-worth measurements, during which a control bank is inserted into the core with the control rod drive mechanism at normal speed. No reactivity compensation is required; thus, the method is much faster than other available methods (Trkov et al., 1995) and is described in more detail in Section 3.1.5. The DMR is also used for other measurements during start-up tests, e.g. for the determination of the isothermal temperature coefficient. It enables the data to be evaluated very quickly and the results to be available shortly after the measurement.

The method is constantly being improved by measurements on the TRIGA reactor, which enables various test arrangements. As part of our studies, four fission chambers were used to determine the flux signal instead of a single ionization chamber (Lengar et al., 2016). The DMR is used at the TRIGA reactor for staff training during the preparation for start-up physics tests at the Krško Nuclear Power Plant (NPP).

3.1.5. Rod insertion method

The Rod Insertion Method is a fast, effective and accurate method for determining the reactivity worth of control rods in a nuclear reactor, also yielding their integral and differential reactivity worth curves. It is applicable to both research and power reactors. The method was first developed at the JSI TRIGA reactor in late 1980s (Čopič, 1976; Glumac and Škraba, 1989; Trkov et al., 1992, 1995; Trkov and Ravnik, 1995) and implemented at the Krško NPP, which was the first power plant to use it as the primary control rod worth measurement method. The method has been used routinely during the start-up tests at the Krško NPP since 1989; it shortened the time required for the tests from a couple of days to 12 h (Glumac and Škraba, 1989). After the successful implementation in Krško NPP, the Rod Insertion Method was adopted by others and is used today in several power plants around the world (Chao et al., 1992). A comprehensive historic overview is given in Merljak et al. (2018b), Merljak (2018).

The experimental part of the Rod Insertion Method is quite straightforward. The measurement is started from a critical configuration, the control rod is inserted at its maximum but constant insertion speed, and the flux signal from a neutron detector is recorded. At the fully inserted position a waiting time of some 30 s to 45 s is required, then the control rod is withdrawn. This experimental sequence and the corresponding neutron flux and reactivity signals are illustrated in Fig. 18.

The simplicity of execution is complemented with a necessity of simulation-based post-processing of measured signals. If the correction for the difference between the dynamic and static reactivity is implemented, the Rod Insertion Method yields quantitatively and qualitatively the same results as the historic standard method of boration-dilution (deviation $\lesssim |\pm 3\%|$) (Merljak et al., 2018b; Merljak, 2018), but the measurements are performed more than an order of magnitude faster.

Recent research and development of the Rod Insertion Method include (among others (Merljak et al., 2014, 2016)) combining simultaneous measurements from multiple detectors (Lengar et al., 2016), using not only ex-core detectors but also miniature in-core fission chamber detectors (Merljak et al., 2017b), time-dependent stochastic simulation (Valtavirta et al., 2018), compensation of the so-called reactivity overshoot (Merljak et al., 2018b,a), and a 3D stochastic

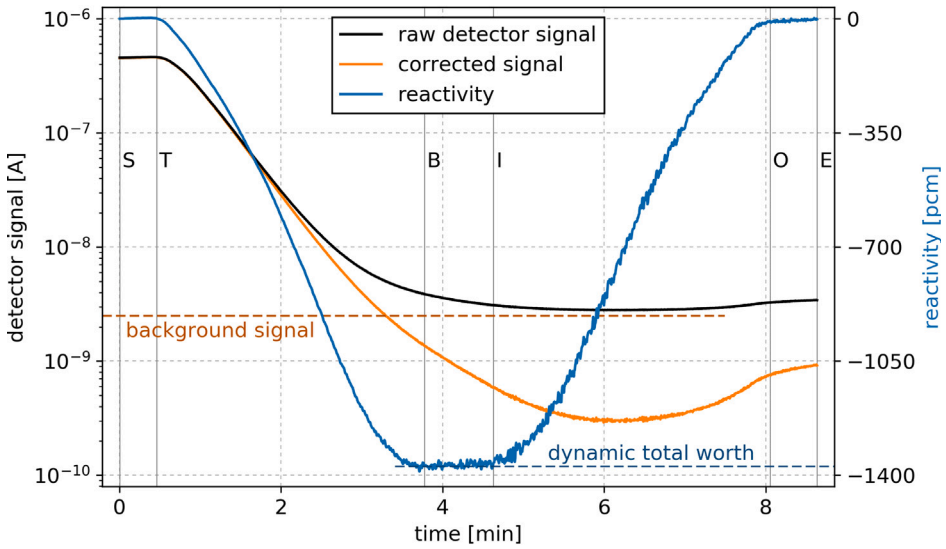

Fig. 18. Rod Insertion Method sequence with the corresponding neutron flux signal and reactivity — an example for the Krško NPP. The first and last of the "S, T, B, I, O, E" labels indicate the *start* and the *end* of the experimental procedure, while the other four correspond to the control rod bank position: *top*, *bottom*, *in* and *out*. Note how the usable (raw − background = corrected) neutron signal is almost "drowned" in the background even before the control rod bank has reached its fully inserted state.

approach to determine factors to compensate for the flux redistribution effect (Goričanec et al., 2023).

Furthermore, the Rod Insertion Method was studied by comparing the static and dynamic reactivity (Merljak et al., 2016) of the TRIGA reactor. The dynamic-to-static conversion factors were calculated using the GNOMER code (Trkov and Merljak, 1994; Merljak et al., 2017a). The TRIGA kinetic parameters during the Rod Insertion Method were further studied using the RAPID (Walters et al., 2018) code system with its tRAPID (Mascolino and Haghighat, 2024) kinetic algorithm, which has the ability to perform 3D kinetic parameter simulations. An experimental campaign was conducted in 2019 in which the response of four differently placed fission chambers (FC) was measured during a rod insertion experiment. All the experimental results and the simulations are presented in Mascolino et al. (2024), Mascolino (2021). The tRAPID simulation was performed to determine detector responses (FCs) at all times during the transient. The positions of the FCs and comparison of experimentally measured and tRAPID calculated response is shown in Fig. 19.

The validation of tRAPID using the JSI TRIGA reactor not only demonstrates the accuracy and effectiveness of using the RAPID Code System for simulating neutron kinetics problems, but also acts as a demonstration for the potential application of RAPID for the JSI TRIGA core monitoring and control. A tool like tRAPID, in fact, would enable on-line simulations of reactor transients, such as pulses or rod insertions, in support of experiments at research reactors, allowing for on-the-fly reassessment of flux redistribution factors based on the reactor configuration (Merljak et al., 2018b). Additional information about tRAPID's development and validation efforts using the JSI TRIGA reactor are included in Section 5.7.

3.2. Radiation physics

The role of JSI TRIGA reactor in radiation physics and nuclear instrumentation is an example of a profound synergy between theoretical innovation and experimental validation. This section highlights this integration by detailing the reactor's contributions to the characterization of the radiation field and to the development, testing and qualification of nuclear detectors. As a well characterized reactor, JSI TRIGA enables diverse experiments using a variety of detectors and instrumentation to study the intricacies of nuclear phenomena. This comprehensive approach not only improves our understanding of radiation interactions, but also drives the development of detector technology by combining computational simulations with empirical data to refine our methods and models in nuclear science.

3.2.1. Radiation field characterization

The radiation field characterization within the TRIGA reactor is a cornerstone of nuclear physics research. The focus is on the precise measurement and comprehensive analysis of the gamma-ray and neutron fields inside the reactor core, using advanced detectors and simulation tools. Through rigorous experimental protocols and detailed simulations, this work achieves a high degree of accuracy in dose measurement, which is essential for validating nuclear models and improving reactor safety. The thorough approach to characterizing radiation fields is an example of the reactor's ability to support sophisticated investigations and contributes significantly to our understanding of radiation dynamics and its practical applications.

3.2.1.1. Unfolding — dosimetry.

Reference neutron fields in irradiation facilities are crucial for experimental research work in nuclear science and technology in general, and at the fundamental level for the measurement of neutron cross sections and validation of evaluated cross-section data. Monte Carlo particle transport techniques in conjunction with state-of-the-art nuclear data libraries are becoming the reference in the broad context of nuclear reactor analysis, and are extensively used for detailed computational characterization of irradiation facilities, including the calculation of neutron spectra. However, adjustment of the neutron spectra based on experimental data is still required. The characterization of the neutron spectra in the three most important irradiation channels of the JSI TRIGA reactor with different spectral characteristics was performed (Radulović et al., 2020b), as an important step in developing the experimental capabilities of the reactor for the purpose of nuclear data validation through activation dosimetry measurements. The characterized neutron spectrum in pneumatic tube (PT) irradiation channel of the JSI TRIGA is presented in Fig. 20.

In the first step we performed detailed Monte Carlo calculations of the neutron spectra, comparing the results obtained using different nuclear data libraries. In the second step the JSI developed GRUPINT spectrum adjustment code was employed for the characterization of the neutron spectra, on the basis of the calculated neutron spectra and measured reaction rate ratios using dosimetry measurements. A comprehensive overview of the methodology employed in the code and

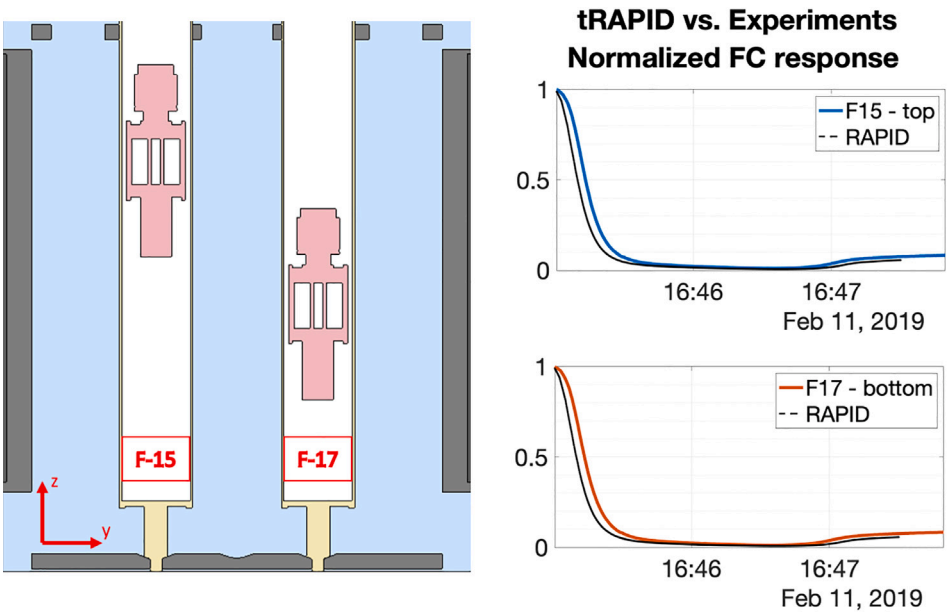

Fig. 19. Left: Axial location of large FCs in the JSI TRIGA Mark-II Serpent model. Right: Comparison of tRAPID-calculated and measured detector responses during the Rod Insertion Method experiments performed at the JSI TRIGA reactor on February 11, 2019 (Mascolino et al., 2024).

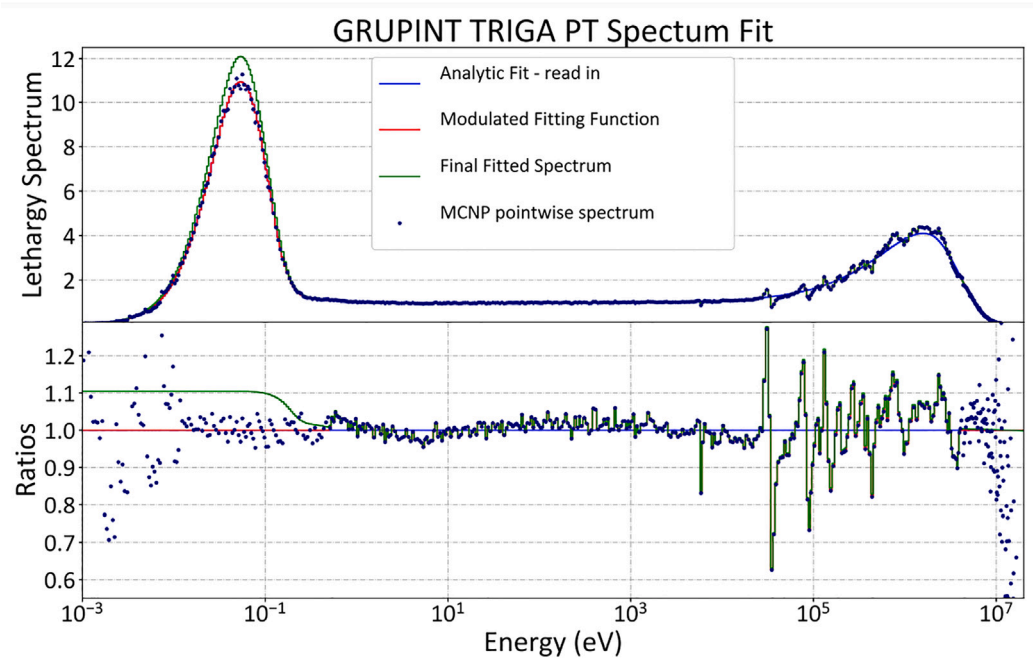

Fig. 20. Characterization of the neutron spectrum in the pneumatic tube. Top graph: Spectrum obtained from Monte Carlo simulation (labeled "MCNP (point-wise)"), fitted analytic function (labeled "Analytic fit - read in"), fitted analytic function multiplied by the form function (labeled "Modulated fitting function") and final result of the adjustment procedure (labeled "Final fitted spectrum"). Bottom graph: ratios of all the spectra vs. the fitted analytic function.

its abilities is given in Radulović et al. (2020b); its use in neutron spectrum unfolding on the basis of measurements with Bonner spheres is presented in Kos et al. (2017). We observe that a positive compensation of up to 10% in the thermal part of the spectrum is needed (as seen in Fig. 20), while no compensation is needed in the epithermal and fast parts.

Absolute neutron flux levels were computed from the adjusted neutron spectra and absolute reaction rate measurements, and compared to the results of a previous analysis using only Monte Carlo calculations. Table 3 from reference (Snoj et al., 2012c) reports the total and 3-group neutron flux levels, with the following energy boundaries: 0–0.625 eV (thermal), 0.625 eV–100 keV (epithermal) and 100 keV–20 MeV (fast). Table 3 also reports the values from the previous computational analysis (Snoj et al., 2012c). The quoted uncertainties in the absolute neutron flux levels derived in this work correspond to the experimental uncertainties of the absolute $^{197}\mathrm{Au}(n,\gamma)$ reaction rates used for normalization. The uncertainties in the values obtained computationally are generally affected by statistical computational uncertainties (which can be reduced to negligible levels), modeling uncertainties and uncertainties in the normalization factor. The uncertainties in the total flux values quoted in our previous computational analysis (Snoj et al., 2012c) correspond to the statistical uncertainties only, the

Table 3
Absolute neutron flux levels (cm^{-2} s^{-1}) and associated uncertainties (%) derived from the spectrum adjustment procedure performed in this work and absolute reaction rate measurements.

	CC, this work	CC, Snoj et al. (2012c)
Total	$1.92 \times 10^{13}(1 \pm 0.024)$	$1.92 \times 10^{13}(1 \pm 0.050)$
Thermal	$5.47 \times 10^{12}(1 \pm 0.024)$	$5.12 \times 10^{12}(1 \pm 0.050)$
Epithermal	$6.47 \times 10^{12}(1 \pm 0.024)$	$6.50 \times 10^{12}(1 \pm 0.050)$
Fast	$7.28 \times 10^{12}(1 \pm 0.024)$	$7.59 \times 10^{12}(1 \pm 0.050)$
	PT, this work	PT, Snoj et al. (2012c)
Total	$6.76 \times 10^{12}(1 \pm 0.023)$	$6.94 \times 10^{12}(1 \pm 0.050)$
Thermal	$3.34 \times 10^{12}(1 \pm 0.023)$	$3.29 \times 10^{12}(1 \pm 0.050)$
Epithermal	$1.73 \times 10^{12}(1 \pm 0.023)$	$1.84 \times 10^{12}(1 \pm 0.050)$
Fast	$1.69 \times 10^{12}(1 \pm 0.023)$	$1.81 \times 10^{12}(1 \pm 0.050)$
	IC40, this work	IC40, Snoj et al. (2012c)
Total	$1.94 \times 10^{12}(1 \pm 0.023)$	$2.09 \times 10^{12}(1 \pm 0.050)$
Thermal	$1.19 \times 10^{12}(1 \pm 0.023)$	$1.26 \times 10^{12}(1 \pm 0.050)$
Epithermal	$4.78 \times 10^{11}(1 \pm 0.023)$	$5.24 \times 10^{11}(1 \pm 0.050)$
Fast	$2.75 \times 10^{11}(1 \pm 0.023)$	$3.03 \times 10^{11}(1 \pm 0.050)$

contribution of other sources was not evaluated. Based on work presented in Radulović et al. (2014) we find that a realistic estimate of the overall uncertainty in the calculated results (including the normalization to the reactor power level) is 5%, which is the level we quote in this work.

The neutron spectrum unfolding for the JSI TRIGA serves as the basis for future experimental and analytical work, in particular extending the scope of the measured capture and threshold dosimetry nuclear reactions, to support a thorough characterization of the neutron spectra in the irradiation channels of the reactor. This effort will enable the JSI TRIGA reactor to support a broad scope of experiments for fundamental research as well as development or testing activities at the highest level.

3.2.1.2. Gamma-rays — TLD dosimeters.

In-core gamma-ray and neutron field measurements have been performed in the core of the JSI TRIGA reactor using TLD dosimeters.

In 2016, TLD400 (CaF_2:Mn) and TLD700 (^{7}LiF:Mg,Ti) obtained from ThemoFischer Scientific were irradiated in a dry in-core irradiation facility in the A-ring (Central channel) and one of the positions in F-ring (see Fig. 4), along with the position in the rotary groove carousel to measure the gamma-ray field dose after reactor shutdown, ranging from 0.02–200 minutes after reactor SCRAM from different power levels (Gruel et al., 2020). Measurements with calibrated fission and ionization chambers were performed in parallel. The TLDs were enclosed within aluminum boxes, in order to measure the absorbed dose in aluminum and provide charged-particle equilibrium. The experiments have been faithfully reproduced by simulations using the JSIR2S code (Ambrožič and Snoj, 2020). Agreement between measured and simulated doses were within their respective uncertainties, as shown in Fig. 21.

Another set of TLD measurements were performed in 2017. A series of MCP-N (^{nat}LiF:Mg, Cu, P) and MCP-7 (^{7}LiF:Mg, Cu, P) TLDs provided by IFJ PAN, Kraków were packaged within polyethylene wraps, and inserted into dry irradiation channels in positions A-ring (Central Channel), one of the positions in F-ring (see Fig. 4), and an irradiation position in the rotary groove carousel (Ambrožič et al., 2020). The dosimeters were irradiated at reactor power between 50 W and 100 kW, during which measurements with calibrated fission and ionization chambers were also performed. The experimental campaign was faithfully modeled for simulation, highlighting large discrepancies between measured and calculated values. The investigation led to the identification of major differences in the TLD readout techniques. Moreover, further experiments were performed by attaching a themocouple to a few of the TLDs irradiated in the reactor core, where temperatures in excess of 100 °C were observed, leading to potential self-annealing of TLDs.

3.2.1.3. Gamma-rays — RadFETs.

The development and the calibration of low cost semiconductor dosimeters based on the Radiation sensitive thick oxide field effect transistors (RadFETs) has been performed at the JSI TRIGA reactor. Here, the threshold voltage changes with the accumulated dose. The detectors are of small size, the accumulated dose can be read out electronically, the detectors can also be electronically annealed.

Dosimeters produced by NÜRDAM, Turkey, were exposed to almost 700 kGy of reactor gamma rays inside the reactor core along with a calibrated ionization chamber. The data obtained from the ionization chamber, along with detailed simulations of both prompt and delayed gamma rays using the MCNP and JSIR2S code served to relate the measured air-kerma dose rates to dose rates in silicon without assuming charged particle equilibrium. The agreement between sets of samples irradiated at different dose-rates with different read-out schemes was found to be very good, and the threshold voltage dependence on the received dose was characterized over the entire absorbed dose range. The sensitivity, dynamic range, as well as the saturation and the breakdown voltage of sensors were investigated. After the irradiation, isothermal annealing was performed at various temperatures, to determine the sensors' response over extended periods of time (Kramberger et al., 2020).

3.2.1.4. Water activation.

In the past, activity analysis of the primary coolant has been performed (Stepišnik et al., 2009). Basic water activation experiments are routinely performed for educational purposes by using a simple open water loop, conveying water activated in the reactor core to a measurement area on the reactor platform (Zohar et al., 2021).

In 2023 the work on a new closed water activation loop called KATANA was started in the JSI TRIGA research reactor, which will serve as a well-defined and stable 6 MeV–7 MeV gamma-ray source. Such a high-energy irradiation facility will allow various experiments based on water activation, e.g. shielding experiments using ITER relevant materials, investigation of the response of detectors to high-energy gamma radiation, investigation of short-lived moving radiation sources, validation of computational fluid activation codes/methods, etc. A schematic and real experimental setup of the KATANA irradiation facility is shown in Fig. 22.

The final design, chosen based on a prior optimization analysis (Kotnik et al., 2023a, 2021, 2022, 2023c), aims to achieve the highest activity while considering both neutronic and hydraulic aspects. The KATANA facility was successfully licensed and commissioned at the end of 2023 when the first test operation began. In February 2024, the KATANA facility demonstrated the desired operating characteristics in terms of water flow rate, as well as neutron and gamma-ray dose rates (Kotnik et al., 2024). In 2024, we will focus on utilizing KATANA and performing benchmark experiments to validate newly developed fluid activation computer codes. The work was carried out in the work package WPPrIO Preparation of ITER Operation within the EUROfusion consortium.

3.2.2. Nuclear instrumentation and detector development, testing and qualification

Decades of work in simulations and measurements in the JSI TRIGA reactor resulted in JSI TRIGA reactor being one of the best characterized research reactors in the world. Well characterized neutron and gamma-ray fields in the experimental locations in the reactor provide the possibility for testing and qualification of nuclear instrumentation detectors and systems. Numerous experimental campaigns took place at the JSI TRIGA reactor using fission and ionization chambers, self-powered neutron detectors, semiconductor neutron detectors, Cherenkov light detectors, an autonomous robot and a small submarine device. Some of the experimental campaigns are presented in the following sub-sections, however it must be pointed out that scope of experimental utilization of the JSI TRIGA reactor is wide and

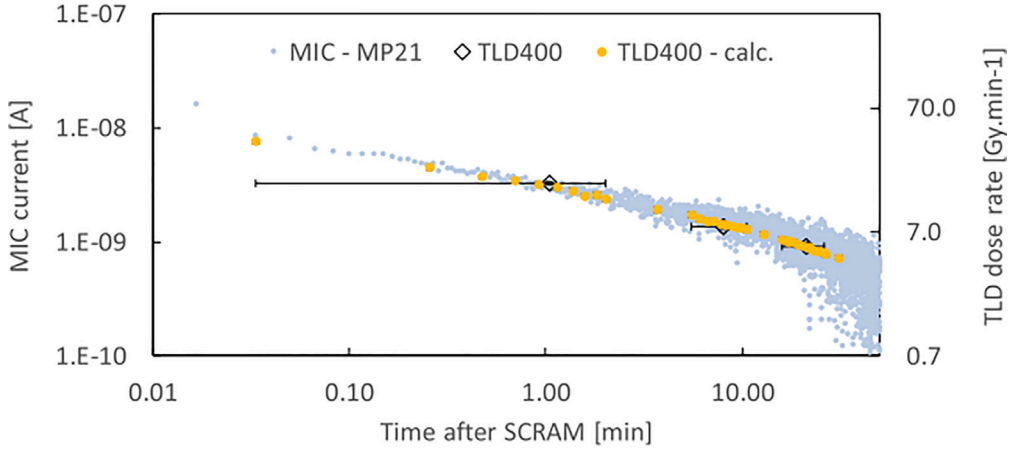

Fig. 21. Comparison of dose rates measured by TLD 400 and the miniature ionization chamber (MIC), compared to calculated dose rates using the JSIR2S code.

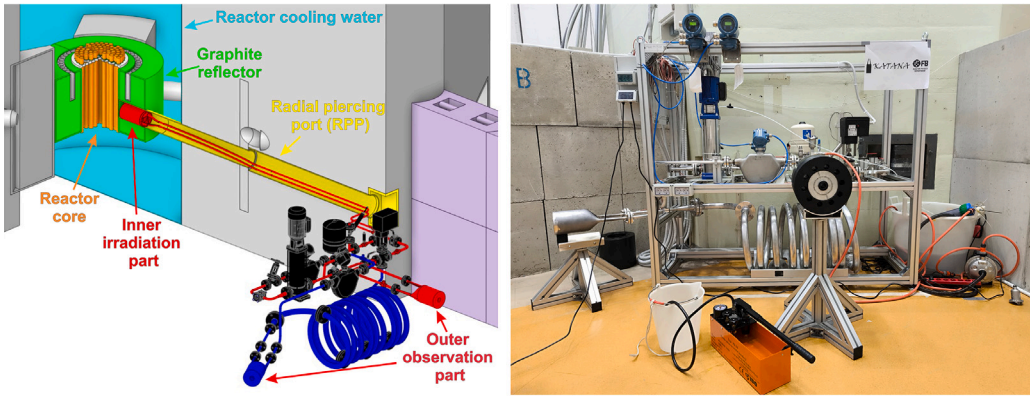

Fig. 22. Schematic (left) and experimental setup (right) of the KATANA irradiation facility at JSI TRIGA reactor that utilizes a closed-water activation loop.

not all experimental campaigns are mentioned in this paper, one of the reasons being constraints and proprietary information related to some of the industrial applications. The experimental campaigns were well supported with calculations usually performed with the MCNP code (Goorley et al., 2013) using a verified and validated computational model of the JSI TRIGA reactor, based on the criticality model (Jeraj and Ravnik, 1999). In the preparation of the experimental campaigns, preliminary calculations are usually performed in order to determine the experimental conditions, and later final calculations are performed to support the measurements. For the individual experiments, explicitly modeled experimental setups including detectors are added to the benchmark model (Jeraj and Ravnik, 1999) to match the experimental conditions as accurately as possible.

3.2.2.1. Fission and ionization chambers.

Since 2010, numerous experiments, including neutron spectrum characterization, in-core flux mapping using ionization chambers and various fission chambers (^{235}U, ^{238}U, ^{237}Np and ^{242}Pu) have been conducted in collaboration with Commissariat à l'Énergie Atomique et aux Énergies Alternatives (CEA) Cadarache (Snoj et al., 2011b; Štancar et al., 2012; Žerovnik et al., 2013; Barbot et al., 2013; Žerovnik et al., 2014b; Kaiba et al., 2015; Radulović et al., 2015; Žerovnik et al., 2015; Goričanec et al., 2018; Štancar et al., 2018). These experiments aimed at both assessing the neutron and gamma-ray measurement methods and equipment and utilizing the gathered data to verify and validate the computational model of the JSI TRIGA reactor. Utilizing miniature fission chambers developed by CEA (Geslot et al., 2009) and a pneumatic positioning system developed by JSI (Štancar et al., 2012) has enabled the precise measurement of axial and radial fission rate profiles, with a typical spatial resolution of 10 mm and an accuracy of 0.2 mm. This stands in contrast to traditional reaction rate measurements in irradiation channels, which provide information on flux profiles on a single plane. Significant advantage of this system lies in its capability to fully characterize the neutron and gamma-ray profiles in three dimensions. Fig. 23 presents measured and calculated axial profiles of fission rates in one of the experimental campaigns using CEA designed miniature fission chambers. Several experimental campaigns using miniature fission and ionization chambers included measurements with a single detector within the reactor core, measurements with multiple in-core detectors in different measuring positions, fission chambers covered with different neutron shields sensitive to different energy ranges in the neutron spectrum, etc. In the experimental campaigns, measurements were performed at different power levels, from low reactor power, of the order of 1 W, to full reactor power, 250 kW.

Our work on the characterization of the in-core and ex-core irradiation facilities of the JSI TRIGA research reactor has gained the interest of commercial manufacturers of nuclear instrumentation detectors and has resulted in several contracts for detector testing and qualification activities.

3.2.2.2. Self-powered neutron detectors.

The DISCOMS project (DIstributed Sensing for COrium Monitoring and Safety) (Ferdinand et al.; Barbot et al., 2018), carried out by the CEA and other partners between 2014 and 2018, was part of the French National Research Agency (ANR) Post-Fukushima projects related to nuclear safety. The project aimed at developing new instrumentation based on Optical Fiber Sensors and Self Powered Neuron Detectors (SPNDs) for corium monitoring in case of a severe accident in a nuclear

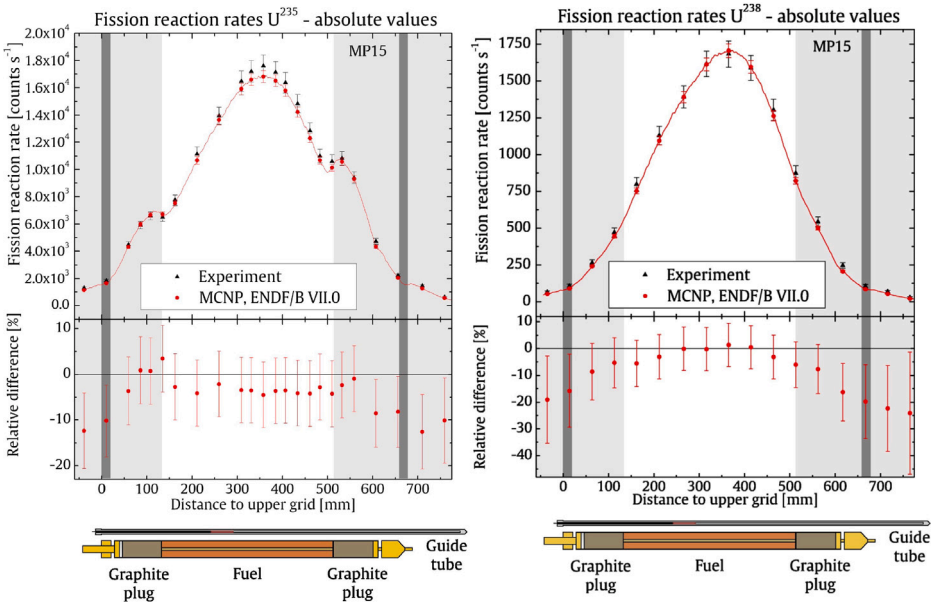

Fig. 23. Experimental and calculated axial fission rate profiles (absolute values) in measurement position MP15 in the core of the JSI TRIGA Mark II reactor. The profiles represent the data collected with ^{235}U (left) and ^{238}U (right) CEA designed miniature fission chambers (Štancar et al., 2018).

reactor. For this purpose, an SPND and thermocouple instrumented sensor was co-developed by CEA and the THERMOCOAX company and tested in the mixed neutron and gamma-ray field in the JSI TRIGA research reactor (Radulović et al., 2018a). In order to ensure accurate centering of the DISCOMS sensor during the irradiations, two centering elements have been designed and manufactured by the JSI workshop. Both elements consist of an aluminum tube with an inside diameter of 13 mm into which the DISCOMS sensor is inserted. The DISCOMS sensors were irradiated inside thermal column, in one of the fuel element positions in F ring and in central channel (A ring). In different measuring positions, the neutron spectrum has different degrees of thermalization and different ratios of the total neutron vs. total gamma-ray. Measurements were performed in different power levels from low reactor powers (50 mW) to full reactor power (250 kW), and allowed for the qualification of the response of the neutron and gamma-ray detectors.

3.2.2.3. Semiconductor neutron detectors.

With the aim of improving border and port security, the NATO Science for Peace and Security programme funded the research project "Engineering Silicon Carbide for Border and Port Security" (E-SiCure) in 2016, in which prototypes of radiation-resistant detectors based on silicon carbide (SiC) for detecting special nuclear materials (SNM) were developed. The detector prototypes were made with SiC Schottky barrier diodes (SBDs) and neutron converter films. In the first few experimental test campaigns carried out in the TRIGA reactor of the Jožef Stefan Institute (JSI) numerous SiC detector prototypes equipped with B and LiF converter layers were subjected to irradiation in the reactor's dry chamber (Radulović et al., 2020c,a). The SiC detector prototype and its components can be seen in Fig. 24 (left), as well as a prototype detector set up in a vacuum chamber in the TRIGA reactor dry chamber — Fig. 24 (right). The SiC prototype detectors showed a recognizable signal due to neutron reactions that exhibits a linear correlation with the neutron flux. The pulse-height spectra obtained from the SiC detectors (see Fig. 25) show features that can be attributed to the nature and energy of the secondary particles that are produced in the nuclear reactions with B and Li isotopes.

The detectors with active volumes 1 mm × 1 mm × 25 μm, 1 mm × 1 mm × 69 μm and 1 mm × 1 mm × 170 μm showed sensitivity of about 2×10^{-5} counts per second per unit of neutron flux [s^{-1} / $cm^{-2}s^{-1}$] (for neutron energies from 0 to 5 eV). The scaling analysis of the SiC detection sensitivity to an active area of e.g. 20 cm^2 showed their response to be comparable to large B or ^{3}He detectors and theoretically resulted in a total sensitivity of about 2 s^{-1}/ $cm^{-2}s^{-1}$ (Radulović et al., 2020c; Coutinho et al., 2021).

In the E-SiCure2 project, the prototype of the SiC detector was further tested and optimized. New development work was carried out on pixelated SiC SBDs and the larger SBDs, scaled up to an area of 5 mm × 5 mm (Bernat et al., 2023). In addition, new fast neutron converters were tested to extend the capabilities of the SiC detector to detect not only thermal neutrons (Žohar et al., 2021). The experimental results obtained did not confirm the contribution of the converter to fast neutron detection, however an intrinsic response of the SiC detector to fast neutrons was observed (Žiber and Radulović, 2022), consistent with the literature. The extensive irradiation tests of the SiC SBDs and the SiC prototype detector in the JSI TRIGA reactor have contributed to a better understanding of the SiC material, which has proven to be promising for the production of solid-state detectors as it is resistant to harsh environment conditions (including high temperatures and radiation fields) and has excellent electronic properties compared to other semiconductors.

3.2.2.4. Cherenkov light detectors.

The development of a Cherenkov light-based power measurement system for the JSI TRIGA reactor began with a simple idea: the intensity of the Cherenkov light is, in principle, linearly dependent on the power of the reactor in operation. The Cherenkov light intensity measurement system consists of four components: a radiator, a light guide, a detector, and a data acquisition system. Peric et al. (2023). Its implementation can be seen in Fig. 26. A closed aluminum tube, inserted in the reactor core periphery was used as the basis of the Cherenkov power meter. A small volume of water at the bottom of the tube at the reactor core level served as the source of Cherenkov light. Part of the emitted light reflected off the inner surface of the aluminum tube and reached the top, at the reactor platform level, where a silicon photomultiplier (SiPM) detector was located. The acquisition system used was based on a RedPitaya module, developed by the Instrumentation Technologies company, as an accessible but very capable measurement tool for scientific and educational purposes.

The Cherenkov reactor power meter was developed, refined and tested both in steady-state as well as pulse operation modes. The

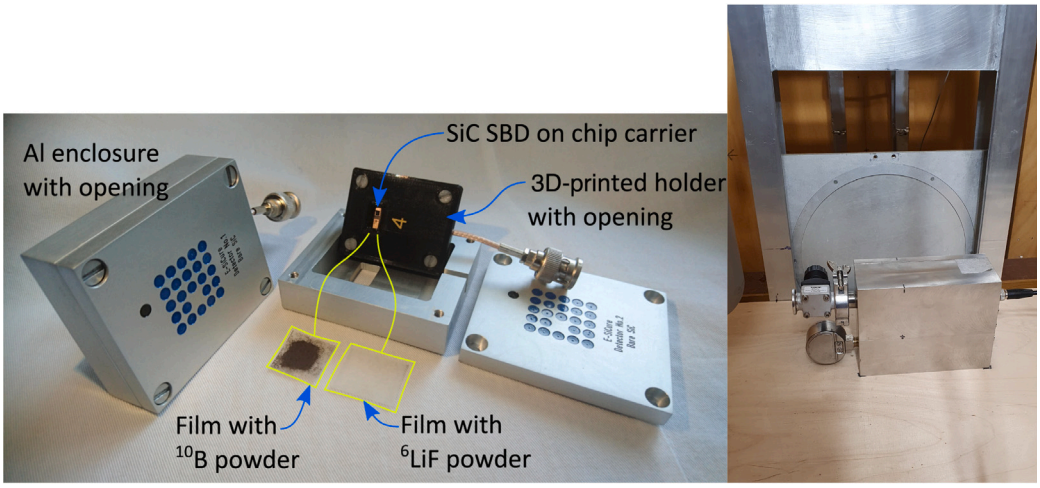

Fig. 24. On the left the assembled SiC detector prototype developed in the E-Sicure project and its components: SiC SBD mounted onto chip carrier with contacts, installed in 3D printed holder with opening, converter films (with ^{10}B and LiF powder), open aluminum enclosure with opening. On the right the testing of the detector in the dry chamber of the JSI TRIGA.

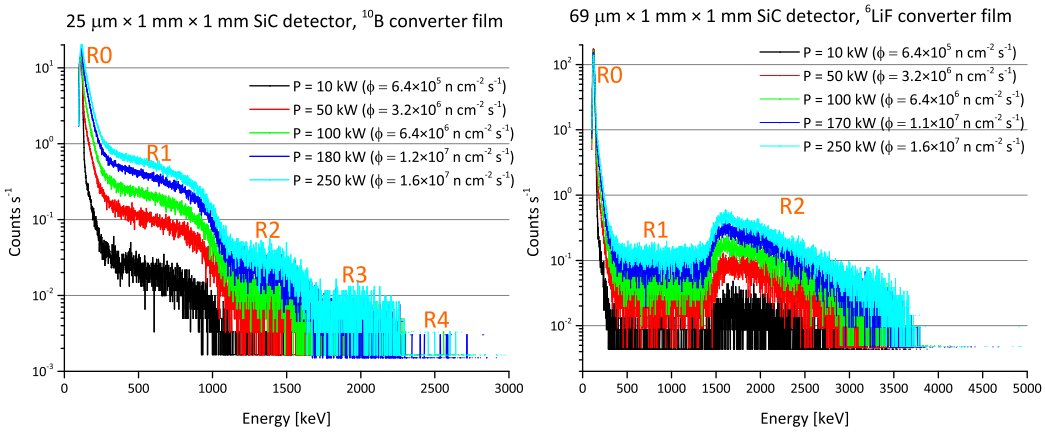

Fig. 25. Left: Pulse-height spectra of a 25 μm thick SiC diode with a ^{10}B converter. Right: Pulse-height spectra of a 69 μm thick SiC diode with a ^{6}LiF converter.

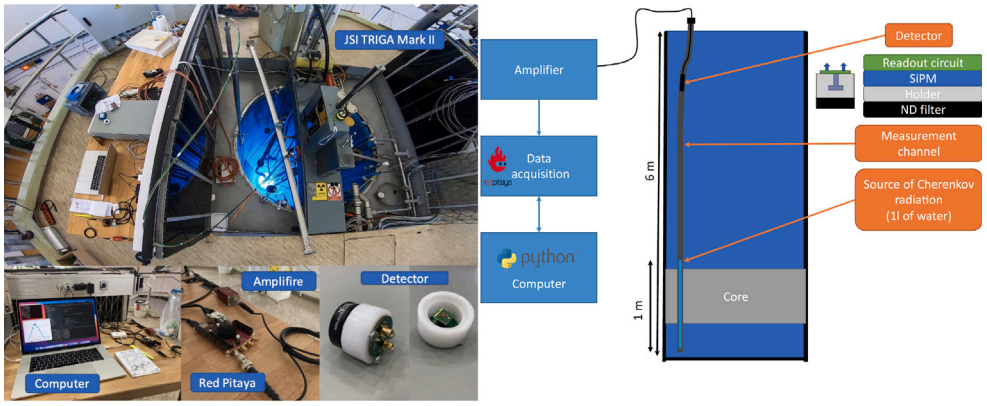

Fig. 26. Experimental setup of the Cherenkov Power Meter (left) and its schematic representation (right) in the JSI TRIGA reactor.

Cherenkov reactor power meter excelled in the latter in particular, thanks to the wide dynamic range and acquisition speed of the Red-Pitaya instrument, enabling to follow the reactor power time response in detail. The Cherenkov power meter was used as an alternative measurement technique in the framework of a bilateral collaboration project between the CEA and JSI with the aim to determine the applicability of reactor pulse operation for extending the experimental capabilities of the JSI TRIGA reactor for detector testing activities, as well as to test the performance of a state-of-the-art fission chamber data acquisition system named Libera MONACO 3, developed by CEA and commercialized by I-Tech (Barbot et al., 2023; Peric et al., 2023; Radulović et al., 2021).

3.2.2.5. Autonomous Robot.

In early 2020, a group of students from Lancaster University chose the JSI TRIGA reactor to test the performance of their autonomous

Fig. 27. Testing of an autonomous robot developed at the Lancaster University at the JSI TRIGA reactor.

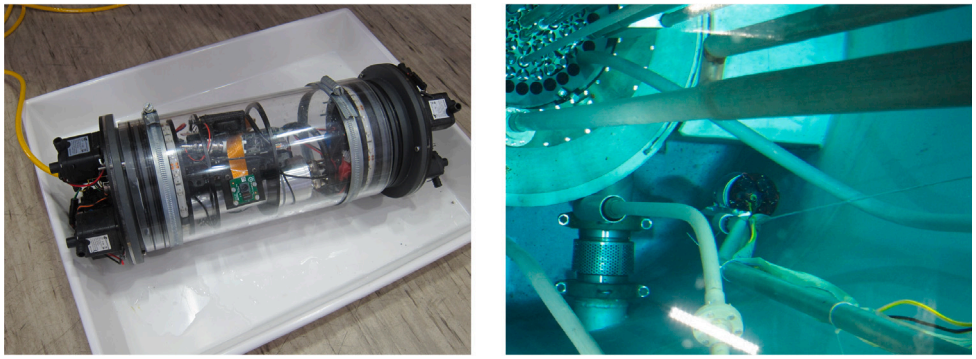

Fig. 28. Submersible ROV developed at the Lancaster University during irradiation tests at the JSI TRIGA reactor.

vehicle (see Fig. 27). The robot was designed to enter areas with increased dose rate levels and measure the dose rate map. It carried detectors sensitive to gamma-ray and neutron radiation. It was also capable of analyzing the gamma-ray spectrum and identifying individual sources of radiation (hot spots), i.e. determining their location and the radionuclides present. During the test run, we opened one of the horizontal beam ports to increase the dose rate inside the reactor hall. The robot provided a detailed dose rate map in the reactor hall and clearly identified some radiation sources safely stored behind in shielded positions (West et al., 2021; Tsitsimpelis et al., 2020).

3.2.2.6. Submarine.

In 2018, our reactor was used as a test facility for a Submersible Remotely Operated Vehicle (ROV) (Jones et al., 2018) designed by students from the Lancaster University (see Fig. 28). Their goal was to develop a robot that would investigate the flooded reactors in Fukushima. Their initial goal was to develop an expensive radiation-hard device, however they decided to focus on an inexpensive design, which could replace the ROV in case its design could not be completed successfully. The Submersible ROV was designed to carry a camera, gamma-ray and neutron probes, a gamma-ray spectrometer, and sonar. At the JSI TRIGA reactor, we exposed the ROV to gamma-ray and neutron radiation. The dose levels at which the robots started failing were determined.

3.3. Safeguards

The Fission Track Thermal Ionization Mass Spectrometry (FT-TIMS) method is considered as the reference method for particle analysis in the field of nuclear safeguards for measurements of isotopic compositions (fissile material enrichment levels) in micrometer-sized particles collected in the framework of nuclear inspection programmes. An integral phase in the method is the irradiation of samples – capsules containing polycarbonate disks onto which the collected particles are deposited – in a very well thermalized neutron spectrum. A bilateral collaboration project was carried out between the JSI and the CEA to determine whether the JSI TRIGA reactor could be used for irradiations of samples for the FT-TIMS method.

On the basis of Monte Carlo simulations and experimental measurements, a heavy water based irradiation device was designed and built in the Thermal Column Beam Port for the purpose of FT-TIMS irradiations (Radulović et al., 2018b). The device was qualified by a test irradiation of a capsule containing polycarbonate disks with deposited micrometer-sized particles of different ^{235}U abundances. The fission tracks in the polycarbonate material, irradiated in the JSI TRIGA reactor were compared against the fission tracks created in an irradiation in the Orphée reactor at the CEA Saclay site, in use at the time for FT-TIMS irradiations. The fission tracks were equally visible for both irradiation locations and no significant differences in the polycarbonate opacity were observed, as is presented in Fig. 29. These results validated the use of the TRIGA reactor for the FT-TIMS method developed at the CEA. The presented approach and device design can be adopted at other TRIGA-type or similar reactors in the world, thus increasing their versatility. As the Orphée reactor, where irradiations of FT-TIMS samples were performed was shut down in 2019, it was important at the time to have an available replacement irradiation facility. It is shown in Radulović et al. (2018b) that although the JSI TRIGA reactor is of

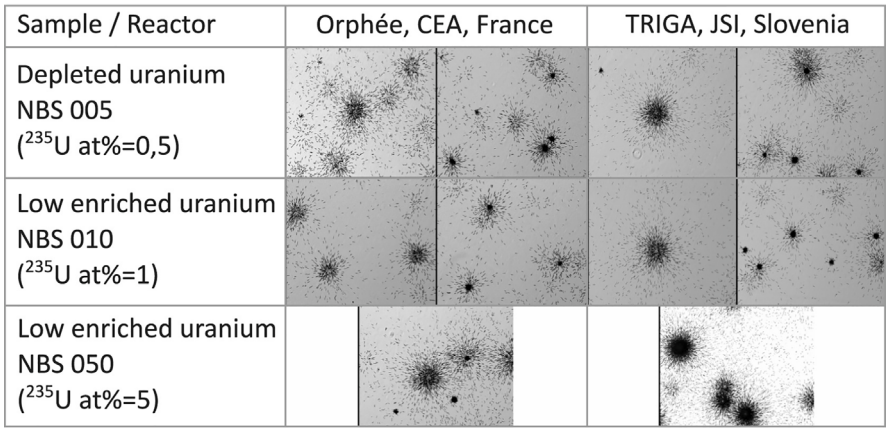

Fig. 29. Comparison between the fission tracks around micrometer sized uranium particles deposited on polycarbonate substrate after irradiation in the Orphée reactor at the CEA Saclay centre and the JSI TRIGA reactor, for three different ^{235}U enrichment levels. Each image displays an area of 0.8 mm × 1 mm. The fission tracks are equally well visible under microscope, there are no significant differences in the opacity of the substrate material. Radulović et al. (2018b).

much lower power (250 kW) than the Orphée reactor (14 MW), it can successfully be used for the FT-TIMS application by employing a smart design approach strongly supported by calculations and subsequent validation by measurements.

3.4. Neutron activation analysis

Neutron Activation Analysis (NAA) is one of the primary relative methods, which is frequently used for the characterization of the chemical composition of various environmental samples (organic and inorganic materials) including man-made materials. In principle, it is a bulk analysis technique with panoramic analysis of many elements in the sample. The method is based on the irradiation of samples in a neutron field. Nuclear reactions, most commonly (n, γ) reactions, generate radionuclides within the sample material during irradiation. Subsequently, induced activities for individual radionuclides are measured using a High Purity Germanium (HPGe) detector. This allows the determination of the mass fraction for a multitude of elements in the sample. NAA is a very sensitive, versatile and reliable non-destructive analytic method.

3.4.1. Analysis

In NAA, the sample mass for analysis is typically about 200 mg, for some studies, the sample mass may be increased up to some grams or more in order to achieve lower detection limits of the method. To detect the elemental content in a sample, a standard of an element or multi-standard should be irradiated simultaneously with the sample and after a suitable cooling time measured independently on a HPGe detector. Then, the produced gamma-ray spectra are processed with gamma-ray spectrum evaluation software to obtain the net peak areas for distinct peaks due to radionuclides originating from activation reactions on isotopes of the element to be measured. On the basis of the measured net peak areas the mass fraction of an element in the sample is determined. Typically, two irradiations are necessary in order to obtain as much information as possible from the studied sample: a short irradiation (up to some minutes) and a long irradiation (some hours or days), respecting the half-life of the induced radionuclides. In this way, about 70 % elements of the periodic table can be detected.

3.4.2. Certification and intercomparisons

Due to the recognition of NAA as one of the reference techniques for the determination of major, minor and trace elements, it can also be used for the characterization of proposed new certified reference materials (CRMs). During the last 50 years, we participated in numerous certification campaigns for new CRMs as well as in different inter-laboratory studies. Some of the studies organized by the Institute for Reference Materials and Measurements (IRMM), Belgium, are listed in the Table 4.

Table 4
Characterization of new CRMs by NAA.

Material	Analytes	Year
BCR-277R estuarine sediment, BCR-280R lake sediment and BCR-320R channel sediment	Al, As, Ba, Br, Cd, Ce, Cl, Co, Cr, Cs, Cu, Dy, Eu, Fe, Hf, Hg, I, K, La, Mn, Na, Nd, Rb, Sb, Sc, Se, Sm, Sn, Sr, Ta, Tb, Ti, U, V, Yb and Zn	2002
Two polyethylene reference materials ERM®-EC680k and ERM®-EC681k	As, Cd, Cl, Cr, Hg, Sb and Sn	2006
Two polymer reference materials ERM-EC590 & ERM-EC591	Br and Sb	2008
ERM-CD281 rye grass	As, Cr, Mn, Mo, Sb, Se, Sn and Zn	2008
ERM-CZ120 Fine Dust	As and Cd	2010
ERM®-CE278k mussel tissue	Ag, As, Cd, Cr, Cu, Fe, Hg, Mn, Rb, Se, Sr and Zn	2011
ERM®-DB001 human hair	As, Cd, Cu, Hg, Se and Zn	2011
ERM®-CD200 Bladderwrack (Fucus vesiculosus)	As, Cd, Hg, Se and Zn	2011
ERM®-BD150 and ERM®-BD151 skimmed milk powders	Ca, Cl, Co, Fe, K, Mg, Na, Se and Zn	2012
ERM®-EF411 (hard coal), ERM®-EF412 (brown coal) ERM®-EF413 (furnace coke)	As, Co, Cr, Mn, Sb, Se, V, Zn, Ca, Mg, Na, K, Cl and Hg	2012
Determination of trace elements in Lu foil	Major elements and trace elements	2013
Mass fraction in Al-0.1%Au alloy: ERM®-EB530A, B and C	Au	2013
The minor elements and trace elements mass fraction in TiAl6V4: BCR®-089	Fe, Cr, Mo, Zr, Cu, Co, Mn, W, Zn, Hf, Ta, Hg, La, Ce, Sb, As and Ga	2013
Two polyethylene reference materials ERM®-EC680 m and ERM®-EC681 m	As, Br, Cd, Cl, Cr, Hg, Sb, Sn and Zn	2015

3.4.3. k0-method: development and improvements

At the JSI, the k0-standardization method of NAA (k0-NAA) was installed and validated in the early 1990s (De Corte et al., 1997, 2001). In principle, the method is mono-standard and uses gold (Au) as the standard and comparator for the simultaneous determination of elements in an unknown sample. The k0-method of NAA is continuously improving, along with the underlying nuclear data. The JSI participated in efforts

to improve the accuracy and reliability of nuclear data in the k0-library (Jaćimović et al., 2014). After the method validation (Jaćimović et al., 2003) and after international recognition as an expert laboratory in NAA, we were able to participate in different studies and international projects including inter-laboratory comparisons (ILCs) at the highest level (CCQM, SIM, APMP, etc.) as well as characterization studies for new CRMs.

3.5. Radiation hardness studies

The JSI TRIGA reactor has become an important reference centre performing radiation hardness studies of materials, components and assemblies used in large particle physics experiments, and recently for applications like the development of radiation-hard LEDs, cameras, glass, etc. We regularly perform irradiations of various nanomaterials or ceramics in which we expose them to different neutron fluence or gamma-ray dose levels and then investigate radiation-induced effects. A paper was published (Trkov and Radulović, 2015) showing how the constants used in NAA are related to the microscopic cross sections, which opens the way for nuclear data validation, and possible enhancements of the NAA technique.

3.5.1. CERN

One of the challenges in particle physics experiments is to ensure successful long-term operation of sensors used for the detection of particles originating from collisions at high energies. Detectors at the LHC (Large Hadron Collider) which began operation at CERN in 2008 are exposed to 1 MeV neutron non ionizing energy loss fluences of up to 10^{15} cm^{-2}. An upgrade of LHC to HL-LHC (high luminosity LHC) should be completed at the beginning of 2029 and the detector components in experiments will be exposed to more than an order of magnitude higher fluences. In the experiments planned further on, the radiation levels will be even higher. Therefore, extensive research of radiation hardness of all components (sensors, electronics, support elements) integrated in detectors is required.

The first irradiations at the JSI TRIGA reactor for the development of particle physics instrumentation began in 1996, to study displacement damage effects in silicon sensors for charged particle tracking (Žontar et al., 1999). Soon, the JSI TRIGA reactor proved to be a reliable source of fast neutrons where fluences up to 10^{17} cm^{-2} can be reached in one day. A good knowledge of the neutron energy spectra and non ionizing energy loss in silicon, stable experimental conditions and suitable irradiation locations for irradiations of components with sizes up to 10 cm×10 cm motivated the European Union to support transnational access to the JSI TRIGA facility in the framework of several projects (AIDA, AIDA-2020, EURO-LABS). The latest project, EURO-LABS, brings together, for the first time, the three research communities of nuclear physics, accelerator and detector technologies for high energy physics. It will be completed in 2026.

The JSI TRIGA reactor is one of the main irradiation sites for studies of displacement damage in silicon detectors and readout chips (ASICs) needed for development of detectors in experiments at LHC and its upgrade to HL-LHC and other experiments (White et al., 2001). The reactor has been intensively used by several research and development collaborations CERN-RD39, RD42, RD48 and RD50. The reactor has become the reference facility for neutron irradiations, which led to many important findings for particle physics instrumentation as well as fundamental properties of silicon and other semiconductors.

Among them are the accurate understanding of the radiation damage effects in silicon such as the increase of generation current, charge trapping effects, increase of effective doping concentration and the removal of effective dopants. The latter is particularly important for latest generation of silicon particle sensors called Low Gain Avalanche Detectors (LGAD) which use impact ionization of free carriers generated by particles. The measurements of signal enhancement due to multiplication effects in neutron-irradiated strip sensors (Mandić et al., 2010) was one of the initiators of Low Gain Avalanche Detectors development (Pellegrini et al., 2014). High gain allows for very thin sensors with an excellent signal-to-noise ratio and short charge collection time, hence superb timing performance of order of 10 ps.

Apart from R&D purposes an extensive program of irradiations for Quality Assurance during the production phase of silicon sensors for the upgrade of the ATLAS experiment started in 2020 and will run until 2026. Both ITk (ATLAS tracker) and HGTD (ATLAS high granularity timing detector) campaigns are ongoing. For the ITk, two different irradiated samples from each production batch are distributed to several laboratories, where their properties important for efficient tracking of charged particles are measured (Kopsalis et al., 2023). The HGTD production test detectors are measured with charged particles and transient current technique (Kramberger et al., 2023).

The major challenge for performing irradiations relevant for CERN was how to expose large components to neutrons. The standard in-core irradiation channels in the JSI TRIGA reactor are only 3 cm in diameter. The triangular irradiation channel allowed for irradiations of relatively large samples (up to 5 cm in diameter) at a neutron flux level of 3.5×10^{12} n/cm^{2}s 1 MeV eq (Depriest, 2019)s. at full reactor power. In 2016, one of the beam ports was modified in a way that samples with diameters up to 12 cm and lengths of 30 cm could be irradiated at a neutron flux level of 4×10^{11} n/cm^{2}s 1 MeV eq. at full reactor power (Radulovic et al., 2017). Future plans include an upgrade of the existing beam port, firstly with the installation of a cadmium shield, which will limit the activation of irradiated components due to thermal neutrons, and secondly the addition of a heating device to irradiate the samples at higher temperatures.

The collaboration with CERN resulted in the development and the characterization of radiation sensitive field effect transistors, where their electrical properties change under the influence of incident gamma-ray irradiation. The upside of such devices is the capability of an on-line dose readout and miniature size. These transistors were developed in collaboration with Scientific and Technological Research Institution of Turkey and were tested and calibrated in the JSI TRIGA reactor against a calibrated PTW ionization chamber (Kramberger et al., 2020).

3.5.2. Specialized nuclear equipment

Since 2015, we have been collaborating extensively with the Slovenian hi-tech company DITO, who are developing and commercializing heavy-duty lighting for harsh environments, with high radiation dose rates, high temperatures and frequent pressure differences. During our collaboration, they have developed and put to market the world's most radiation-resistant LED luminaire (Dito Lighting, 2024), certified up to a dose of 500 kGy and a neutron fluence of 5×10^{14} cm^{-2} (1 MeV equivalent), suitable for various nuclear environments like the containment of nuclear power plants, hot cell facilities and gamma-ray irradiation facilities. They offer a wide range of luminaires, for example LOCA (loss of coolant accident) compatible LED, underwater, emergency, etc., all made possible by radiation hardness testing at our facility.

In 2016, a collaboration with ISEC Monitoring Systems AB of Sweden was established with the goal to develop a radiation tolerant surveillance camera based on consumer components. The development consisted of two stages: computational analyses aimed at establishing the optimal shielding materials and optical paths, as well as experimental tests of individual modules of the camera. A special large-sample irradiation box was constructed, which allowed for on-line fault detection in modules under irradiation. The irradiations were performed by placing the irradiation box in proximity of six activated TRIGA fuel elements located in one of the fuel racks at the edge of the reactor tank, giving rise to a maximum dose rate of about 100 Gy h^{-1} (Klemen et al., 2017; Ambrožič and Snoj, 2016a,b,c). The findings led to the development of several lines of radiation tolerant surveillance cameras, which have been deployed in NPPs and nuclear waste management facilities throughout the world.

3.5.3. Material testing

Since 2014, we have regularly collaborated with the Azerbaijan Institute for Radiation Problems. We are regularly performing neutron irradiations of various nanomaterials and observing how neutron exposure affects the material properties (Huseynov, 2018a, 2020; Huseynov et al., 2021, 2022, 2020). We are investigating methods to modify the properties of materials at the nano-scale. Over the last decade, experiments were conducted at the JSI TRIGA reactor, involving a range of nanoparticle types, including nano Si_3N_4, SiO_2, 3C-SiC, BN, B_4C, and pure Si particles. In the initial approach, it is possible to induce changes in the physical properties of nanoparticles through neutron exposure, even when they possess a crystalline structure. Modifying the properties of nanoparticles, particularly those with a nanocrystalline structure, proves challenging when operating within dimensions under 20 nm. The utilization of the JSI TRIGA reactor as a neutron source for the generation of dopant elements in nanocrystalline particles holds significant practical value. Nevertheless, the agglomeration of nanocrystalline particles or the initiation of amorphous transformations is possible under neutron irradiation. It should be noted that the degree of aggregation of nanoparticles depends directly on the amorphous layer on the surfaces of the nanoparticles (Huseynov, 2017). It is evident that the concentration of doping elements in nanoscale particles is crucial when applied in electronics. We utilized neutrons at the JSI TRIGA facility to investigate the electrical and dielectric properties of varying nanoparticles (Huseynov et al., 2014, 2015). Moreover, impedance spectroscopy has been applied to comprehend the influence of neutrons on various nanoscale particles (Huseynov, 2018b; Huseynov et al., 2019).

A similar collaboration is ongoing with the Electronic Ceramics Department of the JSI, in which we perform neutron irradiations of different ceramic materials and observe their properties (Sarkar et al., 2023; Uršič et al., 2022). As part of this collaboration, the $(1\text{-}x)Pb(Mg_{1/3}Nb_{2/3})O_3\text{–}xPbTiO_3$ (PMN–100xPT) ceramics were irradiated with a neutron fluence of 10^{15} to 10^{17} $1/cm^2$ with the mean energy of 1 MeV, along with simultaneous exposure to γ-irradiation. The functional properties of PMN–100xPT solid solution, a group of relaxor-ferroelectric materials, vary depending on the molar fraction of PT. Therefore, three different compositions with $x = 0$, 0.1, and 0.35 were investigated before and after neutron and γ-irradiation. We note that PMN is a prototype relaxor, while the ferroelectric ordering is becoming more pronounced with increasing PT content. The irradiation had a partial impact on the functional characteristics of the PMN–35PT ceramics, specifically on the polarization versus electric field hysteresis loops. It influenced the ferroelectric long-range order by introducing defects that most likely inhibit the movement of domain walls, resulting in a slightly modified domain-switching mechanism. On the other hand, the relaxor-like PMN and PMN–10PT compositions showed no significant changes in functional properties (Uršič et al., 2022). This suggests that PMN and PMN–10PT ceramics have the potential for use in radiation-resistant sensors, actuators, and solid-state cooling devices based on the electrocaloric (EC) effect, i.e., the temperature change in a material exposed to an applied electric field at adiabatic conditions. When considering using EC-based cooling in harsh conditions, the radiation hardness of the EC material is one of the criteria that needs to be fulfilled. Mn-doping of PMN-10PT allowed the down-shift of the maximum EC-temperature range closer to room temperature. PMN-10PT and Mn-doped PMN-10PT ceramics were exposed to 1 MeV equivalent neutron fluence for silicon of 10^{16} cm^{-2} and 10^{17} cm^{-2} of and γ-ray dose of 145 kGy and 1200 kGy. The neutron and gamma radiation caused a decrease in the saturated polarization, an increase in the internal bias field and a reduction in the EC temperature change compared to PMN-10PT. This radiation-induced degradation of the EC response was attributed to the presence of the Mn-oxygen-vacancy defect complexes and their interaction with the irradiation-induced defects. However, annealing at 450 °C partially healed the radiation-induced changes in the electrocaloric response of Mn-doped PMN-10PT (Sarkar et al., 2023).

Operational stability of voltage-tunable microwave devices such as phase shifters, filters or antennas working in harsh conditions, including space, is an important part of device design. We studied the influence of neutron (1.1×10^{14} cm^{-2}) and γ-ray (167 kGy) irradiation on the kHz- and GHz-range dielectric properties of $Ba_{0.5}Sr_{0.5}TiO_3$ thin films. The about 600 nm thick films, which were deposited on polycrystalline alumina substrates and annealed at 900 °C, were either quite porous, with fine, ≈35 nm equiaxed grains, or dense, with predominantly columnar grains with an in-plane size of ≈100 nm. Microstructural features, such as grain boundaries, pores and cracks, as well as crystal-lattice defects, have an effect on the irradiation-damage accumulation rate. The films with the columnar microstructure were less sensitive to neutron and γ-ray exposure (Glinšek et al., 2015).

3.6. Radiation catalyzed chemistry

In 2022, a project was initiated as a collaboration between the JSI and the Slovenian National Institute of Chemistry (NIC), with the aim of exploring the possibilities of using nuclear radiation as an exploitable energy source to catalyze chemical processes, as a basis for efficient carbon capture technologies and as a means of conversion or synthesis of high value chemicals starting from abundant and low value materials, as glycol, plastic, etc. The project started with Monte Carlo simulations to obtain predictive assessments of physical quantities of interest, e.g. the energy deposition rates in various chemical compounds (CO_2, plastics, biomass, hydrocarbons, etc.) under neutron and gamma-ray irradiation and chemical reaction rates in the presence of solid catalysts and gaseous/liquid medium in the JSI TRIGA reactor. Irradiation testing activities at the JSI TRIGA reactor as well in a high-energy electron beam available in a transmission electron microscope, followed by post-irradiation analysis and quantification will be performed in the second part of the project. Neutron and gamma-ray equivalence principles for LET (linear energy transfer) will be used to establish relations between irradiations in the JSI TRIGA reactor and other large-scale facilities such as nuclear power plants, spent fuel storage facilities, high intensity gamma ray sources as well as future fusion nuclear reactors.

3.7. Environmental sciences

3.7.1. Radiochemical neutron activation analysis

The determination of the chemical yields in analytical processes is one of the outstanding possibilities in radioanalytical methodology, originally the only purpose was to correct for possible losses of determinant during a radiochemical separation. The advantage of radiochemical analysis is the possibility of measuring the chemical yield for each sample aliquote. Radiotracer techniques are often the most accurate and simple way of doing this. The basic role in the use of radiotracers is that all the isotopes of a given element have the same chemical properties. At the JSI, many techniques using radiochemical neutron activation analysis were developed where tracers prepared in the TRIGA reactor were used (see Table 5).

3.7.2. ^{197}Hg radiotracer

Mercury, a well known toxic metal found throughout our planet's biosphere, hydrosphere, geosphere, and atmosphere, poses significant environmental challenges due to its unique physicochemical properties that enable long-distance transport. Once released into the atmosphere, mercury cycles between air, water, and land, with the potential for methylation, especially in aquatic environments, being a crucial aspect. The resulting monomethylmercury (MeHg) readily accumulates and biomagnifies along food webs, posing a threat to aquatic organisms and humans alike.

Table 5
Neutron activation tracers for chemical yield determination for different trace analysis applied for RNAA at JSI (Smodiš et al., 2018).

Measurand	Tracer	Nuclear reaction
As	^{77}As	^{76}Ge (n, γ) ^{77}Ge → ^{77}As
Co	^{58}Co	^{58}Ni (n,p) ^{58}Co
Cu	^{67}Cu	^{67}Zn (n,p) ^{67}Cu
Hg	^{203}Hg	^{202}Hg (n, γ) ^{203}Hg
Mn	^{54}Mn	^{54}Fe (n,p) ^{54}Mn
^{237}Np	^{239}Np	^{238}U (n, γ) ^{239}U → ^{239}Np
^{231}Pa	^{233}Pa	^{232}Th (n, γ) ^{233}Th → ^{233}Pa
Sb	^{125}Sb	^{124}Sn (n, γ) ^{125}Sn → ^{125}Sb
Se	^{81m}Se	Enriched ^{80}Se (n, γ) ^{81m}Se
U	^{238}Np	^{237}Np (n, γ) ^{238}Np

The Department of Environmental Sciences has focused extensively on mercury biogeochemical studies, driven largely by the legacy of the former Idrija mercury mine, which left behind heavily contaminated soil, river catchments of Idrijca and Soča, and deposition in the Gulf of Trieste. Access to the JSI TRIGA research reactor has facilitated fundamental studies, particularly in understanding mercury transformation processes in river and coastal environments, notably the Gulf of Trieste. Mercury methylation, the conversion of Hg^{2+} to MeHg, occurs in various aquatic compartments through microbial metabolism or chemical processes, underscoring the need to evaluate methylation potential using radiotracer techniques.

Mercury radiotracing techniques, essential for studying methylation, involve spiking samples with isotopes like $^{203}Hg^{2+}$ and assessing MeHg production. While ^{197}Hg serves as an alternative, its production is limited. To address this, enriched stable isotope ^{196}Hg is used to produce radioactive tracer ^{197}Hg, enabling experiments at lower, ecologically relevant mercury levels. The process involves dissolving ^{196}Hg-enriched mercury, irradiating it in a reactor, and preparing working solutions for analysis. Emissions from the ^{197}Hg radiotracer, including X-ray and γ-ray emissions, are measured using HPGe detectors.

The studies using ^{197}Hg and main achievements are summarized in Table 6, illustrating the diverse applications of ^{197}Hg tracer, including studies on mercury methylation and reduction in riverine, lagoon, and marine environments. Additionally, the validation of novel materials for mercury removal from water and the calibration and sampling of atmospheric gaseous oxidized mercury have expanded mercury atmospheric research at the JSI.

3.7.3. Radioactive tracer CeO_2

The JSI TRIGA reactor has been used for tracer studies involving dissolution and uptake of CeO_2 nanoparticles (Schymura et al., 2021). Innovative dual label approach has been used where cerium oxide nanoparticles have been irradiated in the JSI TRIGA reactor, which resulted in a homogeneous distribution of ^{141}Ce radiolabel throughout the nanoparticles. As a second radiolabel, nanoparticles were labeled by in-diffusion of cyclotron produced ^{139}Ce. As such, we achieved the presence of ^{139}Ce radiolabel preferentially on the surface of the nanoparticles, whereas ^{141}Ce was homogeneously distributed throughout the nanoparticles. The different distribution of the radiolabels in the particles does not only allow easy dose determination in uptake studies but also enables us to track the uptake pathways of the anthropogenic cerium. By measuring the activity as well as the isotope ratio we tracked the uptake, transformation and excretion of CeO_2 nanoparticles in freshwater shrimp. We found that 99.99% of the uptaken particles are excreted, leaving the gut with excrement. The remaining 0.01% were internalized via a dissolution-based pathway and accumulated in the hepatopancreas of the shrimp at a dose range of pg CeO_2 per shrimp. Most importantly, our results show that dissolution is not only coincidental but instrumental in the uptake of the cerium into the internal organs of the shrimp.

3.7.4. Irradiation of organic materials

Radiolysis of organic materials present in radioactive waste can yield different smaller molecules, which can alter migration properties of radionuclides and compromise safe disposal of radioactive waste. To simulate the acquired gamma-ray dose over the lifespan of the radioactive disposal facility, we have used JSI TRIGA reactor in shutdown conditions as a gamma-ray source (Plant et al., 2021). To be able to do that, a well characterized dose rate is needed as radiation dose decreases with time after shutdown due to the decay of short-lived activation and fission products. As such, the JSI TRIGA reactor is a very useful irradiation facility also during shutdown. We have performed study of radiolytic degradation of polycarboxylate and polyaryl ether superplasticizers used as cement additives to improve cement workability. We have found out that initially liquid superplasticizers first turned into gel, which means that conditions favoring crosslinking of polymers prevailed and larger molecules have been formed. However, after an irradiation dose of 3 MGy, part of the sample turned back to liquid, which contained polyethylene glycol as a main constituent, which means that this can be expected as a main degradation product due to radiolysis. As polyethylene glycol can form crown ether like structures, it can also potentially create complexes with radionuclides and increase their mobility in radioactive waste.

3.7.5. Arsenic

Several organoarsenic compounds were irradiated in the JSI TRIGA reactor and ^{76}As activities and As concentrations of the arsenic-containing decomposition products formed were measured by previously developed chromatographic techniques with element-specific detection. Since the recoil energy available during irradiation is high enough to break molecular bonds, a range of radiolabelled arsenic compounds was produced, depending on the conditions (type of compound, matrix and irradiation time). The most extensively investigated compound, viz. arsenobetaine, yielded, when irradiated as solid material for 60 min, 11 radiolabelled arsenic compounds, of which eight could be identified. Theoretically, an overall specific activity of 3.7 GBq/g was expected, but experimental specific activities were found ranging from 0.5 GBq/g (for arsenobetaine) to more than 3800 GBq/g (for arsenate) (Šlejkovec et al., 1999). The ^{76}As labeled species (mono-, di and trimethylated) were then additionally used to calibrate and improve the column separations (Šlejkovec et al., 1993).

Isotopic exchange based approaches have for many years been applied in soil and solute research. The experiments were carried out with arsenate from IAEA-SOIL-5 in contact with water or phosphate solution in dynamic equilibrium. After contacting the soil suspension for 28 days, the amount of arsenate released is 2.8% and 6.3% of arsenic in the soil, respectively. The addition of a radioactive arsenate ^{73}As(V)-spike and the following of the distribution of this radiotracer from the aqueous to the solid phase in time shows that the accessible fraction, i.e. available for exchange, is in both cases 12 %; the remainder of the arsenic is enclosed in the lattice of minerals and for that reason unavailable for exchange. From deconvolution of compartmental analysis results the distribution of accessible arsenate in the soil could be attributed to sorption onto external surfaces and sorption onto internal surfaces after diffusion through soil particle pores. The mean residence time in two out of three compartments was of the order of minutes for the external surfaces and of the order of days for the diffusion-controlled internal surfaces (van Elteren et al., 2008).

3.8. Nuclear data evaluation and validation

Within the scope of the activities of the International Atomic Energy Agency (IAEA) and the International Network of Nuclear Data Evaluators (INDEN),[1] several improvements to the evaluated nuclear

[1] https://www-nds.iaea.org/INDEN/

Table 6
Overview of key achievements using ^{197}Hg tracer in the department of environmental sciences.

Ribeiro Guevara et al. (2007)	A novel methodology for studying mercury methylation and reduction in sediments and water using ^{197}Hg radiotracer was introduced. This methodology presented a new avenue for investigating the complex processes of mercury cycling in aquatic environments, with a specific focus on methylation and reduction mechanisms.
Žižek et al. (2008)	Validated methodology was developed for determining mercury methylation potential in river sediments using ^{197}Hg radiotracers. This study established a reliable and rigorous approach for evaluating the ability of sediments to methylate mercury.
Bratkič et al. (2017) Bratkič et al. (2017) Koron et al. (2012) Baldi et al. (2012) Hines et al. (2012) Guevara and Horvat (2013)	Studies of mercury transformations in aquatic environments, particularly focusing on coastal areas and lagoon sediments were performed. Researchers examined the behavior of mercury in different marine settings, including the Gulf of Trieste in the northern Adriatic Sea and the Marano & Grado Lagoons in Italy.
Chouhan et al. (2023)	Experimental data demonstrated the efficiency and effectiveness of the magnetite/graphitic carbon nitride nanocomposite in removing Hg^{2+} ions from contaminated water samples, providing insights into the development of advanced materials for environmental remediation applications.
Gačnik et al. (2021a) Gačnik et al. (2021b) Gačnik et al. (2022) Ali et al. (2024)	The papers collectively focus on various aspects of mercury analysis and speciation, aiming to optimize methodologies, validate calibration approaches, and assess the behavior of sorbent traps and trapping solutions used in atmospheric mercury speciation. The research spans optimization of pre-concentration methods for analyzing mercury isotopes in low-concentration foliar samples, calibration approaches for gaseous oxidized mercury using nonthermal plasma oxidation of elemental mercury, and validation of an evaporative calibrator for gaseous oxidized mercury.

data files of important materials in nuclear technology were made, like ^{235}U, ^{238}U, ^{233}U, iron and silicon isotopes, boron isotopes ^{19}F and others (Brown et al., 2018). Several of these evaluations were included in full or in part in the major data libraries such as ENDF/B-VIII.0 (Brown et al., 2018), JEFF-4T3 (Nuclear Energy Agency, 2024) and JEFF3.3 (Plompen et al., 2020). A contribution to the review of evaluations for neutron dosimetry with significant improvements and extension to 60 MeV in the IRDFF-II library was made and is available from the IAEA web site (Trkov et al., 2020). Benchmarking of evaluated data files is an integral part of modern evaluation methods, which provides prompt feedback on the performance of a new evaluation. Benchmarks from the Handbook of International Criticality Safety Benchmark Experiments (ICSBEP) and Shielding Integral Benchmark Archive and Database (SINBAD) are used for the purpose. Improved data libraries result in enhanced accuracy of modeling reactor systems, allowing better characterization of irradiation facilities and the associated radiation fields.

3.8.1. *Epithermal neutron dosimetry — (n, γ) and (n,n') reactions*

Most advanced reactor concepts currently being developed in the framework of the Generation-IV forum are designed to operate with neutrons in the fast and intermediate – epithermal – energy range (1 keV–1 MeV), due important advantages, in particular increased efficiency of the use of uranium resources and the ability to transmute long-lived actinides, which are the most problematic in nuclear waste management. In nuclear fusion reactors, e.g. tokamaks, neutrons originating from fusion reactions are also in the fast energy range, and the neutron spectrum in the immediate vicinity of the reactor is characterized by a fast component, and an epithermal component, which is due to neutrons slowing down by interactions with the surrounding materials. The ability to accurately measure neutrons in the fast and epithermal range is therefore of critical importance in future advanced fission reactors and fusion reactors, in particular to monitor the reactor power level, achieved by on-line nuclear instrumentation, and to assess neutron fluence levels in critical reactor components, giving rise to radiation induced effects in materials and systems.

Various measurement techniques exist at a mature technological level by which thermal and fast neutrons can be detected and quantified. However, there is a general lack of measurement capabilities and suitable instrumentation with sensitivity specifically to the epithermal energy range. Neutron activation dosimetry is the reference neutron flux measurement technique and consists of irradiating material samples with a well-known composition and observing the photon emission due to the radionuclides generated.

The need for a better understanding of the epithermal energy range has resulted in recent work aimed at improvements in neutron activation dosimetry (Sergeyeva et al., 2015), however a general lack of measurement capabilities and suitable instrumentation still remains. New research at the JSI in collaboration with the French CEA in the framework of three research projects has been performed, aimed at extending the capabilities of neutron activation dosimetry in the epithermal energy region by the use of specific radiative capture reactions ((n, γ) reactions) in conjunction with boron-based neutron filters and inelastic scattering reactions ((n,n') reactions) (Radulović and Thiollay, 2018).

3.8.2. *^{241}Am cross section*

In spent nuclear fuel, ^{241}Am is a dominant contributor to decay heat and radiotoxicity for decades to centuries. The neutron capture cross section in ^{241}Am is difficult to measure for different reasons.

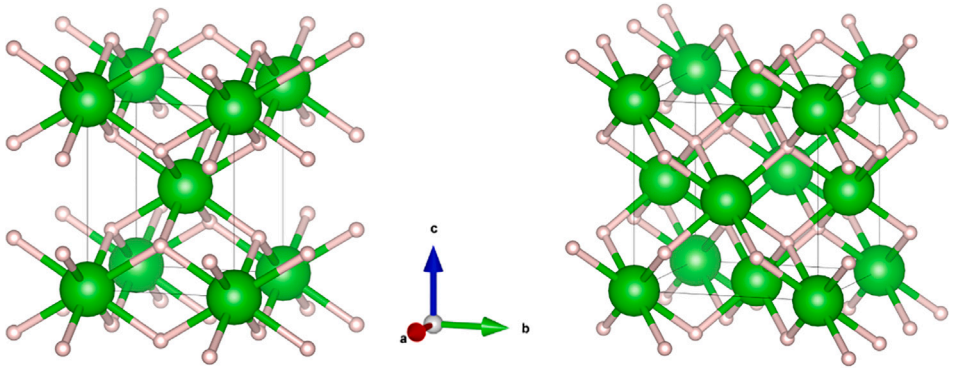

Fig. 30. Unit cells for ϵ-phases left and δ-phases right. Green spheres present Zr atoms and white spheres presents H atoms.

Namely, the ^{241}Am cross section includes two resonances below and near the cut-off energy of the Cd transmission filter (~ 0.55 eV). The ^{241}Am activation process generates both ground and metastable states, with the latter possessing a considerably longer half-life (141 years for ^{242m}Am compared to ~ 16 hours for ^{242g}Am), contributing to the relatively intricate decay scheme of the activation products. In addition, its γ-ray emission compromises the accuracy of the time-of-flight measurements, but alternative methods like activation or pile oscillation can provide more accurate results. In neutron activation analysis, α-particle spectrometry is preferred due to difficulties in γ-ray spectrometry related with the absence of prominent high-energy peaks in the photon emission spectra of the activation products. Pile oscillations offer an alternative to activation measurements, significantly simplifying the analysis but requiring samples containing significantly larger amounts of ^{241}Am.

In order to validate the thermal neutron cross section in ^{241}Am from different nuclear data libraries, a series of irradiations of samples including ^{241}Am (Žerovnik et al., 2021) was performed at the JSI TRIGA reactor. Irradiations of two samples, with and without Cd cover, were performed in each of the following irradiation channels:central channel (A-ring in Fig. 4), one of the positions in F-ring and one of the positions in rotary grove. Since central channel is located in the center of the core and rotary grove in the reflector, they possess very different thermal-to-epithermal spectral ratios, which are related to the reaction rate ratios with and without the Cd transmission filter. The comparison of calculations with experiments (Žerovnik et al., 2023) consistently showed a better agreement with the JEFF-3.3 (Plompen et al., 2020) nuclear data library compared to the ENDF/B-VII.0 (Chadwick et al., 2006) and ENDF/B-VII.1 (Chadwick et al., 2011) nuclear data libraries.

3.8.3. Thermal scattering in ZrH

Recent advances in computing power have enabled state-of-the-art atomistic simulations in chemistry and physics, using algorithms such as density functional theory to model crystal lattices and molecules. Our focus is on zirconium hydride (ZrH_x), which is crucial for hydrogen storage in research reactors. Our goal is to update outdated thermal scattering data and eliminate discrepancies in benchmark results (Švajger et al., 2021) and Švajger et al. (2020). ZrH_x exhibits several phases, most notably the δ-phase (for $1.56 < x < 1.64$) and the ϵ-phase (for $x > 1.74$). Our study focuses on the atomic structures, mechanical properties, frequency distributions, phonon density and thermal scattering cross sections and compares our results with existing literature and experiments (see Fig. 30).

3.9. Multi physics

Multi-physics analyses of nuclear reactors constitute a dynamic research frontier of nuclear engineering. In the JSI TRIGA reactor, we have integrated thermal-hydraulics and neutron physics to examine the behavior of reactivity coefficients under varying temperatures of the fuel and coolant. The first step in this was the analysis of natural and mixed convection flows in the reactor pool. Two types of experiments were performed in this respect: Stepišnik (2008) (Stepišnik et al., 2009) conducted analyses of primary coolant activities at various points in the reactor pool using radioactive tracers. His measurements offered a qualitative insight into the natural and mixed convection patterns above the core. The goal of the second experiment was the measurement of the temperature field in the reactor pool (Henry et al., 2017a). Around sixty thermocouples, fixed on an antenna-like structure, were used for simultaneous measurements of the temperature field above the reactor core under natural convection conditions with the cooling system switched off and under mixed convection conditions (see Fig. 31). In the second phase of the same experimental campaign, temperatures were also measured inside the cooling channels of the reactor (Henry et al., 2017b). These temperature fields were used for the validation of computational fluid dynamics (CFD) simulations, which predicted velocity and temperature distributions in the pool of the TRIGA reactor, and for the validation of coupled thermal hydraulics — neutron physics simulations of TRIGA.

3.10. Radiation biology

The JSI TRIGA reactor exhibits biological overgrowth, which varies with intensity of reactor operation. The biofilm negatively effects water quality in the tank as it covers the reactor components and reduces both water purity and visibility. Hence, it needs to be removed on a regular basis, typically once a year. Despite its detrimental impact on the physical properties of the reactor water, the biofilm offers a unique insight into what conditions are survived by the native microbiota. We have studied the colonization dynamics of microbial biofilm within the containment tank of a TRIGA nuclear reactor, characterized by oligotrophic conditions and periodic exposure to high pulses of ionizing radiation (Bratkic et al., 2023).

Through rigorous analysis (see Fig. 32), the study unveils a rich microbial diversity thriving in this extreme environment. Microbial sampling and sequencing reveal a plethora of species, with over 10 distinct microbial taxa identified within the biofilm community. The succession of microbial genera, particularly Bacilli and Actinobacteria, leads to the establishment of a photoautotrophic and diazotrophic community within a short timeframe. Furthermore, vertical stratification of microbial genera is observed, with Bacillus strains dominating closer to the reactor core, exhibiting surprising resilience to ionizing radiation.

Actinobacteria, including Frigoribacterium and Arthrobacter genera, also play a significant role in the microbial community, displaying resilience to ionizing radiation and contributing to the establishment of a diverse ecosystem within the biofilm. The study further demonstrates how the distance from the reactor core, and thus the radiation intensity, influences the microbial diversity, with microbial communities becoming increasingly complex as the distance from the core increases.

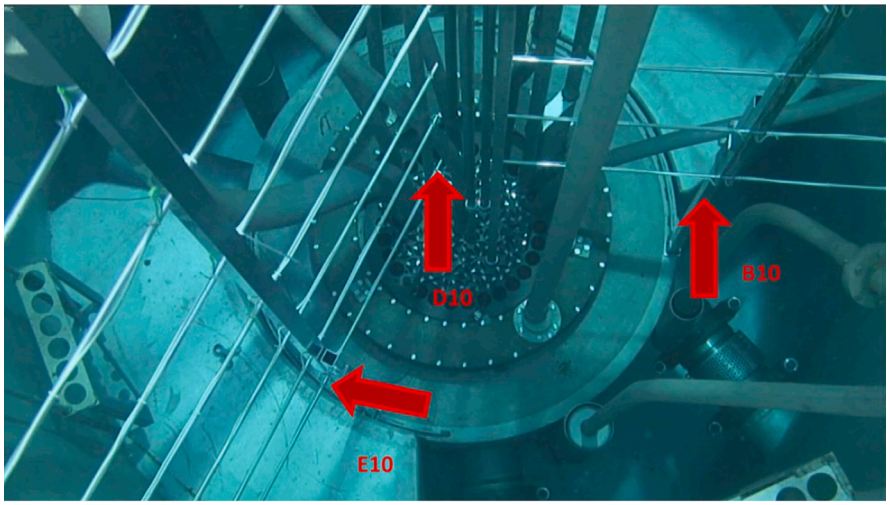

Fig. 31. Support structures with the thermocouples immersed into the TRIGA pool. In the figure letters *E,D,B* depict different column of detector and the number depicts its vertical position (e.g. number *10* depicts the lowest one).

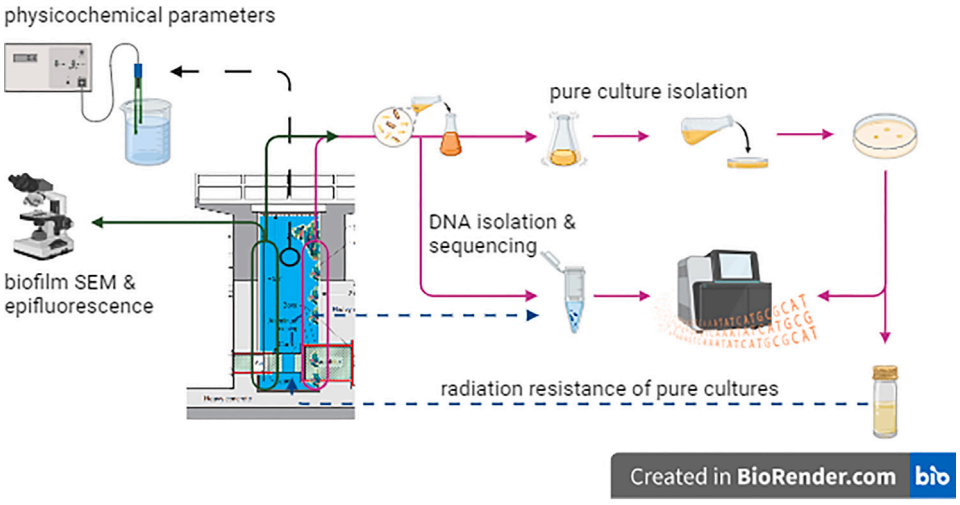

Fig. 32. Experimental and computational procedure for the microbial biofilm analysis performed at the JSI TRIGA research reactor (Bratkic et al., 2023).

The temporal progression of the biofilm community serves as a valuable proxy for understanding microbial responses to radiological contamination events, highlighting the need for improved dose–response models. Furthermore, the study underscores the unique insights provided by the JSI TRIGA reactor in studying ionizing radiation microbiology, elucidating relevant microbial dose thresholds and shedding light on the mechanisms driving microbial survival and adaptation in extreme environments.

Our findings not only contribute to our understanding of microbial ecology in irradiated environments but also have broader implications in radiation biology and environmental microbiology.

3.11. COVID-19 related applications

The beginning of the COVID pandemic posed immediate serious challenges to public health and disrupted supply chains for diverse products, materials and equipment urgently needed. Facemask respirators in particular where in short supply in Slovenia in early 2020. A study was initiated in April 2020 with the objective to investigate the reusability of facemask respirators upon sterilization by gamma-ray radiation. The study was based on test gamma-ray irradiations of facemask respirators in the JSI TRIGA reactor in shutdown conditions, as well as electron beam irradiations in the facilities of the STERIS company in Komenda, Slovenia, to doses relevant for sterilization purposes (20 kGy), and subsequent measurements of their filtration efficiency (Pirker et al., 2021). The study demonstrated that while gamma-ray/electron irradiation effectively sterilizes the respirators, it also reduces their filtration efficiency due to the loss of static charge, the primary filtration mechanism. It was found however, that post-irradiation recharging can restore the filtration efficiency in large part. The study meticulously assessed the structural, chemical, and mechanical impacts of irradiation, establishing a threshold for the applied radiation to ensure the integrity of the polypropylene material used for filtration remains uncompromised. The viability of ionizing radiation for respirator sterilization in emergencies was demonstrated, with limitations on repeated processing to prevent material degradation (see Fig. 33). This investigation, carried out as a collaborative effort across various departments at the JSI during a critical time, underscores the importance of having in place research programs covering diverse scientific fields and able to support multidisciplinary research activities.

4. Education and training

The JSI TRIGA reactor reached its first criticality in 1966 and was the first nuclear installation in Slovenia. From the very beginning it represented the focal point for the development of knowledge and

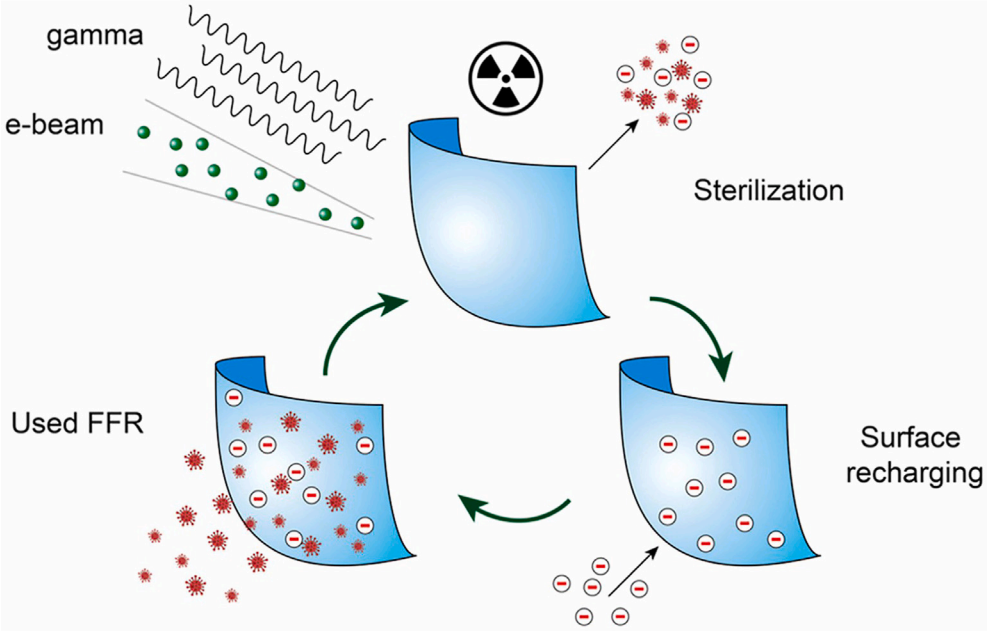

Fig. 33. The study found that the respirators can be sterilized using ionizing radiation. After sterilization, the filtering efficiency can be restored by re-applying the electrostatic charge.

competences in the field of nuclear technology and played a key role in personnel training. When the construction of the Krško NPP started a decade later, several of TRIGA staff were employed in the new NPP. The first radiation protection courses for NPP staff were held at the Reactor centre in Ljubljana in the 1970s, nuclear and reactor physics classes were organized for the first generation of future control room operators of Krško NPP before they were sent to further training in the U.S.A. Since the beginning, education and training activities carried out at the JSI TRIGA have extensively broadened and now include several training courses per year, organized for Slovenian universities and in the framework of international collaborations and initiatives.

4.1. International training courses

The TRIGA Mark II reactor at the JSI serves as a hub for international training and educational collaboration, offering a suite of programs that cater to a diverse audience of nuclear professionals, researchers, and students. These courses are designed to provide hands-on experience, theoretical knowledge, and practical skills in various aspects of nuclear science and technology. Below is an overview of the key international training courses associated with the reactor:

- ENEEP (European Nuclear Experimental Educational Platform) offers a comprehensive curriculum focusing on experimental reactor physics, radiation protection, and the practical aspects of nuclear engineering. The program aims to bridge the gap between theoretical knowledge and practical applications, providing participants with the opportunity to conduct experiments using the TRIGA reactor's facilities. ENEEP started in 2019 as a EU Horizon 2020 project carried out by five universities/research institutions in central Europe (Slovak University of Technology in Bratislava — STU, Czech Technical University — CTU, Vienna University of Technology — TU Wien, Jožef Stefan Institute — JSI, and Budapest University of Technology and Economics — BME) active in the field of nuclear education, in 2023 our activities transitioned to the framework of the ENEEP Association.
- Eastern European Research Reactor Initiative (EERRI) is tailored towards promoting nuclear research and education within Eastern Europe. The initiative fosters collaboration among research reactors in the region, enhancing the capabilities of participating institutions in nuclear research, safety, and education.
- Bilateral collaborations between the JSI and the Massachusetts Institute of Technology (MIT) and the Uppsala University leverage the JSI TRIGA reactor for joint research projects and student exchange programs. The focus is on advancing nuclear science research and developing innovative solutions to contemporary nuclear engineering challenges.
- Politecnico di Milano (Polimi) Partnership emphasizes advanced nuclear engineering and reactor physics education. It provides an opportunity for students and professionals to engage in specialized training sessions, workshops, and collaborative research projects.
- Centre for Nuclear Technology Development (CDT) focuses on the application of nuclear technology in non-energy sectors, including medicine, industry, and agriculture. The training courses cover a wide range of topics, from radiation safety and radionuclide production to the use of nuclear techniques in material science.
- A long-term collaboration between the JSI and the Aix-Marseille University has resulted in the performance of multiple educational activities, both in remote an in-person format, as well as research activities on the development and characterization of silicon carbide and diamond semiconductor neutron detectors and calorimeters for the measurement of nuclear heating.

Fig. 34 displays a photograph of a group of students enrolled in the Masters' programme in instrumentation at the Aix-Marseille University, their lecturers and colleagues from the JSI during a 2-week educational course at the JSI TRIGA reactor in 2023.

4.2. Education of students

The MSc program in Nuclear engineering at the Faculty of Mathematics and Physics, University of Ljubljana, operates in close collaboration with the JSI TRIGA reactor. This two-year program provides students with a comprehensive understanding of mathematics, physics, engineering, and computer science, all within the context of nuclear technology. It caters to a diverse range of students with backgrounds in technical or natural sciences such as physics, mechanical engineering,

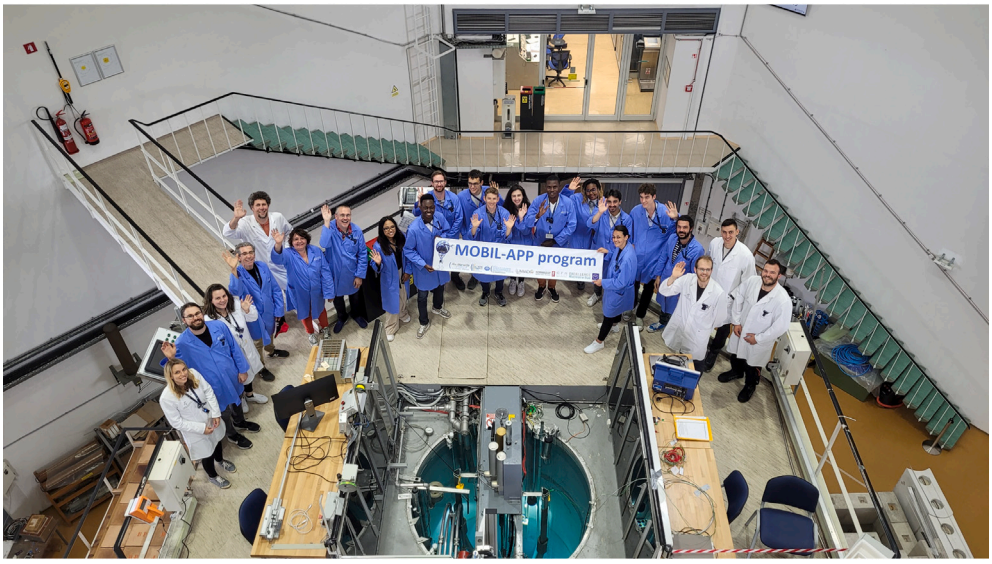

Fig. 34. Students from the Aix-Marseille University during a 2-week educational course at the JSI TRIGA reactor in 2023.

electrical engineering, construction engineering, metallurgy, chemistry, and mathematics. Obtaining a Master's degree in nuclear engineering enhances students' foundational university education by incorporating knowledge from nuclear physics and technology. Additionally, a variety of elective courses allow students to delve into current scientific topics within specific areas of nuclear engineering. The program starts with a couple of general mandatory courses. A key mandatory courses are "Nuclear, Reactor, and Radiological Physics" and "Experimental Reactor Physics" which include practical exercises conducted at the JSI TRIGA reactor. These courses allows students to actively participate in reactor operations, conduct experiments, and write reports on their findings. A key component of the curriculum is an exercise in which students have the opportunity to operate the reactor, providing them with a unique hands-on experience that deepens their understanding of reactor physics and operational safety. Through the further selection of elective courses, students can tailor their studies towards various aspects of nuclear technology, including nuclear physics, with additional course that includes TRIGA reactor exercises, nuclear safety, thermal hydraulics and process engineering, nuclear materials, probabilistic safety analysis, radiation safety, and fusion techniques.

The SARENA (Safe and Reliable Nuclear Applications) program, established under the European Commission's Erasmus Mundus initiative from 2018 to 2024, offers students worldwide the opportunity to pursue a master's degree in nuclear engineering with a focus on either radioactive waste management or nuclear reactor operation. Students receive scholarships for the two-year program, which includes educational periods at various higher education institutions. The program is divided into two tracks, each with specific study locations: The track on nuclear reactor operations (NROS) starts with the first semester ar Institut Mines-Télécom Atlantique (IMT) in France, second semester at LUT University in Finland and the third semester is held along the regular MSc program of Nuclear engineering at University of Ljubljana. One of the central courses of the NROS program is given as a practical course on TRIGA reactor of JSI is held jointly for the Slovenian students of the regular nuclear engineering program and for SARENA students. SARENA students of NROS track prepare their thesis in the fourth semester and receive dual degrees from LUT Lappeenranta and University of Ljubljana.

4.3. Remote exercises in times of pandemic

COVID-19 induced restrictions have prevented reactor physics students from attending in-person reactor physics exercises which are a vital part of their education. JSI has organized remote exercises (Malec et al., 2021) with the help of off-the-shelf technology, including multiple videoconferencing setups, remote desktop software, portable cameras, a dome camera, shared spreadsheets, and a common whiteboard. The students were encouraged to actively participate in the exercises by giving instructions to the reactor operator, asking and answering questions, logging data, operating digital acquisition systems, and performing analysis during the exercise. The first remote exercises were organized as a five-day course of experimental reactor physics for students from Uppsala University (see Fig. 35).

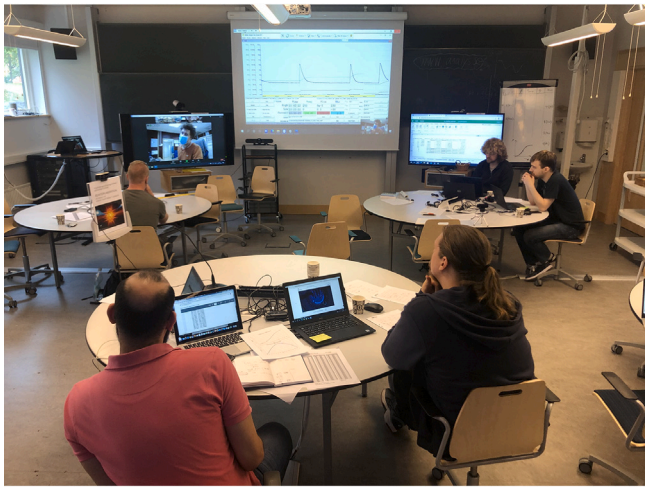

Fig. 35. Students at the Uppsala University attending remote exercises. In addition to the video feed of the lecturer, the students have access to multiple cameras throughout the reactor facility, a common spreadsheet, a stream of the digital whiteboard and real-time control of a computer for data acquisition.

4.4. Training of the Krško NPP Operators

After the Three-Mile-Island nuclear accident in 1979, the training of NPP operators focused on broader understanding of physical phenomena underlying the reactor operation. It was decided to build a Nuclear Training Centre within the Jožef Stefan Institute (in Slovenian language Izobraževalni Center za Jedrsko Tehnologijo or ICJT). The motivation was to use the best available experts in the country for the initial,

theoretical part of training, as well as to complement the theoretical lectures with practical experience by using the TRIGA reactor.

The theoretical training of control room operators lasts approximately 6 months (21 weeks) after which they continue for another 18 months with systems, on-the-job and simulator training at the Krško NPP. Since the establishment of ICJT in 1989, 20 courses for operators were held and 321 participants finished this course.

In addition, a shorter, 8-week course for other technical staff is organized. It is comprised of two parts (4 weeks theory and 4 weeks NPP systems) and is intended for local operators and technicians in the NPP, for technical support organizations, regulatory body staff, radioactive waste agency etc. In the last 35 years, 45 such courses were held with a total of 668 participants. The courses described in the previous paragraph include some practical work on the JSI TRIGA reactor. The most extensive in this regard is the course for future NPP operators.

The following nuclear and reactor physics exercises are routinely performed on the research reactor: Compensated ionization chamber, Critical experiment (fuel/control rod), Step reactivity changes, Temperature reactivity coefficient, Thermal power calibration, Control rod worth (rod swap/rod in), Pulse experiment, Xe poisoning, Void reactivity coefficient, In-core flux mapping, Primary water activation and Reactor operation.

For future NPP operators, the exercise "Reactor operation" is quite thorough and is followed by an exam. If they pass it successfully, they receive a certificate of "Junior research reactor operator" — similar to pilots of passenger jets who first need to obtain a sports pilot license.

Nominally, around 20 % of training is devoted to experimental training, mostly on the TRIGA reactor, with some exercises also in the radiation lab. As the exercises are typically performed by a group of 3–4 trainees, there are around 4 groups for experimental training in each course.

4.5. Public information

In addition to professional training, ICJT has actively been involved in public outreach activities related to nuclear energy (Jenčič and Snoj, 2016). Organized groups, mostly schoolchildren, are invited to ICJT where they attend to a lecture and visit a permanent exhibition on nuclear technology. Our printed materials and web site www.icjt.org have also become a respected source of information for the media and the general public.

For selected groups (with less than 30 participants) a visit of the JSI TRIGA reactor is also organized. For visitors, actually being able to see a nuclear reactor is a unique and convincing experience that nuclear energy should not be feared if managed properly and in a safe manner.

Since 1993, more than 200,000 visitors (10 % of the Slovenian population) attended a lecture for general public at ICJT, with a significant part of them also visiting the TRIGA reactor. These activities are assumed to have contributed to the fact that currently the public acceptance of nuclear energy is high — public opinion polls show that about 70% of respondents support the construction of a second NPP in Slovenia (poll conducted in January 2024) (Ninamedia, 2024). This is of particular importance as by the end of 2024, a referendum on nuclear energy is planned in Slovenia.

5. Development of computer codes and models

5.1. TRIGLAV

In order to support and improve reactor operation and utilization, the first version of the deterministic diffusion code TRIGLAV (Peršič et al., 2017) for reactor calculations was developed in the late 1990s to replace the older TRIGAC code [package ID: IAEA 1214 at the OECD NEA Data Bank], which was based on a 1D two-group diffusion equation solution in cylindrical geometry. TRIGLAV is available from the OECD NEA website on request.[2] The updated version, TRIGLAV-W,[3] features a user-friendly graphical Windows user interface (Zagar et al., 2006). Hence it is suitable for education and training purposes by universities (Wharton et al., 2005) and at international training courses on research reactors, such as the EERRI training course (Snoj et al., 2012a).

The TRIGLAV program package was developed for reactor calculations of mixed cores in the JSI TRIGA research reactor, and can be generalized to any research reactor with annular or cylindrical geometry. It can be applied for fuel element depletion calculations, for thermal power and neutron flux calculations and for critically predictions. The TRIGLAV code package is based on the four-group time independent diffusion equation in two dimensional cylindrical geometry. The diffusion equation is solved using the finite differences method with iteration of fission density. Material constants are assumed to be step functions of local geometrical variables. The geometry in the program is adjusted to the cylindrical core of the JSI TRIGA reactor. Every fuel and non-fuel element position in the core is treated as a unit cell. Group constants for all unit cells are calculated with the transport program WIMSD (Askew et al., 1966), which is integrated in the program package, in dependence of: fuel or non-fuel element geometry, material composition, actual fuel element burnup, temperature, water temperature and density, cladding temperature and ^{135}Xe concentration.

The program enables calculations of a wide variety of possible physical parameters, most importantly the multiplication factor, flux and power distribution, power defect, xenon poisoning, and fuel depletion. It may be used for more advanced applications such as optimization of core loading or estimation of safety parameters such as peaking factors and excess reactivity. The core shuffling is done with a user-friendly shuffling interface, capable of simulating individual fuel element movements (as presented in Fig. 36). The user is able to calculate important core parameters very quickly and efficiently. TRIGLAV-W is not only easy to use and fast; it is also gives reasonably accurate results. The accuracy of the calculated spectra, neutron flux distributions, fission densities, power peaking factors and similar parameters is normally better than 10%.

5.2. MCNP model

During the decades of using MCNP to simulate the JSI TRIGA reactor, the MCNP model of the JSI TRIGA was continuously being improved. The original MCNP model used for the initial benchmark evaluations (Jeraj and Ravnik, 1999) was improved by adding various components that are also specific to certain use cases. For example, when investigating different sample irradiations or detector measurements (e.g. in-core fission chamber or SPND), the required experimental components were added to the model to represent the experimental setup as accurately as possible. The developed MCNP model of the JSI TRIGA also enables quick core reconfigurations (e.g. adding experimental channels such as triangular channel or replacing them with fuel elements), which is essential due to the frequent core reconfigurations to match experimental conditions. For applications where the area of interest is located outside the reactor core (e.g. the investigations of neutron streaming in the reactor building), external structures, such as the biological shield and horizontal channels were also modeled. In general, the computational model of the JSI TRIGA reactor (see Fig. 37) consists of the reactor core, the graphite reflector, the penetrating irradiation channels and the surrounding water enclosed by the aluminum/concrete reactor pool. The components of the reactor core that significantly influence the calculated effective multiplication factor were modeled in detail, wherein the lack of reliable technical

[2] http://www.oecd-nea.org/tools/abstract/detail/iaea1370/
[3] http://www.rcp.ijs.si/triglav/

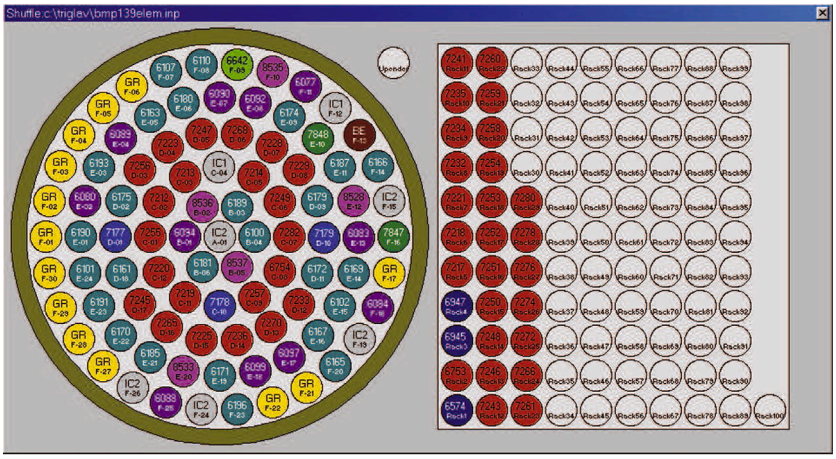

Fig. 36. Core loading pattern editor in the graphical interface of the TRIGLAV code (Peršič et al., 2017). Fuel and other elements can be moved from one location to another using a simple "click and point" procedure.

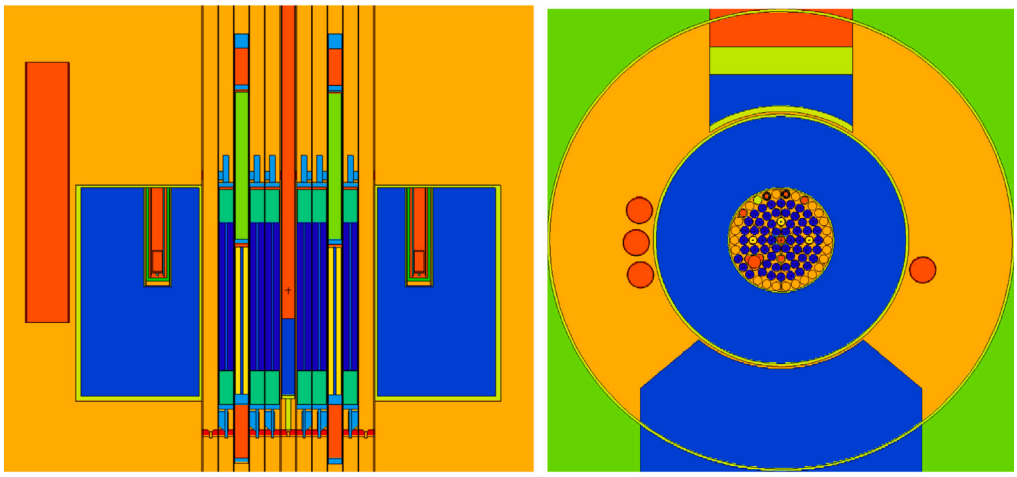

Fig. 37. MCNP geometrical model of the JSI TRIGA xz (left) and xy (right) view.

information often represents the limit. In the majority of calculations performed with the MCNP, the fuel was modeled as fresh, which was a good approximation, supported by the fact that fuel burnup in research reactors, such as a TRIGA reactor is low. However, recent studies of JSI TRIGA fuel burnup by examining the operating history from the beginning of operation (Pungerčič et al., 2023b), showed that fuel depletion can contribute up to ~4500 pcm. Another simplification included in most MCNP calculations is that the reactor core and water are modeled at room temperature and the temperature effects on water density and cross sections (for both water and fuel, including thermal scattering cross sections) have not been considered. The developed MCNP model of the JSI TRIGA reactor has been extensively validated through decades of experimental campaigns including validation of the in-core neutron and gamma-ray distributions. The model has also been used to characterize the gamma-ray field inside the JSI TRIGA irradiation facilities. This has been achieved by firstly simulating the prompt gamma-ray field, and secondly, the delayed gamma-ray field using the in-house developed JSIR2S code (Ambrožič and Snoj, 2020). Several experimental campaigns on gamma-ray field measurements (Gruel et al., 2020; Ambrožič et al., 2018) have been faithfully reproduced by simulations, and agreement between measured and simulated values was observed within their uncertainties.

5.3. ADVANTG model

Streaming, deep penetration, and shielding calculations are challenging and computationally intensive. To perform such calculations with acceptable statistical convergence a two-step hybrid transport approach using the MCNP code for particle transport calculations and the ADVANTG code (Mosher et al., 2015) for variance reduction was implemented. ADVANTG, an AutomateD VAriaNce reducTion Generator, is a code developed by the Oak Ridge National Laboratory, which automatically generates variance reduction parameters, defined in the MCNP input file, for neutron and/or gamma-ray-transport problems. ADVANTG generates energy- and space-dependent mesh-based weight windows parameters, and a biased source distribution based on an approximate deterministic solution of the adjoint and forward transport equation. The basic concept is to increase the rate of tally convergence by using variance reduction parameters and, therefore, to accelerate analogue Monte Carlo simulations in terms of required CPU time.

Our existing MCNP model was extended and now covers the whole reactor building, including the reactor basement and control room, in 2019 (see Fig. 38). The extended model and use of the ADVANTG code allowed us to perform neutron and gamma-ray dose rate calculations inside the reactor hall during reactor operation and in shutdown conditions. This approach was first used to characterize the dose field around

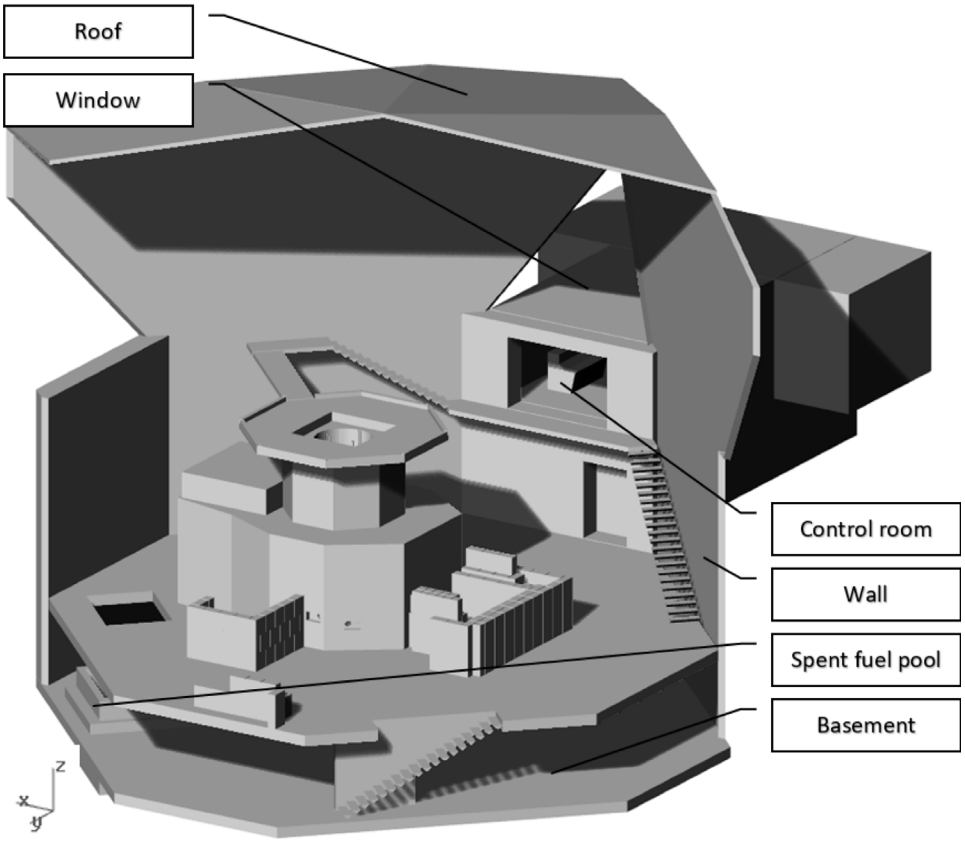

Fig. 38. Schematic view of the extended MCNP JSI TRIGA computational model including reactor hall used for ADVANTG calculations.

beam tube no. 5 (Jazbec et al., 2021a), where a new experimental facility was designed. Using the results, we optimized the shield before the construction phase.

The model also allowed us to simulate the dose field inside the reactor hall during reactor shutdown. This is useful for analyzing various accidental scenarios. The model allowed for the performance of dose field calculations for a hypothetical total loss of coolant scenario (Jazbec et al., 2021b). The obtained dose rates around the reactor were the same as the reference values from older analyses. However, details which became visible with the use of the model were not available before. For example, the major contribution to the dose rate inside the reactor hall does not originate directly from the core region but is backscattered from the reactor building ceiling and walls.

The calculations for the assessment of neutron and gamma-ray dose rates around KATANA (Kotnik et al., 2023b), a new irradiation facility at JSI TRIGA that utilizes a closed-water activation loop (chapter 3.2.1), were performed using MCNP6 v2.0, while the variance reduction parameters, more specifically the weight window parameters, were prepared using ADVANTG. The use of ADVANTG was essential to obtain any statistically significant data at all, as the KATANA facility is located outside the reactor biological shield. The calculations were performed using a fixed source in the reactor core (SDEF source in MCNP terminology), based on a well-converged criticality calculation, due to limitations in the ADVANTG code. The ADVANTG model is case-specific and therefore it has to be optimized for the specific geometry and area of interest. The deterministic ADVANTG calculation related to the KATANA facility was performed with a geometric mesh with 13.7×10^6 voxels that varied in size depending on the geometry, i.e. a finer mesh in the areas of the reactor core and radial piercing port (a few centimeters) and coarser mesh in the surroundings (from several centimeters to one meter), using the 27 neutron and 19 gamma-ray energy group reaction cross-section library a P-3 scattering-angle expansion and an S-4 angular approximation.

5.4. Serpent model

The paper (Ćalić et al., 2016) analyzes the validation of a 3D computational model of the TRIGA research reactor using the Serpent 2 code (Leppänen et al., 2015), version 2.1.24, with the ENDF/B-VII.0 nuclear data library (Chadwick et al., 2006). The detailed TRIGA Serpent model was created based on previous criticality benchmark models (Jeraj et al., 2002; Snoj et al., 2011a; Radulović et al., 2014) and includes structures outside the core, such as the tangential and radial beam ports, thermalizing, and thermal column components. Comparisons were made with experimental data and results from MCNP simulations.

The validation involved a series of experiments, focusing on the criticality benchmark experiment from 1991 and an experiment with Al-Au foils irradiated in various core channels and the rotary groove surrounding it. The comparison between simulations and experiments, particularly regarding reaction rates in the carousel facility, showed close agreement between Serpent and MCNP values (see Fig. 39). The maximum difference was less than 2 %, while discrepancies with experimental results mostly fell within the range of 2 % to 3 %. Overall, the results were consistent within experimental and Monte Carlo uncertainties.

While criticality results agreed well within expected uncertainties and core reaction rates closely matched MCNP and experimental data, some discrepancies were noted in the reflector region, largely due to higher uncertainties. However, given the intended application for depletion calculations, these small discrepancies are less significant for the Serpent code, compared to MCNP.

5.5. OpenMC model

A 3D computational model of the JSI TRIGA research reactor was also developed using the OpenMC code (see Fig. 40 and Fig. 41) (Vavtar

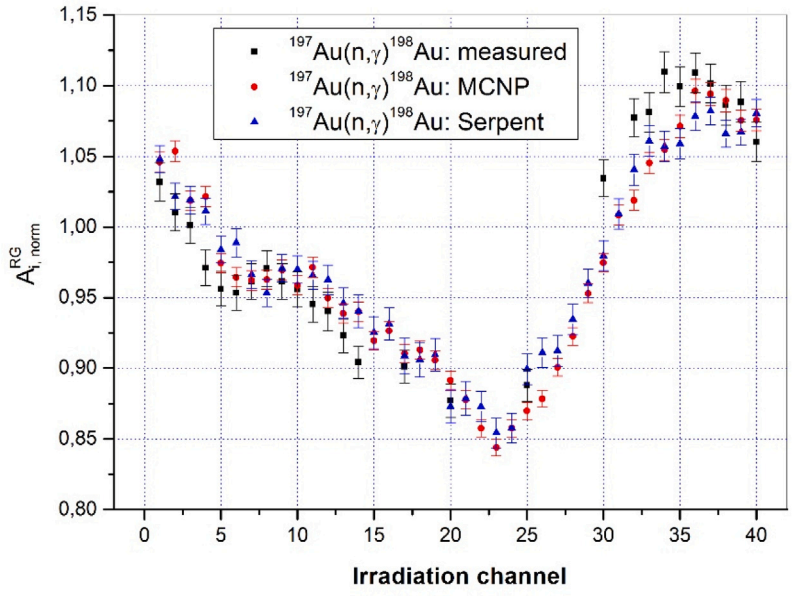

Fig. 39. Calculated and measured reaction rates (^{197}Au(n, γ)^{198}Au) in the irradiation channels of the carousel facility normalized to the average of all irradiation channels.

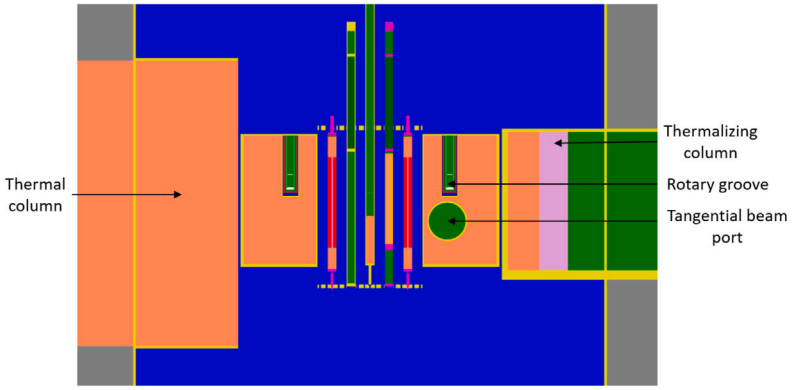

Fig. 40. Detailed geometrical model (yz view) of the TRIGA research reactor in OpenMC.

et al., 2017). The calculated parameters (multiplication factor k_{eff} and radial neutron flux distributions) were compared to the experimental results and to calculations performed with the MCNP code. Results for the effective multiplication factor k_{eff} at critical conditions are within benchmark uncertainty. The results obtained with OpenMC code in comparison to the values obtained with experiments and with MCNP code for neutron flux distributions mostly agree within their uncertainties. The deviation may be the result of a small number of simulated particles and the irregular shape of radial beam port and radial piercing thruport.

The Masters thesis (Sánchez Sanz, 2023) used OpenMC to model both the full reactor core and a simplified unit cell to test how variations in hydrogen distribution within UZrHx fuel affect the neutron multiplication factor and other physical parameters of the JSI TRIGA Mark II reactor. The effect of hydrogen concentration depends on the model used in the simulation: a homogeneous decrease in hydrogen concentration in the full core model results in a decrease in the multiplication factor, while in the simplified unit cell model with no leakage, the effect is the opposite.

5.6. TRIPOLI model

The paper (Henry et al., 2015) investigates the validation of a 3D computational model of the JSI TRIGA research reactor using the TRIPOLI code, version 4 (Petit et al., 2008), and different cross-section libraries: ENDF/B-VI.6 (with thermal scattering $S(\alpha,\beta)$ cross sections for H and Zr from ENDF/B-VII.0), ENDF/B-VII.0 (Chadwick et al., 2006), and JEFF-3.1 (Santamarina et al., 2009). Three types of analyses were performed: comparison of criticality benchmark results obtained with MCNP, comparison of reaction rate calculations with experimental and MCNP results, and comparison of TRIGA reactor kinetic parameters obtained with MCNP for various fuel types and core configurations.

The study addresses systematic biases and errors arising from geometry simplifications and uncertainties in material and geometry data of the benchmark models (Ravnik and Jeraj, 2003). The results show a relatively good agreement between the multiplication factors obtained with TRIPOLI and MCNP (Snoj et al., 2011a). The relative differences between calculated and measured reaction rates are on average around 5 % in the JSI TRIGA core and 4 % in the rotary groove. The calculations of the kinetic parameters show that the mean generation time decreases with increasing ^{235}U content and exhibits a linear relationship to the inverse ^{235}U atomic density.

The paper demonstrates the suitability of the TRIPOLI Monte Carlo code for modeling complex geometries (Snoj et al., 2010), the observed discrepancies in the results are mainly due to nuclear data libraries and not to different methods or codes. In addition, the prompt neutron generation time Λ strongly correlates with fuel type (uranium content) as presented in Fig. 42, while β_{eff} is influenced more by core size

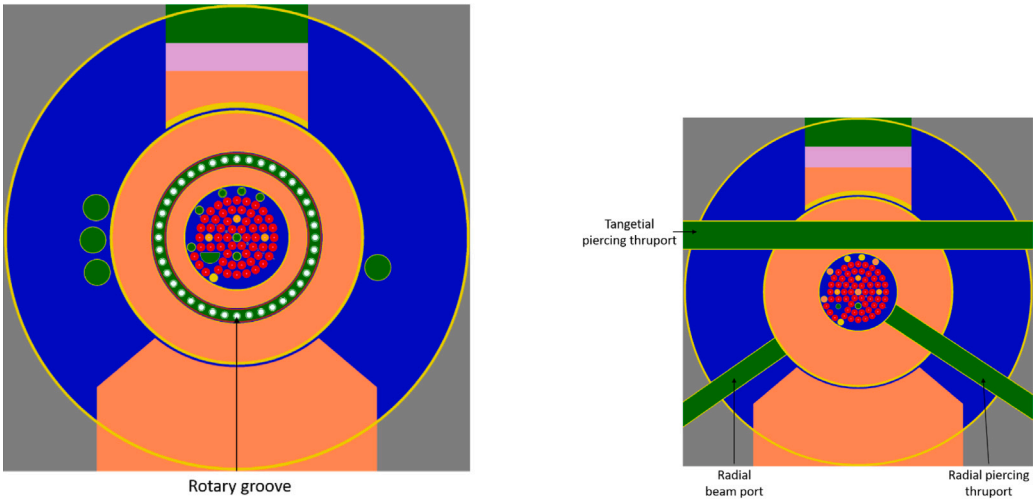

Fig. 41. Detailed geometrical model (xy view) of the TRIGA research reactor at different heights in OpenMC.

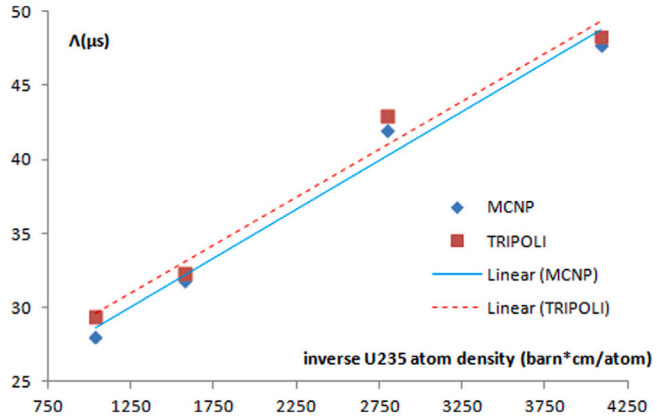

Fig. 42. Mean generation time as a function of inverse ^{235}U atom density.

(leakage), though significant differences in β_{eff} values also arise from variations in delayed neutron data.

5.7. RAPID development and validation

The RAPID code system, developed based on the Multi-stage Response-function Transport methodology (Haghighat et al., 2016), solves response matrix/coefficient form of neutron transport equation in seconds to minutes on a single computer core, by using pre-determined response functions/coefficients for a given problem through detailed continuous-energy Monte Carlo calculations. These coefficients, which are problem dependent, are calculated as a function of several input parameters (e.g., moderator and fuel temperature, material changes) and are then compiled in a database. The database is then used to perform neutron transport calculations (e.g., criticality calculations, time-dependent kinetic calculations, subcritical multiplication, detector responses, ...) in seconds to minutes for every system configuration within the database validity range.

The RAPID code system (Walters et al., 2018) has been validated by comparison with Monte Carlo neutron transport for a number of different nuclear fission systems, such as: spent nuclear fuel pools (Walters et al., 2015; Roskoff et al., 2018), spent fuel casks (Mascolino et al., 2017, 2018), nuclear power reactor cores (Walters et al., 2018; He and Walters, 2019; Topham et al., 2020), and subcritical facilities (Roskoff et al., 2018). More recently, it has been validated using reference computational results and experimental data from the JSI TRIGA research reactor for steady-state operation and for transients that occur due to control rod movements (Mascolino, 2021; Mascolino et al., 2021, 2022, 2024). The effect of control rod insertion on fission matrix coefficients was studied. The results for compensating/shim rod are presented in Fig. 43. In addition to steady-state calculations, kinetic TRIGA parameters (e.g., effective neutron lifetime, L_{eff}; α_{Rossi}) (Mascolino, 2021; Mascolino and Haghighat, 2024; Mascolino et al., 2024), time-dependent 3-D prompt and delayed fission source distribution (Mascolino and Haghighat, 2024; Mascolino et al., 2024) and fuel burnup (Pungerčič et al., 2023b) were studied. RAPID is able to calculate steady-state and time-dependent reactor core parameters and 3-D distributions of nuclear quantities of interest (e.g., neutron source, detector responses).

Once the fission matrix coefficients are pre-calculated, RAPID can simulate the TRIGA reactor core for any combination of control rod positions in the TRIGA in seconds to minutes on one computer core, while for the same calculation Serpent-2 (Leppänen et al., 2015) requires several hours using parallel computers. To achieve the above speedups, RAPID employs several hybrid deterministic/Monte Carlo methodologies to minimize the amount of pre-calculation needed to compile the fission matrix database. One such methodology accounts for the insertion of different control rods by decoupling their effect and combining them into the problem's fission matrix (Mascolino et al., 2022). This methodology has shown the ability to accurately predict the 3-D neutron flux redistribution effects caused by the simultaneous presence of different control rods, even when significant asymmetries are considered.

RAPID is also capable of simulating reactor kinetics transients and calculating the full 3-D time-dependent distribution of the prompt and delayed fission source during the entire transient, a level of detail that is computationally prohibitive to obtain with state-of-the-art Monte Carlo software, especially when complex geometry variations need to be taken into account (e.g., movement of control rods). The TRIGA reactor was used to validate the time-dependent algorithms recently implemented into RAPID, using reference validated Monte Carlo models and experiments (Mascolino and Haghighat, 2024; Mascolino et al., 2024) designed by a collaboration between the JSI and Virginia Tech teams. Fig. 44 shows the volume-integrated time-dependent fission source as calculated by RAPID for the prompt neutrons and six delayed neutron precursors families during a rod insertion experiment at JSI.

5.8. Thermal-hydraulics model

Multi-physics simulations of nuclear reactors, which integrate thermal-hydraulics and neutron physics, present a challenge in nuclear engineering today. Coupled simulations can unveil detailed properties

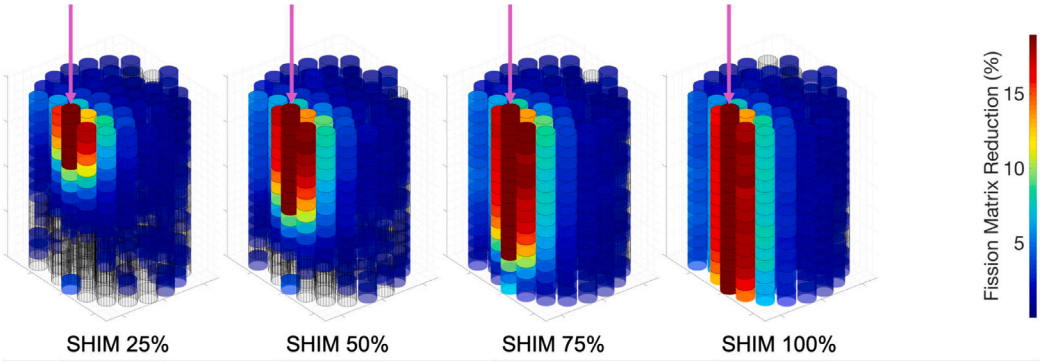

Fig. 43. Percentage variation of integrated fission matrix coefficients, with Shim rod insertion with respect to the all rods out (ARO) case. The arrow indicates the control rod. Variation values smaller than their uncertainties are blanked out (Mascolino et al., 2022).

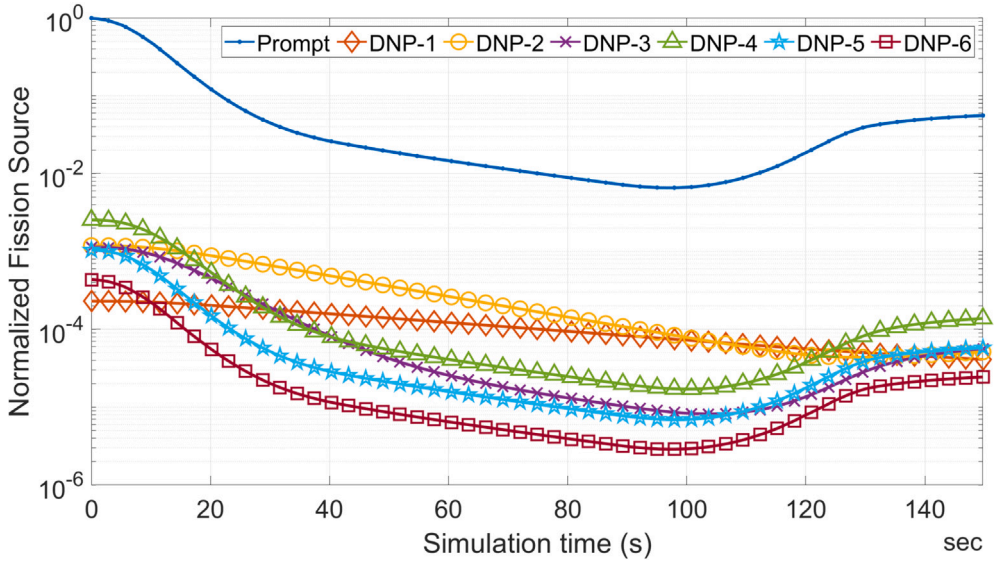

Fig. 44. Space-integrated time-dependent fission neutron source distribution for prompt neutrons and 6 delayed neutrons families (ranging from slowest No. 1 to fastest No. 6) during a Rod Insertion experiment (Mascolino and Haghighat, 2024).

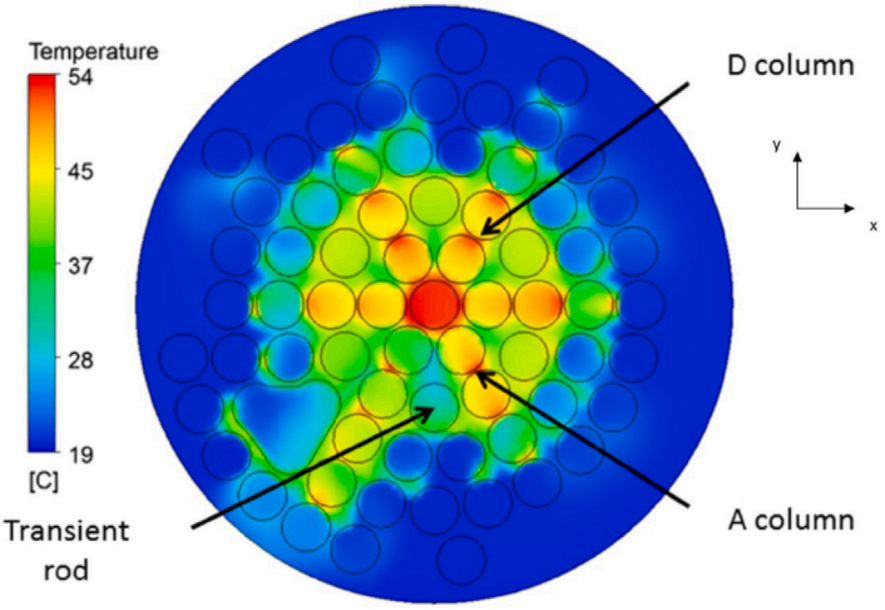

Fig. 45. Calculated water temperature 0.3 m above the top grid of the TRIGA core.

(a) Screenshot of the main panel of the Research Reactor Simulator.

(b) A hardware console was developed for the Research Reactor Simulator.

Fig. 46. Research Reactor Simulator can be controlled using mouse and keyboard (a) or a hardware console (b).

of the reactivity coefficients, which play a pivotal role in assessing the implications of sudden changes in operational parameters of nuclear reactors and ensuring the performance and safety of the core. Henry et al. (2015, 2017b) focused on developing a communication interface to couple the neutron transport code TRIPOLI with the computational fluid dynamics (CFD) code CFX, applied to the TRIGA reactor. The creation of a three-dimensional CFD model of the TRIGA reactor revealed the detailed structure of velocity and temperature fields in the reactor core and in the pool above the core, where natural convection interacts with forced convection imposed by the cooling system (see Fig. 45). CFD simulations were compared with temperature measurements and further coupled with neutron physics analyses, revealing a relatively weak coupling between neutronics and thermal-hydraulics within the TRIGA reactor core. While coolant temperature and density had minimal influence on power distribution, the fuel temperature reactivity coefficient significantly impacted reactivity. Coupled neutron physics-thermal-hydraulic CFD simulations successfully reproduced these phenomena and underscored the localized effects of fuel temperature on power density.

5.9. Reactor simulator

A simulator (Malec et al., 2020) for real-time research reactor operation was developed at the JSI, aimed at educational and training needs of students and prospective reactor operators, particularly in regions without direct access to such facilities (see Fig. 46). The simulator, designed to mimic the reactor kinetics, fuel temperature, and reactivity, utilizes the six-group point kinetics equations augmented with feedback mechanisms, including temperature feedback and xenon poisoning effects. By leveraging graphics acceleration for visualizing simulation outcomes, and employing a straightforward integration approach with minimal simulation steps, the tool enables high responsiveness to user interactions, a critical feature for simulating research reactors capable of rapid transient behaviors. While the focus is on TRIGA-type reactors, the simulator's flexible design allows for on-the-fly modifications of physical parameters, facilitating its adaptation for a broad range of reactor models.

According to the web metrics, the Research Reactor Simulator was downloaded more than 2000 times (as of October 2024) and is currently being used to teach nuclear reactor physics to the physics and nuclear engineering students at Faculty of Mathematics and Physics, University of Ljubljana.

6. Conclusion

The JSI TRIGA Mark II research reactor has been a cornerstone of nuclear research and education, exemplifying the indispensable role that small and medium-sized research reactors play in the nuclear field. Over the past five decades, this reactor has been instrumental in advancing scientific research, technological development, and education, as well as fostering international collaboration. Its contributions span reactor physics, radiation science, and environmental studies, alongside the development and validation of new nuclear technologies and methodologies. The JSI TRIGA reactor has also been a prolific source of scientific output, with more than 450 research articles published between 1966 and 2024,[4] highlighting the reactor's significant impact on the scientific community. This extensive body of work underscores the reactor's role as a vital research facility, enabling a wide range of experiments and studies that have contributed substantially to the advancement of nuclear science and technology.

The ongoing relevance of small and medium-sized research reactors is evident in their versatility and capability to support a broad spectrum of experimental and educational activities. These reactors are crucial for conducting experiments that validate computational models, advance material science, and test radiation detection technologies. Moreover, their role in the education and training of future nuclear scientists and engineers is essential for sustaining and expanding expertise in the nuclear sciences. Looking to the future, the proposed VERONICA reactor (Versatile European Reactor fOr Neutron Irradiation and nuClear reseArch) represents a significant step forward in maintaining and enhancing Europe's capacity for advanced nuclear research and irradiation services. VERONICA is envisioned as a state-of-the-art facility that will address the growing demand for versatile research infrastructure, capable of supporting a wide array of scientific and technological applications. This project will continue the legacy of small and medium-sized reactors, which have been fundamental to the progression of nuclear science (Malec et al., 2019, 2022).

The establishment of VERONICA would not only replace aging reactors but would also push the boundaries of nuclear research, creating new opportunities for scientific discovery and contributing to the development of safer and more efficient nuclear technologies. By continuing to generate high-quality scientific output and fostering innovation, VERONICA and similar projects would ensure that the nuclear research field remains dynamic and capable of addressing the challenges of the future, thereby maintaining Europe's leadership in the global nuclear research community.

Declaration of competing interest

The authors declare the following financial interests/personal relationships which may be considered as potential competing interests: Luka Snoj, Klemen Ambrozic, Dusan Calic, Domen Kotnik, Igor Lengar, Jan Malec, Ingrid Svajger, Andrej Trkov, Bojan Zefran, Tanja Goricanec

[4] https://ric.ijs.si/clanki/

reports financial support was provided by Slovenian Research and Innovation Agency. If there are other authors, they declare that they have no known competing financial interests or personal relationships that could have appeared to influence the work reported in this paper.

Acknowledgments

The research is funded by the research core funding No. P2-0073 from the Slovenian Research Agency, Slovenia.

Data availability

Data will be made available on request.

References

Ali, S.W., Božič, D., Vijayakumaran Nair, S., Živković, I., Gačnik, J., Andron, T.-D., Jagodic Hudobivnik, M., Kocman, D., Horvat, M., 2024. Optimization of a pre-concentration method for the analysis of mercury isotopes in low-concentration foliar samples. Anal. Bioanal. Chem. 1–10.

Ambrožič, K., Gruel, A., Radulović, V., Le Guillou, M., Blaise, P., Destouches, C., Snoj, L., 2018. Delayed gamma determination at the JSI TRIGA reactor by synchronous measurements with fission and ionization chambers. Nucl. Instrum. Methods Phys. Res. Sec. A (ISSN: 0168-9002) 911, 94–103. http://dx.doi.org/10.1016/j.nima.2018.09.103, URL https://www.sciencedirect.com/science/article/pii/S0168900218312567.

Ambrožič, K., Malik, K., Obryk, B., Snoj, L., 2020. JSI TRIGA neutron and gamma field characterization by TLD measurements. EPJ Web Conf. 225, 04034. http://dx.doi.org/10.1051/epjconf/202022504034.

Ambrožič, K., Snoj, L., 2016a. On Development and Calculations of High Radiation Tolerant Surveillance Camera System for ISEC. IJS Work Report IJS-DP-12117, "Jožef Stefan" Institute, Reactor Physics Department, Ljubljana, Slovenia.

Ambrožič, K., Snoj, L., 2016b. On Development and Calculations of Low Radiation Tolerant Surveillance Camera System for ISEC. IJS Work Report IJS-DP-12115, "Jožef Stefan" Institute, Reactor Physics Department, Ljubljana, Slovenia.

Ambrožič, K., Snoj, L., 2016c. Report on Equipment Irradiation Tests for ISEC. IJS Work Report IJS-DP-12116, "Jožef Stefan" Institute, Reactor Physics Department, Ljubljana, Slovenia.

Ambrožič, K., Snoj, L., 2020. JSIR2S code for delayed radiation simulations: Validation against measurements at the JSI TRIGA reactor. Progress Nucl. Energy (ISSN: 0149-1970) 129, 103498. http://dx.doi.org/10.1016/j.pnucene.2020.103498, URL https://www.sciencedirect.com/science/article/pii/S0149197020302432.

Anon, 2017. Strategic planning for research reactors. In: Nuclear Energy Series, (no. NG-T-3.16), INTERNATIONAL ATOMIC ENERGY AGENCY, Vienna, ISBN: 978-92-0-101317-0, URL https://www.iaea.org/publications/10988/strategic-planning-for-research-reactors.

Anon, 2023. Recommendations for planning refurbishment of existing research reactors or construction of new ones. In: TOURR Project Deliverable D3.4, (no. Euratom Fission NFRP-2019-2020), Euroatom Coordination Action - EuroRef. Ares(2023)8057826, URL https://www.tourr.eu/documents.

Askew, J., Fayers, F., Kemshell, P., 1966. General description of the lattice code WIMS. J. Brit. Nucl. Energy Soc..

Baldi, F., Gallo, M., Marchetto, D., Fani, R., Maida, I., Horvat, M., Fajon, V., Zizek, S., Hines, M., 2012. Seasonal mercury transformation and surficial sediment detoxification by bacteria of Marano and Grado lagoons. Estuarine, Coast. Shelf Sci. 113, 105–115.

Barbot, L., De Izarra, G., Destouches, C., Bisiach, D., Cargnelutti, M., Zorzut, S., Škabar, M., Bardorfer, A., Makovac, A., Trnovec, J., Paglovec, P., 2023. Qualification of the industrialized libera MONACO 3 digital acquisition system dedicated to fission/ion chamber measurements in research reactors. In: EPJ Web of Conferences, vol. 288, p. 5, URL https://www.epj-conferences.org/articles/epjconf/abs/2023/14/epjconf_animma2023_04019/epjconf_animma2023_04019.html.

Barbot, L., Domergue, C., Breaud, S., Destouches, C., Villard, J.-F., Snoj, L., Štancar, Ž., Radulović, V., Trkov, A., 2013. Neutron field characterization of irradiation locations applied to the slovenian TRIGA reactor. In: 2013 3rd International Conference on Advancements in Nuclear Instrumentation, Measurement Methods and their Application. ANIMMA, IEEE, pp. 1–5.

Barbot, L., Villard, J.-F., Fourrez, S., Pichon, L., Makil, H., 2018. The self-powered detector simulation 'MATiSSe' toolbox applied to SPNDs for severe accident monitoring in PWRs. EPJ Web Conf. 170, 08001. http://dx.doi.org/10.1051/epjconf/201817008001.

Bernat, R., Knežević, T., Radulović, V., Snoj, L., Makino, T., Ohshima, T., Capan, I., 2023. Radiation response of large-area 4H-SiC Schottky barrier diodes. Materials (ISSN: 1996-1944) 16 (6), http://dx.doi.org/10.3390/ma16062202, URL https://www.mdpi.com/1996-1944/16/6/2202.

Bratkic, A., Jazbec, A., Toplak, N., Koren, S., Lojen, S., Tinta, T., Kostanjsek, R., Snoj, L., 2023. The colonization of an irradiated environment: the case of microbial biofilm in a nuclear reactor. Int. J. Radiat. Biol. 1–14.

Bratkič, A., Koron, N., Ribeiro Guevara, S., Faganeli, J., Horvat, M., 2017. Seasonal variation of mercury methylation potential in pristine coastal marine sediment from the Gulf of Trieste (northern Adriatic Sea). Geomicrobiol. J. 34 (7), 587–595.

Briggs, J.B., et al., 2006. International Handbook of Evaluated Reactor Physics Benchmark Experiments. Tech. Rep., NEA/NSC/DOC Paris, France.

Brown, D., Chadwick, M., Capote, R., Kahler, A., Trkov, A., Herman, M., Sonzogni, A., Danon, Y., Carlson, A., Dunn, M., Smith, D., Hale, G., Arbanas, G., Arcilla, R., Bates, C., Beck, B., Becker, B., Brown, F., Casperson, R., Conlin, J., Cullen, D., Descalle, M.-A., Firestone, R., Gaines, T., Guber, K., Hawari, A., Holmes, J., Johnson, T., Kawano, T., Kiedrowski, B., Koning, A., Kopecky, S., Leal, L., Lestone, J., Lubitz, C., Márquez Damián, J., Mattoon, C., McCutchan, E., Mughabghab, S., Navratil, P., Neudecker, D., Nobre, G., Noguere, G., Paris, M., Pigni, M., Plompen, A., Pritychenko, B., Pronyaev, V., Roubtsov, D., Rochman, D., Romano, P., Schillebeeckx, P., Simakov, S., Sin, M., Sirakov, I., Sleaford, B., Sobes, V., Soukhovitskii, E., Stetcu, I., Talou, P., Thompson, I., van der Marck, S., Welser-Sherrill, L., Wiarda, D., White, M., Wormald, J., Wright, R., Zerkle, M., Žerovnik, G., Zhu, Y., 2018. ENDF/B-VIII.0: The 8th major release of the nuclear reaction data library with CIELO-project cross sections, new standards and thermal scattering data. Nucl. Data Sheets (ISSN: 0090-3752) 148, 1–142. http://dx.doi.org/10.1016/j.nds.2018.02.001, URL https://www.sciencedirect.com/science/article/pii/S0090375218300206. Special Issue on Nuclear Reaction Data.

Ćalić, D., Žerovnik, G., Trkov, A., Snoj, L., 2016. Validation of the Serpent 2 code on TRIGA Mark II benchmark experiments. Appl. Radiat. Isotopes 107, 165–170.

Carlile, C., Petrillo, C., Carpineti, M., Donzelli, M., 2016. Neutron scattering facilities in Europe: Present status and future perspectives. ESFRI Report, Eur. Landsc. Res. Infrast.-ESFRI 123.

Chadwick, M.B., Obložinskỳ, P., Herman, M., Greene, N.M., McKnight, R.D., Smith, D.L., Young, P.G., MacFarlane, R.E., Hale, G.M., Frankle, S.C., et al., 2006. ENDF/B-VII.0: Next generation evaluated nuclear data library for nuclear science and technology. Nucl. Data Sheets 107 (12), 2931–3060.

Chadwick, M.B., et al., 2011. ENDF/B-VII.1 nuclear data for science and technology: Cross sections, covariances, fission product yields and decay data. Nucl. Data Sheets 112 (12), 2887–2996.

Chao, Y.A., Chapman, D.M., Easter, M.E., Hill, D.J., Hoerner, J.A., Kurtz, P.N., 1992. Methodology of the Westinghouse dynamic rod worth measurement technique. Trans. Am. Nucl. Soc.; (United States) (ISSN: 0003-018X) 66, URL https://www.osti.gov/biblio/6983485.

Chouhan, R.S., Gačnik, J., Živković, I., Nair, S.V., Van de Velde, N., Vesel, A., Šket, P., Gandhi, S., Jerman, I., Horvat, M., 2023. Green synthesis of a magnetite/graphitic carbon nitride 2D nanocomposite for efficient Hg 2+ remediation. Environ. Sci.: Nano 10 (10), 2658–2671.

Coutinho, J., Torres, V.J., Capan, I., Brodar, T., Ereš, Z., Bernat, R., Radulović, V., Ambrožič, K., Snoj, L., Pastuović, Ž., Sarbutt, A., Ohshima, T., Yamazaki, Y., Makino, T., 2021. Silicon carbide diodes for neutron detection. Nucl. Instrum. Methods Phys. Res. Sec. A (ISSN: 0168-9002) 986, 164793. http://dx.doi.org/10.1016/j.nima.2020.164793.

De Corte, F., De Wispelaere, A., Van Sluijs, R., Bossus, D., Simonits, A., Kučera, J., Frána, J., Smodis, B., Jaćimović, R., 1997. The installation of KAYZERO-assisted NAA for use in industry and environmental sanitation in three Central European countries: Plans and achievements of a COPERNICUS project. J. Radioanal. Nucl. Chem. 215, 31–37.

De Corte, F., van Sluijs, R., Simonits, A., Kučera, J., Smodiš, B., Byrne, A.R., Wispelaere, A.D., Bossus, D., Frána, J., Horák, Z., et al., 2001. The validation of Kayzero-assisted NAA in Budapest, Řež, and Ljubljana via the analysis of three BCR certified reference materials. Fresenius' J. Anal. Chem. 370, 38–41.

Depriest, K.R., 2019. Historical Examination of the ASTM Standard E722 1-MeV Silicon Equivalent Fluence Metric. Tech. Rep., Sandia National Laboratories (SNL), Albuquerque, NM, and Livermore, CA ....

Dimic, V., 1976. Operation and Maintenance of the 250 kW TRIGA Mark II Reactor at the J Stefan Institute, Ljubljana, Yugoslavia. Tech. Rep., Austria, pp. 11–110, URL http://inis.iaea.org/search/search.aspx?orig_q=RN:40030680. INIS-AT–09N0002.

Dimic, V., 1986. Twenty Years of Operation of Ljubljana's TRIGA Mark II Reactor. Tech. Rep., International Atomic Energy Agency (IAEA), pp. I1–I17, URL http://inis.iaea.org/search/search.aspx?orig_q=RN:40018416. INIS-XA–08N1484.

Dimic, V., Gabrovsek, Z., 1972. Operation, Maintenance, and Utilization of the 250 kW TRIGA Mark II Reactor. Tech. Rep., Italy, pp. 281–287, URL http://inis.iaea.org/search/search.aspx?orig_q=RN:40091468. INIS-IT–09N0001.

Dimic, V., Glumac, B., Kavšek, D., Lipič, L., Mele, I., Pregl, G., Ravnik, M., Trkov, A., 1995. Renewal and Upgrading of the TRIGA Mark II Research Reactor In Ljubljana. GKSS-Forschungszentrum Geesthacht, pp. 190–215, Soavtorji Bogdan Glumac, Darko Kavšek, Ludvik Lipič, Irena Mele, Gvido Pregl, Matjaž Ravnik, Andrej Trkov.

Dimic, V., Petkovsek, J., 1971. Construction and performance of the liquid methane cold source. J. Phys. E: Sci. Instrum. 4 (11), 905. http://dx.doi.org/10.1088/0022-3735/4/11/028.

Dito Lighting, 2024. Dito lighting - lighting solutions. https://www.dito-lighting.com/. (Accessed 14 October 2024).

Ferdinand, P., et al., DISCOMS: Diustributed sensing for corium monitoring and safety. In: International Conference on Smart Materials and Structures, July 2015, Vancouver, Canada.

Filliatre, P., Jammes, C., Barbot, L., Fourmentel, D., Geslot, B., Lengar, I., Jazbec, A., Snoj, L., Žerovnik, G., 2015. Experimental assessment of the kinetic parameters of the JSI TRIGA reactor. Ann. Nucl. Energy 83, 236–245.

Gačnik, J., Živković, I., Ribeiro Guevara, S., Jaćimović, R., Kotnik, J., De Feo, G., Dexter, M.A., Corns, W.T., Horvat, M., 2021a. Behavior of KCl sorbent traps and KCl trapping solutions used for atmospheric mercury speciation: stability and specificity. Atmos. Meas. Tech. 14 (10), 6619–6631.

Gačnik, J., Živković, I., Ribeiro Guevara, S., Jaćimović, R., Kotnik, J., Horvat, M., 2021b. Validating an evaporative calibrator for gaseous oxidized mercury. Sensors 21 (7), 2501.

Gačnik, J., Živković, I., Ribeiro Guevara, S., Kotnik, J., Berisha, S., Vijayakumaran Nair, S., Jurov, A., Cvelbar, U., Horvat, M., 2022. Calibration approach for gaseous oxidized mercury based on nonthermal plasma oxidation of elemental mercury. Anal. Chem. 94 (23), 8234–8240.

Geslot, B., Berhouet, F., Oriol, L., Bréaud, S., Jammes, C., Filliatre, P., Villard, J., 2009. Development and manufacturing of special fission chambers for in-core measurement requirements in nuclear reactors. In: 2009 1st International Conference on Advancements in Nuclear Instrumentation, Measurement Methods and their Applications. IEEE, pp. 1–4.

Glinšek, S., Pečnik, T., Cindro, V., Kmet, B., Rožič, B., Malič, B., 2015. Role of the microstructure in the neutron and gamma-ray irradiation stability of solution-derived Ba0.5Sr0.5TiO3 thin films. Acta Mater. (ISSN: 1359-6454) 88, 34–40. http://dx.doi.org/10.1016/j.actamat.2015.01.028, URL https://www.sciencedirect.com/science/article/pii/S1359645415000415.

Glumac, B., Škraba, G., 1989. Rod Insertion Method for Rod Worth Measurement. In: IAEA Technical Committee Meeting on Operational Safety Experience of Two-Loop Pressurized Water Reactors. (no. IAEA/TC-650), International Atomic Energy Agency, pp. 280–297.

Goorley, J.T., James, M., Booth, T., Brown, F., Bull, J., Cox, L., Durkee, J., Elson, J., Fensin, M., Forster, A., et al., 2013. Initial MCNP6 Release Overview-MCNP6 version 1.0, LA-UR-13-22934. Los Alamos National Laboratory 43.

Goričanec, T., Kos, B., Ambrožič, K., Trkov, A., Snoj, L., Kromar, M., 2023. Determination of neutron flux redistribution factors for a typical pressurized water reactor ex-core measurements using Monte Carlo technique. Front. Energy Res. 11, 1137867. http://dx.doi.org/10.3389/fenrg.2023.1137867.

Goričanec, T., Žerovnik, G., Barbot, L., Fourmentel, D., Destouches, C., Jazbec, A., Snoj, L., 2018. Evaluation of neutron flux and fission rate distributions inside the JSI TRIGA Mark II reactor using multiple in-core fission chambers. Ann. Nucl. Energy 111, 407–440. http://dx.doi.org/10.1016/j.anucene.2017.08.017.

Gruel, A., Ambrožič, K., Destouches, C., Radulović, V., Sardet, A., Snoj, L., 2020. Gamma-Heating and Gamma flux measurements in the JSI TRIGA Reactor: Results and prospects. IEEE Trans. Nucl. Sci. 67 (4), 559–567. http://dx.doi.org/10.1109/TNS.2020.2974968.

Guevara, S.R., Horvat, M., 2013. Stability and behaviour of low level spiked inorganic mercury in natural water samples. Anal. Methods 5 (8), 1996–2006.

Haghighat, A., Royston, K., Walters, W., 2016. MRT methodologies for real-time simulation of nonproliferation and safeguards problems. Ann. Nucl. Energy 87, 61–67.

He, D., Walters, W.J., 2019. A local fission matrix correction method for heterogeneous whole core transport with RAPID. Ann. Nucl. Energy 134, 263–272.

Henry, R., Tiselj, I., Matkovič, M., 2017a. Natural and mixed convection in the cylindrical pool of TRIGA reactor. Heat Mass Transf. 53, 537–551.

Henry, R., Tiselj, I., Snoj, L., 2015. Analysis of JSI TRIGA MARK II reactor physical parameters calculated with TRIPOLI and MCNP. Appl. Radiat. Isotopes 97, 140–148.

Henry, R., Tiselj, I., Snoj, L., 2017b. CFD/Monte-Carlo neutron transport coupling scheme, application to TRIGA reactor. Ann. Nucl. Energy 110, 36–47.

Hines, M.E., Poitras, E.N., Covelli, S., Faganeli, J., Emili, A., Žižek, S., Horvat, M., 2012. Mercury methylation and demethylation in Hg-contaminated lagoon sediments (Marano and Grado Lagoon, Italy). Estuarine, Coast. Shelf Sci. 113, 85–95.

Huseynov, E.M., 2017. Investigation of the agglomeration and amorphous transformation effects of neutron irradiation on the nanocrystalline silicon carbide (3C-SiC) using TEM and SEM methods. Physica B: Condens. Matter 510, 99–103.

Huseynov, E.M., 2018a. Dielectric loss of neutron-irradiated nanocrystalline silicon carbide (3C-SiC) as a function of frequency and temperature. Solid State Sci. 84, 44–50.

Huseynov, E.M., 2018b. Electrical impedance spectroscopy of neutron-irradiated nanocrystalline silicon carbide (3C-SiC). Appl. Phys. A 124 (1), 19.

Huseynov, E.M., 2020. Thermal stability and heat flux investigation of neutron-irradiated nanocrystalline silicon carbide (3C–SiC) using DSC spectroscopy. Ceram. Int. 46 (5), 5645–5648.

Huseynov, E., Garibov, A., Mehdiyeva, R., 2015. Influence of neutron irradiation and temperature on the electric conductivity of SiO2 nanoparticles. J. Electrost. 74, 73–78.

Huseynov, E., Garibov, A., Mehdiyeva, R., Andreja, E., Rustamov, A., 2014. Influence of neutron flux, frequency and temperature to electrical impedance of nano silica particles. AIP Adv. 4 (11).

Huseynov, E., Jazbec, A., Snoj, L., 2019. Temperature vs. impedance dependencies of neutron-irradiated nanocrystalline silicon carbide (3C-SiC). Appl. Phys. A 125, 1–8.

Huseynov, E.M., Naghiyev, T.G., Abbasov, N.R., 2022. The paramagnetic approach of the color-changing of nano h-BN particle under the neutron irradiation. Physica E: Low-Dimens. Syst. Nanostruct. 139, 115124.

Huseynov, E.M., Naghiyev, T.G., Aliyeva, U.S., 2020. Thermal parameters investigation of neutron-irradiated nanocrystalline silicon carbide (3C–SiC) using DTA, TGA and DTG methods. Physica B: Condensed Matter 577, 411788.

Huseynov, E.M., Naghiyev, T.G., Garibov, A.A., Abbasov, N.R., Samedov, O.A., Gasimov, R.C., Bayramov, M.A., 2021. EPR spectroscopy of neutron irradiated nanocrystalline boron nitride (h-BN) particles. Ceramics Int. 47 (5), 7218–7223.

IAEA, Research reactor database - RRDB. [Online database]. https://www.iaea.org/resources/databases/research-reactor-database-rrdb.

Jaćimović, R., De Corte, F., Kennedy, G., Vermaercke, P., Revay, Z., 2014. The 2012 recommended k_0 database. J. Radioanal. Nucl. Chem. 300, 589–592.

Jaćimović, R., Maučec, M., Trkov, A., 2003. Verification of Monte Carlo calculations of the neutron flux in typical irradiation channels of the TRIGA reactor, Ljubljana. J. Radioanal. Nucl. Chem. 257, 513–517.

Jacimovic, R., Stegnar, P., Ravnik, M., 2002. Fast Pneumatic Transfer System for the TRIGA Mark II Reactor, Ljubljana, Slovenia. Tech. Rep., International Atomic Energy Agency (IAEA), p. 3, URL http://inis.iaea.org/search/search.aspx?orig_q=RN:40010592. INIS-XA–08N1446.

Jaćimović, R., Trkov, A., Stegnar, P., 2012. Error in k 0-NAA measurement due to temporal variation in the neutron flux in TRIGA Mark II reactor. J. Radioanal. Nucl. Chem. 294 (1), 155–161.

Jazbec, A., Kos, B., Ambrožič, K., Snoj, L., 2021a. Dose rate calculations at beam tube no. 5 of the JSI TRIGA mark II research reactor using Monte Carlo method. Appl. Radiat. Isotopes 168, 109510.

Jazbec, A., Pungerčič, A., Kos, B., Ambrožič, K., Snoj, L., 2021b. Delayed gamma radiation simulation in case of loss of water event using Monte Carlo method. Nucl. Eng. Des.gn 378, 111170.

Jenčič, I., Snoj, L., 2016. The use of Ljubljana TRIGA reactor for training and public information. In: Report of the IAEA Technical Meeting on “Role of Research Reactors in Providing Support To Nuclear Power Programmes”. IAEA, Vienna.

Jeraj, R., Ravnik, M., 1999. TRIGA Mark II reactor: U[20] - Zirconium Hydride fuel rods in water with graphite reflector, IEU-COMP-THERM-003. In: International Criticality Benchmark Evaluation Project Handbook. NEA/NSC/DOC[95]03, Paris.

Jeraj, R., Žagar, T., Ravnik, M., 2002. Monte Carlo simulation of the TRIGA Mark II benchmark experiment with burned fuel. Nucl. Technol. 137 (3), 169–180.

Jones, A.R., Nancekievill, M., Lennox, B., Watson, S., Katakura, J.-I., Okumura, K., Kamada, S., Katoh, M., Nishimura, K., Snoj, L., Jazbec, A., Joyce, M.J., 2018. The integration of a CeBr3 detector with a submersible ROV for reactor assessment at Fukushima Daiichi. In: 2018 IEEE Nuclear Science Symposium and Medical Imaging Conference Proceedings. NSS/MIC, pp. 1–3. http://dx.doi.org/10.1109/NSSMIC.2018.8824759.

Kaiba, T., Žerovnik, G., Jazbec, A., Štancar, Ž., Barbot, L., Fourmentel, D., Snoj, L., 2015. Validation of neutron flux redistribution factors in JSI TRIGA reactor due to control rod movements. Appl. Radiat. Isotopes 104, 34–42. http://dx.doi.org/10.1016/j.apradiso.2015.06.026.

Klemen, A., Luka, S., Lars, Ö., Jan, G., Niklas, B., 2017. On the development of radiation tolerant surveillance camera from consumer-grade components. EPJ Web Conf. 153, 07044. http://dx.doi.org/10.1051/epjconf/201715307044.

Kopsalis, I., Allport, P., Bach, E., Bhardwaj, A., Chisholm, A., Cindro, V., Fadeyev, V., Federicova, P., Fernandez-Tejero, J., Fleta, C., et al., 2023. Establishing the quality assurance programme for the strip sensor production of the ATLAS tracker upgrade including irradiation with neutrons, photons and protons to HL-LHC fluences. J. Instrum. 18 (05), C05009.

Koron, N., Bratkič, A., Guevara, S.R., Vahčič, M., Horvat, M., 2012. Mercury methylation and reduction potentials in marine water: An improved methodology using 197Hg radiotracer. Appl. Radiat. Isotopes 70 (1), 46–50.

Kos, B., Radulovic, V., Kodeli, I.-A., 2017. Results of EURADOS exercise on neutron spectrum unfolding in bonner sphere spectrometry using GRUPINT. In: Proceedings, 26th International Conference Nuclear Energy for New Europe.

Kotnik, D., Basavaraj, A.K., Lengar, I., 2022. Analysis of water activation loop at the JSI TRIGA research reactor. In: 2022 International Conference Nuclear Energy for New Europe - NENE 2022.

Kotnik, D., Basavaraj, A.K., Snoj, L., Lengar, I., 2023a. Design optimization of the closed-water activation loop at the JSI irradiation facility. Fusion Eng. Des. (ISSN: 0920-3796) 193, 113632. http://dx.doi.org/10.1016/j.fusengdes.2023.113632.

Kotnik, D., Pahor, K., Snoj, L., Lengar, I., 2021. Parametric analysis of the closed-water activation loop at the JSI TRIGA reactor. In: 2021 International Conference Nuclear Energy for New Europe - NENE 2021.

Kotnik, D., Peric, J., Govekar, D., Snoj, L., Lengar, I., 2024. KATANA - water activation facility at JSI TRIGA, part I: Final design and activity calculations. Nucl. Eng. Technol. (ISSN: 1738-5733) http://dx.doi.org/10.1016/j.net.2024.09.036, URL https://www.sciencedirect.com/science/article/pii/S1738573324004820.

Kotnik, D., Snoj, L., Lengar, I., 2023b. Assessment of the gamma and neutron dose field around the closed-water activation loop at the JSI TRIGA reactor. In: EPJ Web of Conferences, vol. 288, EDP Sciences, p. 04003.

Kotnik, D., Snoj, L., Lengar, I., 2023c. Overview of the closed water activation loop at JSI Triga research reactor. In: Transactions: RRFM European Research Reactor Conference - RRFM 2023. ENS, p. 6 str.

Kramberger, G., Ambrožič, K., Gürer, U., Hiti, B., Karacali, H., Mandić, I., Yilmaz, E., Yilmaz, O., Zavrtanik, M., 2020. Development of MOS-FET dosimeters for use in high radiation fields. Nucl. Instrum. Methods Phys. Res. Sec. A (ISSN: 0168-9002) 978, 164283. http://dx.doi.org/10.1016/j.nima.2020.164283, URL https://www.sciencedirect.com/science/article/pii/S0168900220306793.

Kramberger, G., et al., 2023. Fast QA tests for LGADs. presented at 42nd RD50 workshop, Tivat.

Kristan, J., Udovc, H., Kobal, I., Jerancic, S., Zavrtanik, D., 1978. Radiation protection measurements around the TRIGA reactor of the Institute 'J Stefan', Ljubljana (RS). Tech. Rep., Serbia, pp. 411–425, URL http://inis.iaea.org/search/search.aspx?orig_q=RN:40038208. INIS-RS–09N0001.

Lazaru, A., Ilić, R., Skvarč, J., Krištof, E., Stafilov, T., 1999. Neutron induced autoradiography of some minerals from the allchar mine. Radiat. Meas. (ISSN: 1350-4487) 31 (1), 677–682. http://dx.doi.org/10.1016/S1350-4487(99)00170-5, URL https://www.sciencedirect.com/science/article/pii/S1350448799001705. Proceedings of the 19th International Conference on Nuclear Tracks in Solids.

Lee, H., Calvin, K., Dasgupta, D., Krinner, G., Mukherji, A., Thorne, P., Trisos, C., Romero, J., Aldunce, P., Barret, K., et al., 2023. IPCC, 2023: Climate change 2023: Synthesis report, summary for policymakers. Contribution of working groups I, II and III to the sixth assessment report of the intergovernmental panel on climate change [Core Writing Team, H. Lee and J. Romero (eds.)]. IPCC, Geneva, Switzerland.

Lengar, I., Merljak, V., Kromar, M., Snoj, L., 2016. Control rod measurements by rod insertion using signal from multiple fission chambers at TRIGA reactor. In: PHYSOR 2016: Unifying Theory and Experiments in the 21st Century. American Nuclear Society.

Lengar, I., Trkov, A., Kromar, M., Snoj, L., 2012. Digital meter of reactivity for use during zero-power physics tests at the Krško NPP. J. Energy Technol..

Leppänen, J., Pusa, M., Viitanen, T., Valtavirta, V., Kaltiaisenaho, T., 2015. The Serpent Monte Carlo code: Status, development and applications in 2013. Ann. Nucl. Energy 82, 142–150.

Malec, J., Pungerčič, A., Kos, B., Ambrožič, K., Žohar, A., Radulović, V., Jazbec, A., Merljak, V., Čufar, A., Štancar, Ž., Snoj, L., 2019. Towards a new research reactor in Slovenia. NENE-Nucl. Energy New Europe, Portorož, Slovenija.

Malec, J., Radulovic, V., Lengar, I., Jazbec, A., Rupnik, S., Österlund, M., Al-Adili, A., Solders, A., Snoj, L., 2021. Remote research reactor exercises during pandemic induced lockdown. In: 30th International Conference on Nuclear Energy for New Europe (NENE), SEP 06-09, 2021, Bled, SLOVENIA. Nuclear Society Slovenia.

Malec, J., Toškan, D., Snoj, L., 2020. PC-based JSI research reactor simulator. Ann. Nucl. Energy 146, 107630.

Malec, J., et al., 2022. New research reactor developments in Slovenia. In: NENE2022 Proceedings. Portorož, Slovenija.

Mandić, I., Cindro, V., Gorišek, A., Kramberger, G., Mikuž, M., Zavrtanik, M., 2010. Observation of full charge collection efficiency in heavily irradiated n+p strip detectors irradiated up to 3×1015neq/cm2. Nucl. Instrum. Methods Phys. Res. Sec. A (ISSN: 0168-9002) 612 (3), 474–477. http://dx.doi.org/10.1016/j.nima.2009.08.004, URL https://www.sciencedirect.com/science/article/pii/S0168900209015721.

Mascolino, V., 2021. Development and Benchmarking of Advanced FM-based Particle Transport Algorithms for Steady-state and Transient Conditions, Implementation in RAPID and Its VRS Web-application (Ph.D. thesis). Virginia Tech.

Mascolino, V., Haghighat, A., 2024. A novel hybrid deterministic and Monte Carlo neutron transport formulation and algorithm (tRAPID) for accurate and fast 3-D reactor kinetics. Nucl. Sci. Eng. 198 (3), 592–627.

Mascolino, V., Haghighat, A., Roskoff, N.J., 2017. Evaluation of RAPID for a UNF cask benchmark problem. In: EPJ Web of Conferences, vol. 153, EDP Sciences, p. 05025.

Mascolino, V., Haghighat, A., Snoj, L., 2021. Verification and validation of RAPID formulations and algorithms based on dosimetry measurements at the JSI TRIGA Mark-II Reactor. Nucl. Sci. Eng. 195 (9), 937–953.

Mascolino, V., Haghighat, A., Snoj, L., 2022. Development and validation of new algorithms for control rods insertion modeling in the RAPID code system using the JSI TRIGA Mark-II reactor. Ann. Nucl. Energy 166, 108711.

Mascolino, V., Pungerčič, A., Snoj, L., Haghighat, A., 2024. Experimental validation of the 3-D neutron kinetics algorithm of RAPID using the JSI TRIGA mark-II reactor. Prog. Nucl. Energy (ISSN: 0149-1970) 176, 105391. http://dx.doi.org/10.1016/j.pnucene.2024.105391, URL https://www.sciencedirect.com/science/article/pii/S014919702400341X.

Mascolino, V., Roskoff, N.J., Haghighat, A., 2018. Benchmarking of the rapid code system using the GBC-32 cask with variable burnups. Proc. PHYSOR 2018: Reactor Phys. Paving Way Towards Effic. Syst. 22–26.

Mele, I., Ravnik, M., Trkov, A., 1994a. TRIGA Mark II benchmark experiment, Part II: pulse operation. Nucl. Technol. 105 (1), 52–58.

Mele, I., Ravnik, M., Trkov, A., 1994b. TRIGA Mark II benchmark experiment, Part I: Steady-state operation. Nucl. Technol. 105 (1), 37–51.

Merljak, V., 2018. Analysis of the Rod Insertion Method for Control Rod Worth Measurement (Ph.D. thesis). University of Ljubljana, URL https://repozitorij.uni-lj.si/IzpisGradiva.php?id=99946&lang=slv.

Merljak, V., Kromar, M., Snoj, L., Trkov, A., 2016. Control Rod Insertion Method Analysis – Dynamic vs. Static Reactivity. In: PHYSOR 2016: Unifying Theory and Experiments in the 21st Century. American Nuclear Society, URL https://www.researchgate.net/publication/303343854_Control_Rod_Insertion_Method_Analysis_-_Dynamic_vs_Static_Reactivity.

Merljak, V., Kromar, M., Trkov, A., 2017a. Verification of kinetic capabilities of the GNOMER neutron diffusion code. Ann. Nucl. Energy (ISSN: 0306-4549) 109, 431–439. http://dx.doi.org/10.1016/j.anucene.2017.04.037, URL http://www.sciencedirect.com/science/article/pii/S0306454916308325.

Merljak, V., Kromar, M., Trkov, A., 2018a. Numerical verification of dynamic reactivity overshoot as observed after control rod repositioning. In: NENE 2018 – 27th International Conference Nuclear Energy for New Europe, (no. Paper no. 223).

Merljak, V., Kromar, M., Trkov, A., 2018b. Rod insertion method analysis – A methodology update and comparison to boron dilution method. Ann. Nucl. Energy (ISSN: 0306-4549) 113 (Supplement C), 96–104. http://dx.doi.org/10.1016/j.anucene.2017.11.020, URL http://www.sciencedirect.com/science/article/pii/S0306454917304012.

Merljak, V., Trkov, A., Lengar, I., 2014. Comparison of measured and calculated reactivity-worth curves of control rods in a TRIGA reactor. In: NENE 2014 – 23rd International Conference Nuclear Energy for New Europe, (no. Paper no. 709), URL http://www.djs.si/proc/nene2014/pdf/NENE2014_709.pdf.

Merljak, V., Žerovnik, G., Snoj, L., Barbot, L., Fourmentel, D., Destouches, C., Villard, J.-F., 2017b. Using the CEA in-core miniature fission chambers for control rod calibration by the rod insertion method. In: Proceedings of the 26th International Conference Nuclear Energy for New Europe. Nuclear Society of Slovenia.

Mosher, S., Johnson, S., Bevill, A., Ibrahim, A., Daily, C., Evans, T., Wagner, J., Johnson, J., Grove, R., 2015. ADVANTG – An Automated Variance Reduction Parameter Generator, Rev. 1. Tech. Rep., Oak Ridge National Laboratory.

Najzer, M., Byrne, A.R., Dimic, V., Mavko, B., Pregl, G., Rant, J., 1974. Recent Research Programs at The TRIGA Mark II Reactor in Ljubljana. Tech. Rep., United States, URL http://inis.iaea.org/search/search.aspx?orig_q=RN:06215657. CONF-7410123–.

Nemec, T., Rant, J., Apih, V., Glumac, B., 1999. Study of building materials impregnation processes by quasi-real-time neutron radiography. Nucl. Instrum. Methods Phys. Res. A (ISSN: 0168-9002) 424 (1), 242–247. http://dx.doi.org/10.1016/S0168-9002(98)01301-1, URL https://www.sciencedirect.com/science/article/pii/S0168900298013011.

Ninamedia, 2024. Ninamedia polling archive. https://ninamedia.si/arhivi/1257. (Accessed 14 October 2024).

Nuclear Energy Agency, 2024. Joint evaluated fission and fusion (JEFF) 4t3 nuclear data library. https://www.oecd-nea.org/dbdata/jeff/jeff40/t3/.

Nuclear Energy Agency (NEA), 2022. Meeting Climate Change Targets: The Role of Nuclear Energy. OECD Publishing, Paris.

Pellegrini, G., Fernández-Martínez, P., Baselga, M., Fleta, C., Flores, D., Greco, V., Hidalgo, S., Mandić, I., Kramberger, G., Quirion, D., et al., 2014. Technology developments and first measurements of Low Gain Avalanche Detectors (LGAD) for high energy physics applications. Nucl. Instrum. Methods Phys. Res. Sec. A 765, 12–16.

Peric, J., Radulović, V., Barbot, L., Izzara, G.D., 2023. Radiation measurements in reactor pulse mode at the JSI TRIGA reactor – Power meter based on Cherenkov light intensity measurements. In: EPJ Web of Conferences, vol. 288, p. 7, URL https://www.epj-conferences.org/articles/epjconf/abs/2023/14/epjconf_animma2023_04020/epjconf_animma2023_04020.html.

Peršič, A., Ravnik, M., Žagar, T., 2000. TRIGA Mark II criticality Benchmark experiment with burned fuel. Nucl. Technol. 132 (3), 325–338.

Peršič, A., Žagar, T., Ravnik, M., Slavič, S., Žefran, B., Ćalić, D., Trkov, A., Žerovnik, G., Jazbec, A., Snoj, L., 2017. TRIGLAV: A program package for TRIGA reactor calculations. Nuclear Engineering and Design 318, 24–34.

Petit, O., Hugot, F.-X., Lee, Y.-K., Jouanne, C., Mazzolo, A., 2008. TRIPOLI-4 Version 4 User Guide. Tech. Rep., CEA Saclay.

Pirker, L., Krajnc, A.P., Malec, J., Radulović, V., Gradišek, A., Jelen, A., Remškar, M., Mekjavić, I.B., Kovač, J., Mozetič, M., Snoj, L., 2021. Sterilization of polypropylene membranes of facepiece respirators by ionizing radiation. J. Membr. Sci. (ISSN: 0376-7388) 619, 118756. http://dx.doi.org/10.1016/j.memsci.2020.118756.

Plant, A.G., Kos, B., Jazbec, A., Snoj, L., Najdanovic-Visak, V., Joyce, M.J., 2021. Nuclear-driven production of renewable fuel additives from waste organics. Commun. Chem. 4 (1), 132.

Plompen, A.J., Cabellos, O., De Saint Jean, C., Fleming, M., Algora, A., Angelone, M., Archier, P., Bauge, E., Bersillon, O., Blokhin, A., et al., 2020. The joint evaluated fission and fusion nuclear data library, JEFF-3.3. Eur. Phys. J. A 56, 1–108.

Pungerčič, A., Čalič, D., Snoj, L., 2020. Computational burnup analysis of the TRIGA Mark II research reactor fuel. Progress Nucl. Energy (ISSN: 0149-1970) 130, 103536. http://dx.doi.org/10.1016/j.pnucene.2020.103536, URL https://www.sciencedirect.com/science/article/pii/S0149197020302845.

Pungerčič, A., Cirillo, R., Walkiewicz, J., Novák, E., Gajewski, J., Szentmiklósi, L., Van Puyvelde, L., Starflinger, J., Cano, D., Pohlner, G., et al., 2023a. Identified opportunities in utilization of the European research reactor fleet as a part of the TOURR project. In: EPJ Web of Conferences, vol. 288, EDP Sciences, p. 04013.

Pungerčič, A., Mascolino, V., Haghighat, A., Snoj, L., 2023b. Verification of a novel fuel burnup algorithm in the RAPID code system based on Serpent-2 simulation of the TRIGA Mark II research reactor. Nucl. Eng. Technol. 55 (10), 3732–3753.

Radulović, V., Ambrožič, K., Snoj, L., Capan, I., Brodar, T., Ereš, Z., Pastuović, Ž., Sarbutt, A., Ohshima, T., Yamazaki, Y., Coutinho, J., 2020a. E-SiCure collaboration project: Silicon carbide material studies and detector prototype testing at the JSI TRIGA reactor. EPJ Web Conf. 225, 07007. http://dx.doi.org/10.1051/epjconf/202022507007.

Radulović, V., Barbot, L., Izzara, G.D., Peric, J., Lengar, I., 2021. Reactor Pulse Operation for Nuclear Instrumentation Detector Testing – Preparation of a Dedicated Experimental Campaign at the JSI TRIGA Reactor, vol. 253, EPJ, p. 6.

Radulović, V., Fourmentel, D., Barbot, L., Villard, J.-F., Kaiba, T., Žerovnik, G., Snoj, L., 2015. Measurements of miniature ionization chamber currents in the JSI TRIGA Mark II reactor demonstrate the importance of the delayed contribution to the photon field in nuclear reactors. Nucl. Instrum. Methods Phys. Res. Sec. A 804, 149–154.

Radulović, V., Goričanec, T., Kos, B., Ambrožič, K., 2018a. Report on Experimental Tests of a Combined SPND and Thermocouple Sensor for the DISCOMS Project at the JSI TRIGA Reactor, vol. 12547, Institut Jožef Stefan, p. 98.

Radulović, V., Jaćimović, R., Pungerčič, A., Vavtar, I., Snoj, L., Trkov, A., 2020b. Characterization of the neutron spectra in three irradiation channels of the JSI TRIGA reactor using the GRUPINT spectrum adjustment code. Nuclear Data Sheets 167, 61–75.

Radulovic, V., Kaiba, T., Cindro, V., Snoj, L., Kavsek, D., Stepisnik, M., Mikuz, M., 2017. Large object irradiation facility in the tangential channel of the JSI TRIGA reactor. In: European Research Reactor Conference 2017.

Radulović, V., Kolšek, A., Fauré, A.-L., Pottin, A.-C., Pointurier, F., Snoj, L., 2018b. Qualification of heavy water based irradiation device in the JSI TRIGA reactor for irradiations of FT-TIMS samples for nuclear safeguards. Nucl. Instrum. Methods Phys. Res. Sec. A 885, 139–144.

Radulović, V., Štancar, Ž., Snoj, L., Trkov, A., 2014. Validation of absolute axial neutron flux distribution calculations with MCNP with 197Au (n, γ) 198Au reaction rate distribution measurements at the JSI TRIGA Mark II reactor. Appl. Radiat. Isotopes 84, 57–65.

Radulović, V., Thiollay, N., 2018. Nuclear reactions suitable for epithermal neutron dosimetry using boron-based filters: preparation of an experimental campaign at the JSI TRIGA reactor. In: Proc. 27th Int. Conf. Nucl. Energy for New Europe. Nuclear Society of Slovenia.

Radulović, V., Yamazaki, Y., Pastuović, Ž., Sarbutt, A., Ambrožič, K., Bernat, R., Ereš, Z., Coutinho, J., Ohshima, T., Capan, I., et al., 2020c. Silicon carbide neutron detector testing at the JSI TRIGA reactor for enhanced border and port security. Nucl. Instrum. Methods Phys. Res. Sec. A 972, 164122.

Rant, J., Copic, M., Dimic, V., Ilic, R., Sirca, F., 1972. Neutronography and Microneutronography and Their Applications. Tech. Rep., Italy, pp. 3125–3131, URL http://inis.iaea.org/search/search.aspx?orig_q=RN:40091482. INIS-IT–09N0001.

Ravnik, M., 1997. Experimental verification of adiabatic Fuchs-Hansen pulse model. In: 4th Regional Meeting Nuclear Energy in Central Europe.

Ravnik, M., Jeraj, R., 2003. Research reactor benchmarks. Nucl. Sci. Eng. 145 (1), 145–152. http://dx.doi.org/10.13182/NSE03-A2370.

Ravnik, M., Mele, I., Dimic, V., 1990. PULSTRI-1 computer program for mixed core pulse calculation.

Ravnik, M., Strebl, M., Böck, H., Trkov, A., Mele, I., 1992a. Determination of the burn-up of TRIGA fuel elements by calculation and reactivity experiments/Bestimmung des Abbrandes von TRIGA-Brennelementen durch Reaktorberechnungen und Reaktivitätsmessungen. Kerntechnik 57 (5), 291–295.

Ravnik, M., Strebl, M., Böck, H., Trkov, A., Mele, I., 1992b. Determination of the burn-up of TRIGA fuel elements by calculation and reactivity experiments/Bestimmung des Abbrandes von TRIGA-Brennelementen durch Reaktorberechnungen und Reaktivitätsmessungen. Kerntechnik 57 (5), 291–295.

Ravnik, M., Wimmer, H., Trkov, A., Böck, H., Mele, I., 1993. Burn-up measurements at TRIGA fuel elements containing strong burnable poison/Abbrandbestimmung an TRIGA-Brennelementen mit starkem brennbarem Reaktorgift. Kerntechnik 58 (5), 289–294.

Ravnik, M., Zagar, T., Persic, A., 1999. Fuel element burnup determination in mixed TRIGA core using reactor calculations. Nucl. Technol. 128 (1), 35–45.

Ribeiro Guevara, S., Žižek, S., Repinc, U., Pérez Catán, S., Jaćimović, R., Horvat, M., 2007. Novel methodology for the study of mercury methylation and reduction in sediments and water using 197 Hg radiotracer. Anal. Bioanal. Chem. 387, 2185–2197.

Roskoff, N., Mascolino, V., Haghighat, A., 2018. Accuracy of rapid for simulation of pools with diverse spent fuels. In: Proceedings of the PHYSOR 2018: Reactor Physics Paving the Way Towards more Efficient Systems.

Sánchez Sanz, M., 2023. Effect of hydrogen distribution in UZrHx on physical parameters of JSI TRIGA reactor. URL https://repozitorij.uni-lj.si/IzpisGradiva.php?id=149104.

Santamarina, A., Bernard, D., Blaise, P., Coste, M., Courcelle, A., Huynh, T., Jouanne, C., Leconte, P., Litaize, O., Mengelle, S., et al., 2009. The JEFF-3.1. 1 nuclear data library. JEFF Rep. 22 (10.2), 2.

Sarkar, A., Šadl, M., Jazbec, A., Snoj, L., Drnovšek, S., Rojac, T., Brennecka, G.L., Uršič, H., Malič, B., 2023. Influence of neutron and gamma irradiation on the electrocaloric properties of Mn-doped 0.9 Pb (Mg1/3Nb2/3) O3–0.1 PbTiO3 ceramics. J. Phys.: Energy 5 (4), 045006.

Schymura, S., Rybkin, I., Uygan, S.S.S., Drev, S., Rijavec, T., Mansel, A., Lapanje, A., Franke, K., Strok, M., et al., 2021. Dissolution-based uptake of CeO 2 nanoparticles by freshwater shrimp–a dual-radiolabelling study of the fate of anthropogenic cerium in water organisms. Environ. Sci.: Nano 8 (7), 1934–1944.

Sergeyeva, V., Thiollay, N., Vigneau, O., Korschinek, G., Carcreff, H., Destouches, C., Lyoussi, A., 2015. Determination of neutron spectra within the energy of 1 kev to 1 MeV by means of reactor dosimetry. In: 2015 4th International Conference on Advancements in Nuclear Instrumentation Measurement Methods and their Applications. ANIMMA, pp. 1–8. http://dx.doi.org/10.1109/ANIMMA.2015.7465515.

Šlejkovec, Z., Byrne, A., Dermelj, M., 1993. Neutron activation analysis of arsenic species. J.F Radioanal. Nucl. Chem. 173 (2), 357–364.

Šlejkovec, Z., Van Elteren, J.T., Byrne, A.R., de Goeij, J.J., 1999. Separation of radiolabelled arsenic compounds produced by neutron irradiation of organoarsenic compounds. Anal. Chim. Acta 380 (1), 63–71.

Smodiš, B., Benedik, L., Jaćimović, R., 2018. Analytical radiochemistry of neutron activated samples in practice. J. Radioanal. Nucl. Chem. (ISSN: 1588-2780) 318 (3), 1641–1647. http://dx.doi.org/10.1007/s10967-018-6275-5.

Snoj, L., Kavčič, A., Žerovnik, G., Ravnik, M., 2010. Calculation of kinetic parameters for mixed TRIGA cores with Monte Carlo. Ann. Nucl. Energy 37 (2), 223–229.

Snoj, L., Ravnik, M., 2008. Power peakings in mixed TRIGA cores. Nucl. Eng. Des. 238, 2473–2479.

Snoj, L., Sklenka, L., Rataj, J., Böck, H., 2012a. Eastern Europe Research Reactor Initiative Nuclear Education and Training Courses-Current Activities and Future Challenges. Tech. Rep., American Nuclear Society, Inc., 555 N. Kensington Avenue, La Grange Park ....

Snoj, L., Stancar, Z., Radulovic, V., Kaiba, T., Lengar, I., Zerovnik, G., Merljak, V., Trkov, A., Barbot, L., Fourmentel, D., et al., 2016. Benchmark experiments at the TRIGA Mark II reactor. In: PHYSOR 2016–Unifying Theory and Experiments in the 21st Century.

Snoj, L., Trkov, A., Jaćimović, R., Rogan, P., Žerovnik, G., Ravnik, M., 2011a. Analysis of neutron flux distribution for the validation of computational methods for the optimization of research reactor utilization. Appl. Radiat. Isotopes 69 (1), 136–141.

Snoj, L., Trkov, A., Ravnik, M., Žerovnik, G., 2012b. Testing of cross section libraries on zirconium benchmarks. Ann. Nucl. Energy 42, 71–79.

Snoj, L., Žerovnik, G., Radulovič, V., Podvratnik, M., Trkov, A., Barbot, L., Geslot, B., Domergue, C., Gregoire, G., Destouches, C., 2011b. CEA-IJS joint experimental campaign at TRIGA Mark II Reactor at Jožef Stefan Institute. In: Proceedings of the International Conference Nuclear Energy for New Europe.

Snoj, L., Žerovnik, G., Trkov, A., 2012c. Computational analysis of irradiation facilities at the JSI TRIGA reactor. Appl. Radiat. Isot. 70 (3), 483–488.

Štancar, Ž., Barbot, L., Destouches, C., Fourmentel, D., Villard, J.-F., Snoj, L., 2018. Computational validation of the fission rate distribution experimental benchmark at the JSI TRIGA Mark II research reactor using the Monte Carlo method. Ann. Nucl. Energy 112, 94–108.

Štancar, Ž., Barbot, L., Domergue, C., Radulovič, V., Trkov, A., Snoj, L., 2012. Evaluation of the axial absolute power profile measurements at the JSI TRIGA Mark II reactor. In: Proceedings of the International Conference Nuclear Energy for New Europe. pp. 5–7.

Štancar, Ž., Snoj, L., 2017. An improved thermal power calibration method at the TRIGA Mark II research reactor. Nucl. Eng. Des. (ISSN: 0029-5493) 325, 78–89. http://dx.doi.org/10.1016/j.nucengdes.2017.10.007, URL https://www.sciencedirect.com/science/article/pii/S0029549317304788.

Štancar, Ž., Snoj, L., Barbot, L., Lengar, I., Destouches, C., Lell, R., 2017a. Reaction rate distribution experiments at the Slovenian JSI Triga Mark II research reactor. In: International Handbook of Evaluated Reactor Physics Benchmark Experiments. OECD Nuclear Energy Agency, Paris.

Štancar, Ž., Snoj, L., Barbot, L., Lengar, I., Destouches, C., Lell, R., 2017b. Reaction rate distribution experiments at the Slovenian JSI Triga Mark II research reactor, international handbook of evaluated reactor physics benchmark experiments (NEA, 7329).

Stepišnik, M., Pucelj, B., Snoj, L., Ravnik, M., 2009. Activity Analysis of Primary Coolant in TRIGA MARK II Research Reactor. In: Proceedings of International Conference Nuclear Energy for New Europe.

Švajger, I., Čalič, D., Pungerčič, A., Trkov, A., Snoj, L., 2023. Evaluation of reactor pulse experiments. Nucl. Eng. Technol. (ISSN: 1738-5733) http://dx.doi.org/10.1016/j.net.2023.11.021, URL https://www.sciencedirect.com/science/article/pii/S173857332300520X.

Švajger, I., Fleming, N.C., Laramee, B., Noguere, G., Hawari, A., Snoj, L., Trkov, A., 2021. Thermal scattering law data for zirconium hydride from first-principles. In: Proceedings of the 30th International Conference Nuclear Energy for New Europe. Nuclear Society of Slovenia.

Švajger, I., Trkov, A., Snoj, L., 2020. Methodology for thermal neutron scattering cross sections determination. In: Proceedings of the 29th International Conference Nuclear Energy for New Europe. Nuclear Society of Slovenia.

Topham, T.J., Rau, A., Walters, W.J., 2020. An iterative fission matrix scheme for calculating steady-state power and critical control rod position in a TRIGA reactor. Ann. Nucl. Energy 135, 106984.

Trkov, A., Griffin, P.J., Simakov, S.P., Greenwood, L.R., Zolotarev, K.I., Capote, R., Aldama, D.L., Chechev, V., Destouches, C., Kahler, A.C., Konno, C., Koštál, M., Majerle, M., Malambu, E., Ohta, M., Pronyaev, V.G., Radulović, V., Sato, S., Schulc, M., Šimečková, E., Vavtar, I., Wagemans, J., White, M., Yashima, H., 2020. IRDFF-II: A new neutron metrology library. Nucl. Data Sheets 163, 1–108. http://dx.doi.org/10.1016/j.nds.2019.12.001.

Trkov, A., Merljak, V., 1994. GNOMER-Multigroup 3-Dimensional Neutron Diffusion Nodal Code with Thermohydraulic Feedbacks. Jozef Stefan" Institute, Ljubljana, IJS-DP-6688.

Trkov, A., Najžer, M., Škerget, L., 1990. A variant of the Green's function method for neutron diffusion. J. Nucl. Sci. Technol. 27 (8), 766–777. http://dx.doi.org/10.1080/18811248.1990.9731251, URL http://www.tandfonline.com/doi/abs/10.1080/18811248.1990.9731251.

Trkov, A., Radulović, V., 2015. Nuclear reactions and physical models for neutron activation analysis. J. Radioanal. Nucl. Chem. 304 (2), 763–778.

Trkov, A., Ravnik, M., 1995. The neutron flux redistribution effects on the power level reading from the nuclear detectors in a research reactor. In: Nuclear Society of Slovenia, 2^{Nd} Regional Meeting: Nuclear Energy in Central Europe.

Trkov, A., Ravnik, M., Böck, H., Glumac, B., 1992. Reactivity measurements in a close-to-critical TRIGA reactor using a digital reactivity meter. Kerntechnik 57, 296–300.

Trkov, A., Ravnik, M., Wimmer, H., Glumac, B., Böck, H., 1995. Application of the rod-insertion method for control rod worth measurements in research reactors. Kerntechnik 60, 255–261, URL http://www.scopus.com/inward/record.url?eid=2-s2.0-0029405504&partnerID=40&md5=9a1f95e915dd302dee0e608424569bc4.

Tsitsimpelis, I., West, A., Licata, M., Aspinall, M.D., Jazbec, A., Snoj, L., Martin, P.A., Lennox, B., Joyce, M.J., 2020. Simultaneous, robot-compatible γ-ray spectroscopy and imaging of an operating nuclear reactor. IEEE Sensors J. 21 (4), 5434–5443.

Uršič, H., Prah, U., Rojac, T., Jazbec, A., Snoj, L., Drnovšek, S., Bradeško, A., Mirjanić, A., Vrabelj, M., Malič, B., 2022. High radiation tolerance of electrocaloric (1-x) Pb (Mg1/3Nb2/3) O3–xPbTiO3. J. Eur. Ceramic Soc. 42 (13), 5575–5583.

Čopič, M., 1976. Dve Metodi Merjenja Negativnih Reaktivnosti. Tech. Rep., (IJS-DP-1033), Jožef Stefan Institute.

Valtavirta, V., Hessan, M., Leppänen, J., Allelein, H.-J., Merljak, V., Čalič, D., Stancar, Ž., Snoj, L., 2018. Time-Dependent Modelling Of The JSI TRIGA With Serpent 2. In: Proceedings of the 27th International Conference Nuclear Energy for New Europe. Nuclear Society of Slovenia.

van Elteren, J., Kroon, K., Šlejkovec, Z., Verburg, T., Kolar, Z., 2008. Topical isotopic exchange and compartmental analysis approach for probing solute behaviour at the soil/arsenate solution interface. Talanta 75 (1), 253–257.

Vavtar, I., Kos, B., Snoj, L., 2017. Validation of TRIGA Mark II Reactor Model in Open Source Program Openmc Using Experiments and MCNP Code. IJS Work Report IJS-DP-12440, Jožef Stefan Institute, Reactor Physics Department, Ljubljana, Slovenia.

Vavtar, I., Pungerčič, A., Snoj, L., 2020. Utilisation of JSI TRIGA pulse experiments for testing of nuclear instrumentation and validation of transient models. In: EPJ Web of Conferences, vol. 225, EDP Sciences, p. 04027.

Vavtar, I., Snoj, L., 2019. Evaluation of uncertainties in Physical Parameters of Reactor Pulse. In: Proceedings of the 28th International Conference Nuclear Energy for New Europe. Nuclear Society of Slovenia.

Švajger, I., Ćalić, D., Pungerčič, A., Snoj, L., 2020. Evaluation of approximation and uncertainties in theoretical models describing pulse mode operation. In: European Research Reactor Conference RRFM 2020. ENS, ISBN: 978-92-95064-34-8, p. 10.

Švajger, I., Snoj, L., 2020. Evaluation of approximations in reactor pulse. In: PHYSOR 2020, Transition To a Scalable Nuclear Future. University of Cambridge, Cambridge, ISBN: 978-1-5272-6447-2, p. 8.

Švajger, I., Snoj, L., 2021. Evaluation of reactor pulse experiments. In: Mathematics & Computation (M&C) 2021: Proceedings. ANS, La Grange Park, Illinois, pp. 1490–1499.

Walters, W., Roskoff, N.J., Haghighat, A., 2015. A fission matrix approach to calculate pin-wise 3D fission density distribution. Proc. M&C.

Walters, W.J., Roskoff, N.J., Haghighat, A., 2018. The RAPID fission matrix approach to reactor core criticality calculations. Nucl. Sci. Eng. 192 (1), 21–39.

West, A., Tsitsimpelis, I., Licata, M., Jazbec, A., Snoj, L., Joyce, M.J., Lennox, B., 2021. Use of Gaussian process regression for radiation mapping of a nuclear reactor with a mobile robot. Sci. Rep. 11 (1), 13975.

Wharton, W.A., O'Kelly, S., Krause, M., 2005. Educating students on core loading with TRIGLAV. Trans. Am. Nucl. Soc. 93, 33–34.

White, D., Dowell, J., Mahout, G., Jovanovic, P., Mandić, I., Weidberg, A., 2001. Radiation hardness studies of the front-end ASICs for the optical links of the ATLAS SemiConductor tracker. Nucl. Instrum. Methods Phys. Res. A (ISSN: 0168-9002) 457 (1), 369–377. http://dx.doi.org/10.1016/S0168-9002(00)00763-4, URL https://www.sciencedirect.com/science/article/pii/S0168900200007634.

Zagar, T., Ravnik, M., 1996. Determination of the burn-up of TRIGA fuel elements by calculation with new TRIGLAV program. In: 3rd Regional Meeting: Uclear Energy in Central Europe.

Zagar, T., Zefran, B., Slavic, S., Snoj, L., Ravnik, M., 2006. TRIGLAV-W a Windows Computer Program Package with graphical users interface for TRIGA reactor core management calculations.

Žerovnik, G., Kaiba, T., Radulović, V., Jazbec, A., Rupnik, S., Barbot, L., Fourmentel, D., Snoj, L., 2015. Validation of the neutron and gamma fields in the JSI TRIGA reactor using in-core fission and ionization chambers. Applied Radiat. Isotopes 96, 27–35.

Žerovnik, G., Noguère, G., Benedik, L., Kocijančič, D., Radulović, V., 2023. Am-241 thermal neutron capture cross section and neutron capture resonance integral from reactor activation and oscillation measurements. In: EPJ Web of Conferences, Vol. 284 – ND 2022 Special Issue, (no. 01042).

Žerovnik, G., Podvratnik, M., Snoj, L., 2014a. On normalization of fluxes and reaction rates in MCNP criticality calculations. Ann. Nucl. Energy 63, 126–128.

Žerovnik, G., Radulović, V., Benedik, L., Kos, B., Gantar, T., Noguère, G., 2021. Method for analysis of neutron activation measurements of Am-241 with uncertainty propagation. In: NENE 2021 – 30th International Conference Nuclear Energy for New Europe, (Paper no. 1006).

Žerovnik, G., Snoj, L., Trkov, A., Barbot, L., Fourmentel, D., Villard, J.-F., 2013. Improved measurements of thermal power and control rods using multiple detectors at the TRIGA Mark II reactor in Ljubljana. In: 2013 3rd International Conference on Advancements in Nuclear Instrumentation, Measurement Methods and their Applications. ANIMMA, IEEE, pp. 1–5.

Žerovnik, G., Snoj, L., Trkov, A., Barbot, L., Fourmentel, D., Villard, J.-F., 2014b. Measurements of thermal power at the TRIGA Mark II reactor in Ljubljana using multiple detectors. IEEE Trans. Nucl. Sci. 61 (5), 2527–2531.

Žiber, Y., Radulović, V., 2022. Testing Of silicon carbide neutron detector for detection of fast neutrons. In: Proceedings of the 31th International Conference Nuclear Energy for New Europe. Nuclear Society of Slovenia.

Žižek, S., Ribeiro Guevara, S., Horvat, M., 2008. Validation of methodology for determination of the mercury methylation potential in sediments using radiotracers. Anal. Bioanal. Chem. 390, 2115–2122.

Zohar, A., Radulovic, V., Jazbec, A., Lengar, I., Rupnik, S., Snoj, L., 2021. Water activation experiments and calculations at JSI TRIGA research reactor. In: 29th International Conference Nuclear Energy for New Europe - NENE 2021. Nuclear Society of Slovenia, DJS, p. 302.1.

Žohar, A., Radulović, V., Snoj, L., Bernat, R., Bakrac, L., Capan, I., Makino, T., 2021. Silicon carbide neutron detector development-computational support with MCNP. In: Proceedings, 30st International Conference Nuclear Energy for New Europe, (no. 30), Nuclear Society of Slovenia, URL https://www.djs.si/nene2021/proceedings/pdf/NENE2021_316.pdf.

Žontar, D., Cindro, V., Kramberger, G., Mikuž, M., 1999. Time development and flux dependence of neutron-irradiation induced defects in silicon pad detectors. Nucl. Instrum. Methods Phys. Res. Sec. A 426 (1), 51–55.